

Quasi-Bayesian Dual Instrumental Variable Regression

Ziyu Wang*

Yuhao Zhou*

*Tsinghua University
Beijing, 100084, China*

WZY196@GMAIL.COM

YUHAOZ.CS@GMAIL.COM

Tongzheng Ren

UT Austin

Austin, TX 78712, USA

TONGZHENG@UTEXAS.EDU

Jun Zhu

Tsinghua University

Beijing, 100084, China

DCSZJ@MAIL.TSINGHUA.EDU.CN

Abstract

Recent years have witnessed an upsurge of interest in employing flexible machine learning models for instrumental variable (IV) regression, but the development of uncertainty quantification methodology is still lacking. In this work we present a novel quasi-Bayesian procedure for IV regression, building upon the recently developed kernelized IV models and the dual/minimax formulation of IV regression. We analyze the frequentist behavior of the proposed method, by establishing minimax optimal contraction rates in L_2 and Sobolev norms, and discussing the frequentist validity of credible balls. We further derive a scalable inference algorithm which can be extended to work with wide neural network models. Empirical evaluation shows that our method produces informative uncertainty estimates on complex high-dimensional problems.

Keywords: instrumental variable, uncertainty quantification, Gaussian process, contraction rates, causal inference

1. Introduction

Instrumental variable (IV) regression is a standard approach for estimating causal effect from confounded observational data, and is widely used in areas such as economics, epidemiology and clinical research (Angrist and Pischke, 2008; Greenland, 2000; Cuzick et al., 1997). In the presence of confounding, any regression method estimating $\mathbb{E}(\mathbf{y} \mid \mathbf{x})$ cannot recover the causal relation f_0 between the outcome \mathbf{y} and the treatment \mathbf{x} , since the residual $\mathbf{u} = \mathbf{y} - f_0(\mathbf{x})$ is correlated with \mathbf{x} due to the unobserved confounders. IV regression enables identification of the causal effect through the introduction of *instruments*, variables \mathbf{z} that are known to influence \mathbf{y} only through \mathbf{x} .

Recent years have seen great development in adopting flexible machine learning models for IV regression (Hartford et al., 2017; Lewis and Syrgkanis, 2018; Bennett et al., 2019; Singh et al., 2019; Bennett and Kallus, 2020), which bring the promise of better adaptation to complex structures in data. However, their theoretical properties are less well understood than classical nonparametric approaches, as we discuss in Section 7. Moreover, there is a lack of principled uncertainty quantification measures for these flexible IV models.

*. Equal contribution.

Uncertainty quantification is especially important for IV analysis, since unlike in standard supervised learning scenarios, we do not have (unconfounded) validation data. Moreover, it is possible that the instrument of choice is only weakly correlated with \mathbf{x} , in which case point estimators suffer from high variance (Stock et al., 2002). This problem is exacerbated in the nonparametric setting, where IV estimation is typically an ill-posed inverse problem, in which statistical challenges present for the recovery of higher order nonlinear effects. We refer readers to Horowitz (2011) for an introduction to this matter.

Uncertainty quantification for IV regression is challenging. For example, while it may appear natural to consider a Bayesian approach, specification of the likelihood requires knowledge of the data generating process, which is typically not assumed in IV regression. Consequently, existing work on Bayesian IV (Kleibergen and Van Dijk, 1998; Kleibergen and Zivot, 2003; Conley et al., 2008; Lopes and Polson, 2014; Wiesenfarth et al., 2014) typically make stronger assumptions, and assume the following data generating process: $\mathbf{x} = g(\mathbf{z}) + \mathbf{u}_1$, $\mathbf{y} = f(\mathbf{x}) + \mathbf{u}_2$, where $(\mathbf{u}_1, \mathbf{u}_2)$ are correlated and independent of \mathbf{z} . Posterior inference is then conducted on g, f as well as the *distribution* of the unobserved confounders $(\mathbf{u}_1, \mathbf{u}_2)$. Additive, independent error in \mathbf{x} is an unnecessary assumption for point estimators, and is difficult to check in high dimensions. The need to model the generating process of $(\mathbf{u}_1, \mathbf{u}_2)$ also introduces extra risks of model misspecification, and Bayesian inference over the generative model is computationally expensive, especially on complex high-dimensional datasets. None of these issues present if only point estimation is needed.

For the above reasons, it is appealing to turn to an alternative *quasi-Bayesian* approach (Chernozhukov and Hong, 2003; Liao and Jiang, 2011; Kato, 2013). Quasi-Bayesian analysis views IV estimation as a generalized method of moments procedure, and defines the quasi-posterior as a Gibbs distribution constructed from a chosen prior and violation of the conditional moment restrictions. It does not require full knowledge of the data generating process, and thus does not suffer from the aforementioned drawbacks. However, computation of the quasi-posterior is non-trivial in the IV setting, as its density contains a conditional expectation term $\mathbb{E}(\mathbf{y} - f(\mathbf{x}) \mid \mathbf{z})$, which itself needs to be estimated. Moreover, the need to estimate the conditional expectation also brings challenges to theoretical analysis of the frequentist behavior. So far, quasi-Bayesian analysis for nonparametric IV is only developed with classical models such as wavelet basis (Liao and Jiang, 2011; Kato, 2013) or Nadaraya-Watson smoothing (Florens and Simoni, 2012), and with more limited theoretical understanding compared with their frequentist counterparts (see Section 7). Besides, numerical study has been limited in previous work, and thus little is known about the empirical performance of the quasi-Bayesian approach for nonparametric IV.

In this work, we present a novel quasi-Bayesian procedure for IV regression, building upon the recent development in kernelized IV models (Singh et al., 2019). We employ a Gaussian process (GP) prior and construct the quasi-likelihood based on a recently proposed dual formulation of IV estimation (e.g., Muandet et al., 2020; Dikkala et al., 2020). Following this, posterior sampling can be cast as a minimax optimization problem, based on which we construct an inference algorithm. The algorithm is further adapted to work with flexible neural network models, in which case its behavior can be justified by analyzing the neural networks in the kernel regime. We evaluate the proposed method on several synthetic datasets, showing that it produces informative uncertainty estimates on complex nonlinear problems, and is particularly advantageous in the finite-sample setting.

In addition to the methodological contributions, this work also contributes to the theoretical understanding of nonparametric IV methods. We establish optimal posterior contraction rates for both L_2 and Sobolev norms. Comparing with previous work on quasi-Bayesian IV (Kato, 2013), we allow for more flexibility in the choice of models. From these results we deduce optimal convergence rates for the point estimator of kernelized IV, which fill in an important gap in literature, and further establish kernelized IV as a principled estimation method with potential theoretical advantages (see Section 7 for discussion). We further analyze the frequentist coverage properties of the posterior credible balls, and provide intuition on the nonasymptotic behavior of the quasi-posterior. As a side contribution, we apply our proof technique to Gaussian process regression, and improve the result of van der Vaart and van Zanten (2011) by relaxing a joint Hölder and Sobolev regularity assumption. Finally, we note that this work is a substantial extension of a conference paper (Wang et al., 2021), with all theoretical results in Section 4-5 being new.

The rest of the paper is organized as follows: we set up the problem in Section 2 and derive the quasi-posterior in Section 3. We then present the asymptotic analysis in Section 4, and discuss the nonasymptotic behavior of the quasi-posterior in Section 5. The approximate inference algorithm is presented in Section 6. Section 7 discuss related work, and Section 8 presents numerical studies. Finally, we discuss conclusion in Section 9.

2. Notations and Setup

2.1 Notations

We use boldface $(\mathbf{x}, \mathbf{y}, \mathbf{z})$ to represent random variables on the space $\mathcal{X} \times \mathcal{Y} \times \mathcal{Z}$, regular font (x, y, z) to denote deterministic values. $[n]$ denotes the set $\{1, 2, \dots, n\}$. $\{(x_i, y_i, z_i) : i \in [n]\}$ indicates the training data. We use the notations $X := (x_1, \dots, x_n) \in \mathcal{X}^n$, $f(X) := (f(x_1), \dots, f(x_n))$; likewise for Y, Z . For finite-dimensional vectors $\theta, \theta' \in \mathbb{R}^m$, we use $\|\theta\|_2$ and $\langle \theta, \theta' \rangle_2$ to denote the Euclidean norm and inner product w.r.t. the data distribution, respectively. For square-integrable functions, $\|\cdot\|_2$ and $\langle \cdot, \cdot \rangle_2$ refer to L_2 norm and inner product. $\|\cdot\|$ denotes the sup norm. For any operator $A : H_1 \rightarrow H_2$ between Hilbert spaces H_1 and H_2 , we denote its adjoint by $A^* : H_2 \rightarrow H_1$. When $H_1 = H_2$ and $\lambda \in \mathbb{R}$, we use the notation $A_\lambda := A + \lambda I$.

$\lesssim, \gtrsim, \asymp$ represent (in)equality up to constants. The hidden constants may depend on those introduced in the assumptions, but will not depend on data in any other way. Therefore, asymptotic claims such as the contraction results will hold uniformly, over a family of data distributions satisfying the assumptions.

2.2 Instrumental Variable Regression

Denote the treatment and response variables as \mathbf{x}, \mathbf{y} , the instrument as \mathbf{z} , and the true *structural function* of interest as f_0 . Consider the data generating process $\mathbf{y} = f_0(\mathbf{x}) + \mathbf{u}$, where we assume the unobserved residual \mathbf{u} satisfies $\mathbb{E}(\mathbf{u} \mid \mathbf{z}) = 0$, but may correlate with \mathbf{x} . Intuitively, the assumption requires that \mathbf{z} only influence \mathbf{y} through \mathbf{x} . Then f_0 satisfies

$$\mathbb{E}(\mathbf{y} - f_0(\mathbf{x}) \mid \mathbf{z}) = 0 \quad \text{a.s. } [P(dz)], \quad (1)$$

where P denotes the data distribution. This *conditional moment restriction* (CMR) formulation is the standard definition in literature (e.g., Newey and Powell, 2003; Kato, 2013), and is used in the recent work on machine learning models for IV. It connects to GMM as (1) can be viewed as a continuum of generalized moment constraints.

Note that (1) does not place any structural constraint on the conditional distribution $p(\mathbf{x} \mid \mathbf{z})$, such as additive noise; hence, it does not require full knowledge of the data generating process. Also, as discussed in, e.g., Hartford et al. (2017), the setup can also be extended to incorporate observed confounders \mathbf{v} , by including \mathbf{v} in both \mathbf{x} and \mathbf{z} .

IV regression can also be viewed as solving a linear *inverse problem*: introduce the conditional expectation operator $E : L_2(P(dx)) \rightarrow L_2(P(dz)), f \mapsto \mathbb{E}(f(\mathbf{x}) \mid \mathbf{z} = \cdot)$, and define $b(z) := \mathbb{E}(\mathbf{y} \mid \mathbf{z} = z)$. Then (1) can be written as

$$Ef_0 = b.$$

Although IV is more difficult than standard inverse problems, due to the need to estimate E from data, it is often helpful to draw parallels from the inverse problem literature.

2.3 Dual/Minimax Formulation of IV

Let \mathcal{H}, \mathcal{I} be normed function spaces on \mathcal{X}, \mathcal{Z} , respectively. The inverse problem view motivates the use of the following objective

$$\min_{f \in \mathcal{H}} \mathcal{L}(f) := d_n^2(\hat{E}_n f - \hat{b}) + \bar{\lambda} \Omega(f), \quad (2)$$

where $\hat{E}_n : \mathcal{H} \rightarrow \mathcal{I}$ is an empirical approximation to the restriction of E on \mathcal{H} , \hat{b} is an estimator of $b = Ef_0$, $\{d_n\}$ is a sequence of suitable (semi-)norm on \mathcal{I} , and $\Omega : \mathcal{H} \rightarrow \mathbb{R}$ is a regularization term. We restrict our attention to \hat{E}_n which solves a ridge-regularized least square regression problem

$$\hat{E}_n(f) := \arg \min_{g \in \mathcal{I}} \frac{1}{n} \sum_{j=1}^n (f(x_j) - g(z_j))^2 + \bar{\nu} \|g\|_{\mathcal{I}}^2 \quad (3)$$

and define \hat{b} as solving a similar problem as above, with $f(x_j)$ replaced by y_j . Consider setting $\Omega(f) := \frac{1}{2} \|f\|_{\mathcal{H}}^2$ and $d_n^2(g) := \frac{1}{n} \sum_{j=1}^n g(z_j)^2 + \bar{\nu} \|g\|_{\mathcal{I}}^2$. Appealing to the Fenchel duality identity $\frac{1}{2} u^2 = \sup_{v \in \mathbb{R}} (uv - \frac{1}{2} v^2)$, and rearranging terms, we arrive at the dual/minimax objective for IV regression (Muandet et al., 2020; Bennett and Kallus, 2020; Liao et al., 2020; Dikkala et al., 2020; Dai et al., 2016):

$$\min_{f \in \mathcal{H}} \mathcal{L}(f) \equiv \min_{f \in \mathcal{H}} \max_{g \in \mathcal{I}} \frac{1}{n} \sum_{j=1}^n \left((f(x_j) - y_j)g(z_j) - \frac{g(z_j)^2}{2} \right) - \frac{\bar{\nu}}{2} \|g\|_{\mathcal{I}}^2 + \frac{\bar{\lambda}}{2} \|f\|_{\mathcal{H}}^2. \quad (4)$$

The formulation (4) is appealing for two reasons. From the computational aspect, it circumvents the need to directly compute \hat{E}_n , an operator between the typically infinite-dimensional spaces \mathcal{H} and \mathcal{I} , and can be solved efficiently with stochastic gradient descent-ascent (SGDA) if the function spaces can be approximated with parametric models. Its particular choice of d_n also simplifies theoretical analysis and leads to tighter error rates (Dikkala et al., 2020). As we shall see below, both of the above advantages for point estimators carry to our quasi-Bayesian setting.

2.4 Kernelized Dual IV

In this work, we are primarily interested in the case where \mathcal{H} is a reproducing kernel Hilbert spaces (RKHS), although in Section 6 we discuss heuristic application to DNNs. The choice of \mathcal{I} is more flexible, but a major example is when it is another RKHS. In this scenario, we derive an alternative closed-form expression for $\mathcal{L}(f)$.

Let k_x and k_z denote the reproducing kernels of \mathcal{H} and \mathcal{I} , respectively.¹ Define the evaluation operator $S_z : \mathcal{I} \rightarrow \mathbb{R}^n, g \mapsto (g(z_1), \dots, g(z_n))$, and $S_x : \mathcal{H} \rightarrow \mathbb{R}^n$ similarly. Let $\hat{C}_{zz} := \frac{1}{n} S_z^* S_z, \hat{C}_{zx} := \frac{1}{n} S_z^* S_x$ be the empirical kernel (cross-)covariance operators. Using the Woodbury identity, we can verify that $\hat{E}_n = \hat{C}_{zz, \bar{\nu}}^{-1} \hat{C}_{zx}$ matches the definition (3) (recall $\hat{C}_{zz, \bar{\nu}} = \hat{C}_{zz} + \bar{\nu} I$), and \hat{b} admits a similar expression. Then

$$\begin{aligned} \mathcal{L}(f) &= \frac{1}{2} \left\| \hat{C}_{zz, \bar{\nu}}^{-1/2} \left(\hat{C}_{zx} f - \frac{S_z^* Y}{n} \right) \right\|_{\mathcal{I}}^2 + \frac{\bar{\lambda}}{2} \|f\|_{\mathcal{H}}^2 \\ &= \bar{\lambda} \left(\frac{1}{2} (f(X) - Y)^\top ((n\bar{\lambda})^{-1} L) (f(X) - Y) + \frac{1}{2} \|f\|_{\mathcal{H}}^2 \right), \end{aligned} \quad (5)$$

where $L = \frac{1}{n} S_z \hat{C}_{zz, \bar{\nu}}^{-1} S_z^*$ is a linear map from \mathbb{R}^n to \mathbb{R}^n , and thus can be identified with a matrix. Similar derivations appear in previous work (Singh et al., 2019; Muandet et al., 2020, e.g.). (5) will be used to derive a closed-form expression of the quasi-posterior.

3. Quasi-Bayesian Analysis of Dual IV

For any point estimator minimizing the general objective (2), we can conduct quasi-Bayesian analysis by specifying a prior $\Pi(df)$ for f and computing the *quasi-posterior*, defined through the following Radon-Nikodym derivative with respect to the prior:

$$\frac{d\Pi(\cdot \mid \mathcal{D}^{(n)})}{d\Pi}(f) \propto \exp\left(-\frac{n}{\lambda} d_n^2(\hat{E}_n f - \hat{b})\right), \quad (6)$$

where $\lambda := n\bar{\lambda}$ is the scaled regularization coefficient. The connection between the quasi-posterior and the point estimator can be seen from the following variational characterization (Zhang, 2006):

$$\Pi(\cdot \mid \mathcal{D}^{(n)}) = \arg \min_{\Psi} \mathbb{E}_{f \sim \Psi} [\lambda^{-1} n d_n^2(\hat{E}_n f - \hat{b})] + \text{KL}(\Psi \parallel \Pi), \quad (7)$$

showing that the quasi-posterior trades off between the properly scaled *evidence* (the log *quasi-likelihood*) $\frac{n}{\lambda} d_n^2(\hat{E}_n f - \hat{b})$, which characterizes the estimated violation of the GMM constraint (1), and our *prior belief* $\Pi(df)$.

As discussed in Section 2, this work focuses on the dual/minimax formulation (4) which is an instance of (2), and we employ a RKHS regularizer for f . Thus, our quasi-posterior is defined by choosing Π as the standard Gaussian process prior $\Pi := \mathcal{GP}(0, k_x)$, and instantiating (6) with $d_n(\hat{E}_n f - \hat{b})$ defined as

$$d_n^2(\hat{E}_n f - \hat{b}) := \max_{g \in \mathcal{I}} \frac{1}{n} \sum_{j=1}^n \left((f(x_j) - y_j) g(z_j) - \frac{g(z_j)^2}{2} \right) - \frac{\bar{\nu}}{2} \|g\|_{\mathcal{I}}^2. \quad (8)$$

1. In the following, we will abuse notation and use k to refer to both kernels, whenever the denotation is clear.

We now continue the kernelized IV discussion in Section 2.4, and derive the closed-form expression for its quasi-posterior. Observe that in (5), the first term is equivalent to the log density of the multivariate normal distribution $\mathcal{N}(Y \mid f(X), \lambda L^{-1})$, as a function(al) of f and Y .² Hence, (5) can be viewed as the objective of a kernel ridge regression (KRR) problem with a data-dependent noise covariance λL^{-1} . To derive the closed-form expression, we can recall the connection between KRR and Gaussian process regression (GPR; see Kanagawa et al., 2018) and consider the fictitious data generating process

$$f \sim \mathcal{GP}(0, k), \quad p_{\text{fic}}(Y \mid f, X, Z) := \mathcal{N}(Y \mid f(X), \lambda L^{-1}), \quad (9)$$

since its conditional distribution $p_{\text{fic}}(df \mid Y)$ will coincide with (6) (Stuart, 2010, Chapter 6). See Remark 1 below for further discussion.

In the probability space of this fictitious data generating process, for any finite set of test inputs x_* , we have

$$p_{\text{fic}}(f(x_*), Y \mid X, Z) \sim \mathcal{N}\left(0, \begin{bmatrix} K_{**} & K_{*x} \\ K_{x*} & K_{xx} + \lambda L^{-1} \end{bmatrix}\right),$$

where $K_{(\cdot)}$ denote the corresponding Gram matrices with subscript $*$ denoting x_* and x denoting X (so, e.g., $K_{*x} := k(x_*, X)$). Thus, by the Gaussian conditioning formula, the marginal posterior equals

$$\Pi(f(x_*) \mid \mathcal{D}^{(n)}) = p_{\text{fic}}(f(x_*) \mid Y) = \mathcal{N}(m, S), \quad (10)$$

$$\text{where } m := K_{*x}(\lambda I + LK_{xx})^{-1}LY, \quad (11)$$

$$S := K_{**} - K_{*x}L(\lambda I + K_{xx}L)^{-1}K_{x*}, \quad (12)$$

$$L = K_{zz}(K_{zz} + \nu I)^{-1}. \quad (13)$$

In the above $K_{zz} := k(Z, Z)$ denotes the Gram matrix, $\nu := n\bar{\nu}$, and (13) follows by applying the Woodbury identity to the definition of L in Section 2.

Remark 1 (Interpretation of (9), Quasi-Bayes vs Bayes) *The fictitious data generating process (9) is merely introduced for computational convenience. As discussed in e.g., Florens and Simoni (2012), care should be taken in its interpretation. For example, one should not deduce from (9) that the quasi-posterior is only useful when $L^{1/2}(Y - f(X)) \sim \mathcal{N}(0, \lambda I)$ (or when whatever infinite-sample version of this statement holds).*

From a “subjective Bayesian” point of view, in quasi-Bayesian analyses we do not have a full “Bayesian belief” of the data generating process. One quick way to see the difference is to observe that, even though (x_i, y_i, z_i) are i.i.d. draws from the joint data distribution by assumption, $p_{\text{fic}}(y_i \mid f, X, Z)$ depends on all of Z by (13), instead of merely z_i as in a fully Bayesian model. This distinction arises because \hat{E}_n is estimated from data. Nonetheless, Florens and Simoni (2021) shows that the quasi-posterior can be obtained as a certain non-informative limit of a fully Bayesian posterior; but in the context of IV regression, construction of the latter appears unrealistic.

2. Here we assume the invertibility of L for brevity. Alternatively, observe that (5) defines a linear inverse problem with the finite-dimensional observation operator $f \mapsto \sqrt{L}f(X)$ and noise variance $\lambda^{-1}I$. Now we can follow (Stuart, 2010, Chapter 6) to derive the same quasi-posterior.

More generally, *quasi-Bayesian methods should be justified by the variational characterization (7), and analyses of their frequentist properties as in the following. We stress that none of the analyses below relies on Y being distributed as in (9).*

4. Asymptotic Analysis

In this section, we demonstrate that the quasi-posterior provides a useful notion of uncertainty, by establishing the following results:

1. Minimax optimal *contraction rate* (Theorem 3, Corollary 4), showing that the region of high posterior probability rapidly shrinks to the true function f_0 .
2. (Asymptotic near-)validity of the *credible balls* (Theorem 6), showing that the spread of the quasi-posterior is informative of the error of the posterior mean predictor.

These asymptotic results hold under L_2 and Sobolev norms, thus covering the recovery of both f_0 and its (higher-order) derivatives.

4.1 Assumptions in the Analysis

We first introduce our assumptions. As we discuss below, all assumptions come from previous work on nonparametric IV or Bayesian inverse problems. We will also provide an example where the assumptions hold in Example 1 below.

Assumption 1 defines the problem. Note we assume bounded residual for simplicity; for general subgaussian residuals, the contraction rate will change by a logarithm factor.

Assumption 1 *The observed data $\mathcal{D}^{(n)} := \{(x_i, y_i, z_i) : i \in [n]\}$ are n i.i.d. draws from the joint distribution $P(dx \times dy \times dz)$. The data distribution satisfies (1). The residual $y - f_0(\mathbf{x})$ is always bounded by B .*

Assumption 2 is standard. It is used to ensure that *Mercer's representation* exists and constitutes an orthonormal basis (ONB) of $L_2(P(dx))$: consider the integral operator $T : L_2(P(dx)) \rightarrow L_2(P(dx))$, $f \mapsto \int f(x)k(x, \cdot)P(dx)$. Under Assumption 2, by Steinwart and Scovel (2012, Lemma 2.3, 2.12, Theorem 3.1, Corollary 3.5), T has an eigendecomposition $\{(\lambda_i, \bar{\varphi}_i)\}$, which defines a Mercer's representation, and $\{\bar{\varphi}_i\}$ form an ONB.

Assumption 2 *(i) \mathcal{X} and \mathcal{Z} are Polish spaces. (ii) The kernel k_x is measurable, continuous, bounded and L_2 -universal (Sriperumbudur et al., 2011). (iii) $P(dx)$ has full support.*

Assumption 3 is taken from the literature on kernel ridge regression in the “hard learning” scenario (Fischer and Steinwart, 2020; Steinwart et al., 2009). Before introducing it, we need to introduce the notion of *power space*:

Definition 2 (Steinwart and Scovel, 2012, p. 384) *Let $\{(\lambda_j, \bar{\varphi}_j) : j \in \mathbb{N}\}$ defined as above. For $\alpha \in (0, 1]$, define the power space $[\mathcal{H}]^\alpha$ using the norm*

$$\|f\|_{[\mathcal{H}]^\alpha}^2 := \sum_{j=1}^{\infty} \lambda_j^{-\alpha} \langle f, \bar{\varphi}_j \rangle_2^2.$$

The inner product of $[\mathcal{H}]^\alpha$ is defined similarly; see Appendix A.2.1 for further discussion.

Now we introduce Assumption 3. Its part (i) specifies a polynomial eigendecay for \mathcal{H} , which is standard for *mildly ill-posed problems* (Cavalier, 2008). Part (ii) is the “embedding property” in Fischer and Steinwart (2020). It is used to address the mismatch of the regularity of the RKHS \mathcal{H} and that of prior samples (van der Vaart and van Zanten, 2011), which makes GPR fall into the “hard learning” scenario. For Matérn kernels, (ii) holds for all $b_{emb} > 1$ under mild conditions listed in Section 4.2.2.

As any RKHS \mathcal{H} can be continuously embedded into its power space $[\mathcal{H}]^\alpha$, for $\alpha < 1$, condition (ii) is weaker for larger b_{emb} . We merely require the existence of a b_{emb} , which can be arbitrarily close to b . $b_{emb} = b$ would be satisfied as long as f_0 is in an RKHS $\bar{\mathcal{H}}$ with a bounded kernel, since after that we can choose $\mathcal{H} := [\bar{\mathcal{H}}]^{\frac{b+1}{b}}$; see Lemma 10. Requiring the existence of $b_{emb} = b - \epsilon < b$ is only “infinitesimally stronger”, as it is satisfied if $\sup_{x \in \mathcal{X}} \sum_{i=1}^{\infty} i^{b-\epsilon} \bar{\varphi}_i^2(x) < \infty$ (Steinwart and Scovel, 2012, Theorem 5.3), whereas requiring $\bar{\mathcal{H}}$ to have a bounded kernel implies $\sup_{x \in \mathcal{X}} \sum_{i=1}^{\infty} i^b \bar{\varphi}_i^2(x) < \infty$.

Assumption 3 (i) $\lambda_j \asymp j^{-(b+1)}$ for some $b > 1$, and (ii) for some $b_{emb} < b$, the power space $[\mathcal{H}]^{b_{emb}/(b+1)}$ can be continuously embedded into $L_\infty(P(dx))$.

Assumption 4 requires f_0 to be well approximated in \mathcal{H} . The first two inequalities in (b) is equivalent to bounding an L_2 concentration function of f_0 , and is weaker than the sup-norm requirement in previous work on GPR (van der Vaart and van Zanten, 2008a, 2011). For the sup norm, we place the very basic requirement that approximation errors do not diverge.

(a) is a more intuitive condition and implies (b), as shown in Lemma 23. It requires $f_0 \in \bar{\mathcal{H}}$. The power space $\bar{\mathcal{H}}$ is larger than \mathcal{H} , but also has an RKHS structure; see Appendix A.2.1. It often has a clear interpretation: for example, when \mathcal{H} is a Sobolev space (e.g., a Matérn RKHS), $\bar{\mathcal{H}}$ will be a lower-order Sobolev space under mild conditions. (a) implies that our prior knowledge $f_0 \in \bar{\mathcal{H}}$ should be matched by using a more regular RKHS $\mathcal{H} \subset \bar{\mathcal{H}}$. This is a standard practice, and arises from the mismatch between the regularity of \mathcal{H} and that of GP prior samples (van der Vaart and van Zanten, 2011).

Note that throughout this work we only state assumptions in the rate-optimal cases. Suboptimal specifications lead to deteriorated rates, but consistency can still be possible. The conference version of this work (Wang et al., 2021) also established consistency under fewer assumptions.

Assumption 4 Define

$$\bar{\mathcal{H}} := [\mathcal{H}]^{\frac{b}{b+1}}.$$

We require that one of the following holds: (a) $f_0 \in \bar{\mathcal{H}}$, Or (b) For all $j \in \mathbb{N}$, there exists $f_j^\dagger \in \mathcal{H}$ such that

$$\|f_j^\dagger\|_{\mathcal{H}}^2 \lesssim j^{\frac{1}{b+1}}, \quad \|f_0 - f_j^\dagger\|_2^2 \lesssim j^{-\frac{b}{b+1}}, \quad \|f_0 - f_j^\dagger\|^2 \lesssim 1. \quad (14)$$

Assumption 5 restricts to the mildly ill-posed setting, thus matching Assumption 3 (i). The *severely ill-posed* setting is often treated separately; it should be matched by kernels with an exponential eigendecay.

Assumption 5 *The conditional expectation operator $E : L_2(P(dx)) \rightarrow L_2(P(dz))$ has singular values $\nu_j \asymp j^{-p}$, where $p \geq 0$ is a constant.*

Assumption 6 imposes the *link and reverse link conditions* on the orthonormal series $\{\bar{\varphi}_i\}$. Variants of these conditions appear in all previous work on optimal L_2 rate for non-parametric IV (e.g., Horowitz, 2012; Chen and Pouzo, 2012; Kato, 2013),³ and is considered relatively weak in Bayesian inverse problem (Agapiou et al., 2013; Knapik and Salomond, 2018). A stronger assumption, which is also common in the Bayesian literature (Knapik et al., 2011; Szabó et al., 2015), requires that $\{\bar{\varphi}_i\}$ diagonalize the operator E^*E .

Note that (RL) implies injectivity of E , which implies identification in $L_2(P(dx))$. Without assuming identifiability, it is still possible to derive suboptimal rates in the semi-norm $\|E(\cdot)\|_2$; see the conference version of this work.

Assumption 6 *Let $\bar{\varphi}_i$ be defined as above. For any $j \in \mathbb{N}$, denote by Proj_j the L_2 projection onto $\text{span}\{\bar{\varphi}_i : i \leq j\}$. Then we have, for all $f \in L_2(P(dx))$ and $j \in \mathbb{N}$,*

$$\|Ef\|_2^2 \gtrsim j^{-2p} \|\text{Proj}_j f\|_2^2, \quad (\text{RL})$$

$$\|Ef\|_2^2 \lesssim \sum_{j=1}^{\infty} j^{-2p} \langle f, \bar{\varphi}_j \rangle_2^2. \quad (\text{L})$$

Assumption 7 is used to control $\|\hat{E}_n f - Ef\|_2$, and subsequently the estimation error of the quasi-likelihood, for “typical” f sampled from the GP prior. We specify δ_n^2 so that under Assumptions 3 and 5, the estimation error can be optimal. This requirement of optimal error rate is intuitive and appears in all previous work with optimal rates.

Part (i) follows Dikkala et al. (2020) and controls the variance part of the error with local Rademacher complexity. It can be fulfilled by an entropy integral bound (Wainwright, 2019, Corollary 14.3); By standard entropy bounds (e.g., Giné and Nickl, 2021, Chapter 4), when \mathcal{I}_1 is contained in an L_2 -Sobolev or Hölder ball, (i) merely requires the L_2 estimation error (using the Sobolev or Hölder ball) be $O(\delta_n)$. Part (ii) controls the bias, and matches the assumption in most recent work (Muandet et al., 2020; Liao et al., 2020); we consider the restriction of E to $\bar{\mathcal{H}}$ instead of \mathcal{H} , as Assumption 4 matches the regularity of f_0 with $\bar{\mathcal{H}}$. (ii) can be relaxed to allow an L_2 approximation error of $O(\delta_n)$, which enables the use of e.g. Nyström approximation for \hat{E}_n ; see Appendix A.8.1.

Assumption 7 *Denote by \mathcal{I}_1 the unit norm ball of \mathcal{I} . Let δ_n be the critical radius of the local Rademacher complexity of \mathcal{I}_1 (Wainwright, 2019, Eqs. (14.4)). Then (i) functions in \mathcal{I}_1 are uniformly bounded, and $\delta_n^2 \lesssim n^{-\frac{b+2p}{b+2p+1}}$, and (ii) the restriction of E to $\bar{\mathcal{H}}$ has image contained in \mathcal{I} , and is bounded, i.e., $\|Ef\|_{\mathcal{I}} \lesssim \|f\|_{\bar{\mathcal{H}}}$ for all $f \in \bar{\mathcal{H}}$.*

We conclude this subsection with the following example, adapted from Horowitz (2011).

Example 1 *Let $\mathcal{X} = \mathcal{Z}$ be the circle $\mathbb{S}^1 = \mathbb{T}^1$, the joint distribution of X and Z be absolutely continuous w.r.t. the Hausdorff measure, and the corresponding density f_{XZ} be bounded*

3. While it does not appear in recent ML works on IV, they did not establish convergence rates for the recovery of nonparametric f_0 , and only treated Ef_0 . The rates for Ef_0 are also suboptimal; see Section 7.

on both sides. Let $\bar{\mathcal{H}}$ be in the Sobolev space $W^{b/2,2}(\mathbb{T}^1) = \{f : \sum_{i=1}^{\infty} \langle f, \bar{\varphi}_i \rangle_2^2 i^b < \infty\}$ where $\{\bar{\varphi}_i\}$ denotes the sinusoidal basis (Triebel, 1983; Strichartz, 1983). It then follows from Steinwart and Scovel (2012) that $\bar{\mathcal{H}}$ is an RKHS with the (bounded) kernel having the Mercer representation $\bar{k}_x(x, x') = \sum_{i=1}^{\infty} i^{-b} \bar{\varphi}_i(x) \bar{\varphi}_i(x')$.⁴ Suppose $f_0 \in \bar{\mathcal{H}}$, and define $\mathcal{H} := W^{(b+1)/2,2}, \mathcal{I} := W^{(b+2p)/2,2}$ which have similar RKHS structures. Then Assumptions 2, 3, 4 are satisfied. 7 (i) follows from the entropy bound for periodic Sobolev spaces (e.g., Corollary 4.3.38, Giné and Nickl, 2021). The remaining assumptions can be satisfied if we construct E so that its left and right singular vectors match the Mercer basis, as in Section 8.1. We refer to Chen and Reiss (2011, Section 6.1) for another example where the singular vectors do not have to match $\{\bar{\varphi}_i\}$.

The construction generalizes easily to higher dimensional toruses. As discussed above, the assumptions on the kernels can also be satisfied if we work with $[0, 1]^d$ as opposed to the torus \mathbb{T}^d , and use the corresponding Matérn kernels, but explicit construction of valid E is not as straightforward, since we no longer have $\mathbb{E}\bar{\varphi}_{i+1} \equiv 0$. Nonetheless, it is known that p is lower bounded by the differentiability of the joint density: if f_{XZ} has continuous mixed derivatives up to order r , we will have $p \geq r$ (Horowitz, 2011, p. 365).

4.2 Contraction Rates

4.2.1 L_2 CONTRACTION RATES

Theorem 3 below is our main result. (15) establishes an L_2 contraction rate of ϵ_n for the recovery of f_0 , and (16) is a contraction rate in the norm $\|E(\cdot)\|_2$.

Theorem 3 Fix $\lambda = 1, \bar{\nu} = C\delta_n^2$ where $C > 0$ is an universal constant determined by the assumptions. Under the assumptions in Section 4.1, there exists $M > 0$ such that for $\epsilon_n^2 = n^{-\frac{b}{b+2p+1}}$, we have

$$\lim_{n \rightarrow \infty} \mathbb{P}_{\mathcal{D}^{(n)}} \Pi \left(\{f : \|f - f_0\|_2 \geq M\epsilon_n\} \mid \mathcal{D}^{(n)} \right) = 0, \quad (15)$$

$$\lim_{n \rightarrow \infty} \mathbb{P}_{\mathcal{D}^{(n)}} \Pi \left(\{f : \|E(f - f_0)\|_2 \geq M\delta_n\} \mid \mathcal{D}^{(n)} \right) = 0. \quad (16)$$

In addition, if Assumption 1 is relaxed to allow general subgaussian residuals $\mathbf{y} - f_0(\mathbf{x})$, the above equations will hold with ϵ_n and δ_n multiplied by $\log n$.

The proof is deferred to Appendix A.4. It is based on the posterior contraction framework (Ghosal et al., 2000), and shares similarity with the analysis of Bayesian inverse problem under the link condition (Knapik and Salomond, 2018). While IV is also a linear inverse problem, it is more challenging as we need to estimate the “forward operator” E from data. Thus, contrary to Knapik and Salomond (2018), in which the rate for Ef can be established easily and the rate for f is derived from it, in our case (16) and (15) have to be proved simultaneously, since they require to control the same estimation error about E . For this purpose, we combine the argument in (Dikkala et al., 2020) with the interpolation space arguments in (Steinwart et al., 2009).

4. In fact \bar{k}_x is the Matérn kernel, and closed-form expressions are provided in Borovitskiy et al. (2020).

Under our assumptions, the L_2 rate ϵ_n is minimax optimal (Chen and Reiss, 2011, Corollary 1).⁵ The rate for Ef also matches the minimax rate for least square regression on the dataset $\{(y_i, z_i) : i \in [n]\}$, although its optimality is less clear due to the additionally observed X . The contraction rates also imply high-probability convergence rates for the posterior mean estimator, or L_2 rates (for f and Ef) if we truncate prediction with a large constant, as in e.g., Steinwart et al. (2009). We compare with previous work in Section 7.

Finally, observe that under Assumptions 3, 5, 7, our choice for the regularizer $\bar{\nu}$ is asymptotically optimal for the estimation of $\mathbb{E}(f(\mathbf{x}) \mid \mathbf{z})$, for functions f with the same regularity as the GP prior (e.g., $f \in \bar{\mathcal{H}}$). This suggests that this choice may be identified from data using an algorithm in previous work (see Singh et al., 2019, or our Appendix D.1).

4.2.2 SOBOLEV NORM CONTRACTION RATES

Suppose \mathcal{X} is a bounded open subset of \mathbb{R}^d with a smooth boundary, $P(dx)$ has Lebesgue density bounded on both sides, and \mathcal{H} is equivalent to a Sobolev space $W^{\frac{(b+1)d}{2}, 2}$ (e.g., when using the Matérn kernel).⁶ Then for all $b' \in (0, b+1)$, $[\mathcal{H}]^{\frac{b'}{b+1}}$ is norm-equivalent to the Sobolev space $W^{\frac{b'-d}{2}, 2}$; see Adams and Fournier (2003, Sections 7.33, 7.67); Fischer and Steinwart (2020, Section 4). Therefore, we can derive Sobolev norm rates by investigating the power space, for which we have the following:

Corollary 4 *Let all assumptions in Section 4.1 hold; in particular, for Assumption 4 let (a) hold. Set $\bar{\lambda}, \bar{\nu}$ as in Theorem 3. Then for some sufficiently large $M > 0$, we have, for all $0 \leq b' < b$ and $\epsilon_{b',n}^2 := n^{-\frac{b-b'}{b+2p+1}}$,*

$$\mathbb{P}_{\mathcal{D}^{(n)}}(\Pi(\{f : \|f - f_0\|_{[\mathcal{H}]^{\frac{b'}{b+1}}} \geq M\epsilon_{b',n}\} \mid \mathcal{D}^{(n)})) \rightarrow 0.$$

The proof is in Appendix A.5. In the above setting, the rate $\epsilon_{b',n}$ is optimal for estimating integer-order derivatives, i.e., when $bd/2 \in \mathbb{N}$ (Chen and Christensen, 2015, Theorem 2.4).

4.2.3 SIDE RESULT: IMPROVED RATE FOR GAUSSIAN PROCESS REGRESSION

Our proof technique can be applied to GPR for unconfounded regression, i.e., when $\mathbb{E}(\mathbf{y} - f_0(\mathbf{x}) \mid \mathbf{x}) = 0$. In this case, we improve the result in van der Vaart and van Zanten (2011) for Matérn priors, by relaxing their assumption of joint Hölder and Sobolev regularity to Sobolev regularity alone. More generally, our Assumption 4 relaxes their assumption (in the rate-optimal case), by requiring approximability in L_2 norm instead of sup norm. The relaxation makes it clear that the result is minimax optimal. We state the result in power space norms, thus covering both L_2 and Sobolev spaces:

Theorem 5 *Let \mathcal{H} satisfy Assumption 3, and $f_0 \in \bar{\mathcal{H}}$. Let $\Pi(df \mid \mathcal{D}^{(n)})$ be the Gaussian process posterior under a normal likelihood. Suppose the residual $\mathbf{e} := \mathbf{y} - f_0(\mathbf{x})$ is bounded*

5. (Chen and Reiss, 2011) allows for additional assumptions, and thus applies to our setting. Such additional assumptions are common in the analysis of concrete estimators, as opposed to establishing lower bounds.

6. The order $\frac{(b+1)d}{2}$ is determined by the eigendecay assumption; see also (Kanagawa et al., 2018).

by B and $\mathbb{E}(\mathbf{e} \mid \mathbf{x}) = 0$.⁷ Then for sufficiently large $M > 0$, we have, for all $b' \in [0, b)$ and $\epsilon_{b',n}^2 = n^{-\frac{b-b'}{b+1}}$,

$$\mathbb{P}_{\mathcal{D}^{(n)}} \Pi \left(\{f : \|f - f_0\|_{[\mathcal{H}]^{\frac{b'}{b+1}}} \geq M\epsilon_{b',n}\} \mid \mathcal{D}^{(n)} \right) \rightarrow 0.$$

The proof is made possible by a refined bound on the marginal likelihood; see Appendix A.7. Note that Yang et al. (2017) also establishes minimax rate under the same assumptions, but for a different prior scaled by a data-dependent factor. Our result for the unscaled prior appears new.

4.3 Frequentist Properties of the Credible Balls

We now study the frequentist validity of the quasi-Bayesian *credible balls*, $B(\hat{f}_n, \tilde{r}_n(\gamma, \cdot)) := \{f : \|f - \hat{f}_n\|_{(\cdot)} \leq \tilde{r}_n(\gamma, \cdot)\}$, where \hat{f}_n denotes the posterior mean function, (\cdot) denotes an arbitrary norm, $\gamma \in (0, 1)$ is the credibility level, and

$$\tilde{r}_n(\gamma, \cdot) := \inf \left\{ r_n(\mathcal{D}^{(n)}) : \forall \|f_0\|_{\mathcal{H}} \leq 1, \mathbb{P}_{\mathcal{D}^{(n)}} \left(\Pi(\|f - \hat{f}_n\|_{(\cdot)} \leq r_n(\mathcal{D}^{(n)}) \mid \mathcal{D}^{(n)}) \geq \gamma \right) = 1 \right\}$$

is its radius. We will compare $\tilde{r}_n(\gamma, \cdot)$ with the radius of the frequentist *confidence ball*

$$\hat{r}_n(\gamma, \cdot) := \inf \{r_n : \forall \|f_0\|_{\mathcal{H}} \leq 1, \mathbb{P}_{\mathcal{D}^{(n)}}(\|f_0 - \hat{f}_n\|_{(\cdot)} \leq r_n) \geq \gamma\}.$$

Note that \tilde{r}_n is a random variable determined by $\mathcal{D}^{(n)}$, since in its definition the inequality must hold with $\mathbb{P}_{\mathcal{D}^{(n)}}$ probability 1; in contrast, \hat{r}_n is deterministic because confidence balls can fail with probability $1 - \gamma$, which could account for failures in estimating \hat{E}_n .

We shall show that for the power space norms which include the L_2 norm, the radius of the credible balls will eventually have the correct order of magnitude. Formally, for any fixed $\gamma \in (0, 1)$, $\alpha = \frac{b'}{b+1} \in [0, \frac{b}{b+1})$,

$$\lim_{n \rightarrow \infty} \mathbb{P}_{\mathcal{D}^{(n)}}(\tilde{r}_n(\gamma, [\mathcal{H}]^\alpha) \asymp \hat{r}_n(\gamma, [\mathcal{H}]^\alpha)) = 1. \quad (17)$$

Similar results (for other problems) are provided in Knapik et al. (2011); Szabó et al. (2015); Rousseau and Szabo (2017). From a theoretical point of view, asymptotically valid confidence balls can then be constructed by inflating the radius of the credible ball, \tilde{r}_n , with a constant, or a slowly growing function of n (Rousseau and Szabo, 2017), although the inflation often appears unnecessary in practice. A more precise characterization (e.g., showing that $\frac{\tilde{r}_n(\gamma, \cdot)}{\hat{r}_n(\gamma, \cdot)} \approx 1$) is often difficult for general nonparametric models.

For the frequentist confidence ball, Corollary 4 implies $\|\hat{f}_n - f_0\|_{[\mathcal{H}]^\alpha} \leq M\epsilon_{b',n}$ with $\mathbb{P}_{\mathcal{D}^{(n)}}$ probability $\rightarrow 1$, and thus for any fixed γ , $\hat{r}_n(\gamma, [\mathcal{H}]^\alpha) \lesssim \epsilon_{b',n}$; on the other hand, the minimax lower bound implies that $\hat{r}_n(\gamma, [\mathcal{H}]^\alpha) \gtrsim \epsilon_{b',n}$. Thus

$$\hat{r}_n(\gamma, [\mathcal{H}]^\alpha) \asymp \epsilon_{b',n}.$$

7. As in the IV setting, we assume bounded noise for simplicity, and general subgaussian noise can be treated by inflating B (and thus the final rate) by a logarithm factor. We specify normal likelihood for the GP for simplicity. It is also a standard practice as it makes computation easy.

For the credible ball, Theorem 3 implies that for any fixed $\gamma < 1$, we have

$$\mathbb{P}_{\mathcal{D}^{(n)}}(\tilde{r}_n(\gamma, [\mathcal{H}]^\alpha) \leq M\epsilon_{b',n}) \rightarrow 1.$$

Therefore, to prove (17), it suffices to show that $\tilde{r}_n(\gamma, [\mathcal{H}]^\alpha) \gtrsim \epsilon_{b',n}$ with probability $\rightarrow 1$. We prove this using the strategy in Rousseau and Szabo (2017):

Theorem 6 *Under the conditions in Corollary 4, there exists $\rho > 0$ such that as $n \rightarrow \infty$,*

$$\mathbb{P}_{\mathcal{D}^{(n)}}(\Pi(\{\|f - \hat{f}_n\|_{[\mathcal{H}]^\alpha} \leq \rho\epsilon_{b',n}\} \mid \mathcal{D}^{(n)})) \rightarrow 0.$$

Consequently, (17) holds.

The proof is in Appendix A.6.

5. Discussion of the Non-asymptotic Behavior

The asymptotic analysis above relies on various assumptions on the interaction between the kernel and the data distribution. While they are standard in literature, they cannot account for potential misspecification. The analysis also focused on the recovery of the *full parameter* f , which does not provide optimal guarantees for the *evaluation of linear functionals* (e.g., evaluation functionals $f \mapsto f(x_0)$; see Knapik et al., 2011). In this section, we complement the results above, by providing some intuition on the non-asymptotic behavior of the closed-form quasi-posterior (10), without any of the assumptions introduced above.

Fix a bounded linear functional in \mathcal{H} with Riesz representer $k_* \in \mathcal{H}$, and consider the marginal posterior of $\langle k_*, f \rangle_{\mathcal{H}}$.⁸ Repeating the derivation in Section 3, we can see that $\Pi(\langle k_*, f \rangle_{\mathcal{H}} \mid \mathcal{D}^{(n)}) = \mathcal{N}(m, S)$, where m and S are defined as in Eqs (11)-(12), with K_{*X} replaced by $(S_x k_*)^\top$.⁹ Following their definitions, we can reformulate the equality as

$$\Pi(\langle k_*, f \rangle_{\mathcal{H}} \mid \mathcal{D}^{(n)}) = \mathcal{N}(m, S) = \mathcal{N}(\langle k_*, \hat{f}_n \rangle_{\mathcal{H}}, \langle k_*, \mathcal{C} k_* \rangle_{\mathcal{H}}),$$

where we can verify \hat{f}_n matches the posterior mean. The expression of \mathcal{C} can be found in Eq. (70).

To check if the quasi-posterior quantifies the uncertainty in the estimation of linear functional evaluations, it thus suffices to compare the error of the posterior mean predictor, $\langle k_*, \hat{f}_n - f_0 \rangle_{\mathcal{H}}^2$, with the marginal variance $\langle k_*, \mathcal{C} k_* \rangle_{\mathcal{H}}$. With some algebra (see Appendix B.1 for the proof), we can show that:

Proposition 7 *Let the data $\mathcal{D}^{(n)}$ be generated from an unconfounded data generating process: $y_i := f(x_i) + e_i$, where $\{e_i\}$ are i.i.d. random variables with zero mean and variance λ , and $e_i \perp \{x_i, z_i\}$. Then for any $k_* \in \mathcal{H}$ and any choice of (n, X, Z) , we have*

$$\langle k_*, \mathcal{C} k_* \rangle_{\mathcal{H}} = \sup_{\|f_0\|_{\mathcal{H}}=1} \mathbb{E}_{Y|X,Z} \langle k_*, \hat{f}_n - f_0 \rangle_{\mathcal{H}}^2 + \langle k_*, (\Delta \mathcal{C}) k_* \rangle_{\mathcal{H}} \quad (18)$$

$$= \mathbb{E}_{f \sim \mathcal{GP}(0, k_x)} \mathbb{E}_{Y|X,Z} \langle k_*, \hat{f}_n - f_0 \rangle_{\mathcal{H}}^2 + \langle k_*, (\Delta \mathcal{C}) k_* \rangle_{\mathcal{H}}, \quad (19)$$

where $\Delta \mathcal{C}$ is a non-negative operator defined in the proof.

8. While the posterior assigns zero mass on \mathcal{H} , it is known that the above marginal posterior is well-defined (van der Vaart and van Zanten, 2008b; Eldredge, 2016).

9. Observe that $(S_x k_*)^\top = (\langle k_*, k(x_1, \cdot) \rangle_{\mathcal{H}}, \dots, \langle k_*, k(x_n, \cdot) \rangle_{\mathcal{H}})$.

The above proposition is inspired by similar results for GPR (Kanagawa et al., 2018, Proposition 3.8; Srinivas et al., 2012). The first result (18) connects the marginal variance to the worst-case prediction error,¹⁰ but only applies to $f_0 \in \mathcal{H}$. This assumption is different from the optimal choice when recovering the full parameter, where we match the regularity of f_0 with the GP prior; see the discussion around Assumption 4 and the reference therein. However, this trade-off is well-known in literature (Knapik et al., 2011; Srinivas et al., 2012), and is not unique to (quasi-)Bayesian methods. Instead, it stems from the infinite dimensionality of the prior. While it can be avoided for sufficiently smooth functionals, evaluation functionals usually fall out of this category (Knapik et al., 2011).

Nonetheless, Eq. (19) shows that the marginal variance can be useful in the “full parameter regime”, by relating it to the average prediction error. This type of result also appears in the bandit literature (Srinivas et al., 2012). While there are caveats around its interpretation, e.g., sets of misspecified functions can have zero prior measure (Ghosal and Van der Vaart, 2017), it may explain the good coverage of credible intervals observed in practice.

The main limitation of Proposition 9 is that it only applies to the unconfounded case. In the general case, it does not constitute a complete and rigorous analysis, and only hopefully provides some intuition, by accounting for the approximation error within the model, as well as part of the estimation error due to the sampling of X and Z . We restrict to this setting so that the prediction error is available in closed form. Still, the additional term $\langle k_*, \Delta \mathcal{C} k_* \rangle_{\mathcal{H}}$ is non-negative and might compensate for some additional sources of error, see Appendix B.2 for an informal discussion. Also, the main appeal of the discussion in this subsection is that it does not place any assumption on the choice of the models (or hyperparameters); for example, it does not require \mathcal{I} to contain the image of E restricted on $\bar{\mathcal{H}}$. Therefore, it suggests that the quasi-Bayesian uncertainty may still reflect a nontrivial part of prediction error, even if the conditional expectation estimator is badly misspecified.

6. Approximate Inference via a Randomized Prior Trick

We now turn to approximate inference with parametric models, such as random feature models. While other approaches are also possible (e.g., using Nyström approximation), this approach has the advantage of being able to extend to wide NN models. We construct an algorithm by extending the “randomized prior” trick for GPR (Osband et al., 2018), to work with (quasi-)likelihoods with an optimization formulation as in (4).

6.1 Approximate Inference with Random Feature Approximation

We first consider approximate inference with random feature models. Introduce the random feature approximation $k_z(z, z') \approx \tilde{k}_{z,m}(z, z') := \frac{1}{m} \phi_{z,m}(z)^\top \phi_{z,m}(z')$, where $\phi_{z,m}$ takes value in \mathbb{R}^m . Then the map $\varphi \mapsto \frac{1}{\sqrt{m}} \varphi^\top \phi_{z,m}(\cdot) =: g(\cdot; \varphi)$ parameterizes an approximate RKHS $\tilde{\mathcal{L}}$; and for all $c > 0$, the random function $g(\cdot; \varphi)$, where $\varphi \sim \mathcal{N}(0, cI)$, is distributed as $\mathcal{GP}(0, c\tilde{k}_{z,m})$. The notations related to k_x are similar and thus omitted. Now we can state the objective:

10. It applies to the worst-case f_0 . We can remove the average over $P(Y \mid X, Z)$ with the Markov inequality; this is less problematic as Y is finite dimensional.

Proposition 8 *Let $\phi_0 \sim \mathcal{N}(0, \lambda\nu^{-1}I)$, $\theta_0 \sim \mathcal{N}(0, I)$, $\tilde{y}_i \sim \mathcal{N}(y_i, \lambda)$. Then the optima θ^* of*

$$\min_{\theta \in \mathbb{R}^m} \max_{\phi \in \mathbb{R}^m} \sum_{i=1}^n \left((f(x_i; \theta) - \tilde{y}_i)g(z_i; \phi) - \frac{g(z_i; \phi)^2}{2} \right) - \frac{\nu}{2} \|\phi - \phi_0\|_2^2 + \frac{\lambda}{2} \|\theta - \theta_0\|_2^2 \quad (20)$$

parameterizes a random function which follows the quasi-posterior distribution (10), where the kernels are replaced by the random feature approximations.

The proof is in Appendix C.1. Given the above proposition, we can sample from the random feature-approximated quasi-posterior by solving (20) with stochastic GDA; the approximation errors will be analyzed in the following.

The objective (20) is closely related to (4): Appendix C.1.1 shows it is equivalent to

$$\min_{f \in \mathcal{H}} \max_{g \in \tilde{\mathcal{I}}} \sum_{i=1}^n \left((f(x_i) - \tilde{y}_i)g(z_i) - \frac{g(z_i)^2}{2} \right) - \frac{\nu}{2} \|g - g_0\|_{\tilde{\mathcal{I}}}^2 + \frac{\lambda}{2} \|f - f_0\|_{\mathcal{H}}^2, \quad (20')$$

which differs from (4) only in the regularizers: instead of regularizing the norm of f and g , it encourages the functions to stay close to randomly sampled “anchors” (Pearce et al., 2020). A similar relation is also observed in Osband et al. (2018), which transforms GPR to the optimization problem $\min_{f \in \mathcal{H}} \sum_{i=1}^n (f(x_i) - \tilde{y}_i)^2 + \lambda \|f - f_0\|_2^2$. In both cases, the resultant approximate inference algorithm has the same time complexity as ensemble training for point estimation.

6.2 Application to Neural Network Models

While the algorithm can be directly applied to NN models as in Osband et al. (2018), we follow He et al. (2020) and modify the objective, to account for the difference between the neural tangent kernel (NTK; Jacot et al., 2018) of a wide NN architecture and the GP kernel of the corresponding infinite-width Bayesian neural network (Neal, 2012). Concretely, we modify (20) as

$$\min_{\theta} \max_{\phi} \sum_{i=1}^n \left((\tilde{f}_{\theta}(x_i) - \tilde{y}_i)\tilde{g}_{\phi}(z_i) - \frac{\tilde{g}_{\phi}(z_i)^2}{2} \right) - \frac{\nu}{2} \|\phi - \phi_0\|_2^2 + \frac{\lambda}{2} \|\theta - \theta_0\|_2^2, \quad (21)$$

$$\text{where } \tilde{g}_{\phi}(z) := g(z; \phi) - g(z; \phi_0) + \tilde{g}_0(z), \quad \tilde{g}_0(z) := \sqrt{\frac{\lambda}{\nu}} \langle \bar{\phi}_0, \frac{\partial g}{\partial \phi} \big|_{\phi=\phi_0}(z) \rangle,$$

and ϕ_0 denotes the initial value of ϕ , $\bar{\phi}_0 \sim \mathcal{N}(0, I)$ is a set of randomly initialized NN parameters independent of ϕ_0 ; and \tilde{f}_{θ} is defined similarly.

We only give a formal justification for the modification, under the assumption¹¹ that the NNs remain in the kernel regime throughout training, so that $g(z; \phi) - g(z; \phi_0) = \langle \phi - \phi_0, \frac{\partial g(z)}{\partial \phi} \big|_{\phi_0} \rangle_2$ (Lee et al., 2019). Thus, for the purpose of analyzing $g(\cdot; \phi) - g(\cdot; \phi_0)$, we can view g as a random feature model with the parameterization $\phi \mapsto \langle \phi, \frac{\partial g(z)}{\partial \phi} \big|_{\phi_0} \rangle_2$. By the argument in Appendix C.1.1, we can show that the weight regularizer $\|\phi - \phi_0\|_2$ is equivalent to $\|g(\cdot; \phi) - g(\cdot; \phi_0)\|_{\tilde{\mathcal{I}}} = \|\tilde{g}_{\phi} - \tilde{g}_0\|_{\tilde{\mathcal{I}}}$, where $\tilde{\mathcal{I}}$ is determined by the NTK $k_{g,ntk}(z, z') :=$

11. See Liao et al. (2020) for an analysis of the linearization error in a similar setting to ours.

$\langle \frac{\partial g(z)}{\partial \phi} |_{\phi_0}, \frac{\partial g(z')}{\partial \phi} |_{\phi_0} \rangle_2$. Similar arguments can be made for \tilde{f}_θ and \tilde{f}_0 . Consequently, (21) is equivalent to an instance of (20') with $\tilde{\mathcal{H}}, \tilde{\mathcal{I}}$ defined by the NTKs.

Implementation details, including hyperparameter selection, are discussed in Appendix D.

6.3 Convergence Analysis

We provide a quick analysis of the inference algorithm, by showing that for any fixed set of test points x_* , SGDA can approximate the marginal distribution $\Pi(f(x_*) | \mathcal{D}^{(n)})$ arbitrarily well given a sufficient computational budget. This implies that the approximate posterior can be good enough for prediction purposes.

We consider standard random feature models as in Section 6.1. We place several mild assumptions listed in Appendix C.2; they are satisfied by common approximations such as the random Fourier features (Rahimi et al., 2007). The SGDA algorithm is described in detail in Appendix C.4. Now we have the following result, which will be proved in Appendix C.5:

Proposition 9 *Fix the training data $\mathcal{D}^{(n)}$ and hyperparameters $\lambda, \nu > 0$. Then there exist a sequence of choices of m and SGDA step-size schemes, such that for any $l \in \mathbb{N}$, we have*

$$\sup_{x^* \in \mathcal{X}^l} \max(\|\hat{\mu}_m - \mu_m\|_2, \|\hat{S}_m - S_m\|_F) \xrightarrow{p} 0.$$

In the above, $\hat{\mu}_m, \hat{S}_m$ denote the mean and covariance of the approximate marginal posterior for $f(x_*)$, μ, S correspond to the true posterior, $\|\cdot\|_F$ denotes the Frobenius norm, and the convergence in probability is defined with respect to the sampling of random feature basis.

7. Related Work

7.1 Quasi-Bayesian Analysis and IV

Quasi-Bayesian analysis for general GMM problems was first developed in (Zellner, 1995; Kim, 2002; Chernozhukov and Hong, 2003), which studied parametric models. The use of the quasi-posterior is motivated from the maximum entropy principle, based on which similar ideas have been developed in the machine learning literature (e.g., Jaakkola et al., 1999; Dudík et al., 2007; Zhu and Xing, 2009).

For nonparametric IV, Liao and Jiang (2011) established consistency results. Kato (2013) established minimax contraction rates, as well as a Bernstein von-Mises type theorem for smooth functionals, in a setting where the GP prior and \hat{E}_n are modeled with truncated series models. Our theoretical results allow for more flexibility, as we can either adapt the results to work with truncated series models, or use the orthonormal series to construct our kernels. Our result also avoids their requirement that both series models must have the same number of basis. Florens and Simoni (2012) derived a quasi-posterior using general GP priors and Nadaraya-Watson smoothing for \hat{E}_n . They proved an L_2 rate under the different assumption of *source condition*, which requires f_0 to be in the range of $(E^*E)^\beta$. It is unclear if their rate is optimal, but it can only utilize limited smoothness of f_0 ($\beta \leq 2$), and their rate cannot be better than $O(n^{-1/4})$. This is different from our result, where ϵ_n approaches $O(n^{-1/2})$ as $b \rightarrow \infty$. On the empirical side, no numerical study was presented in Liao et al. (2020); Kato (2013), whereas Florens and Simoni (2012) only provided numerical studies for the mean estimator.

7.2 Kernelized IV

Our quasi-Bayesian procedure builds upon the kernelized IV¹² methods (Singh et al., 2019; Muandet et al., 2020) and the dual formulation of IV regression (Bennett et al., 2019; Muandet et al., 2020; Liao et al., 2020; Dikkala et al., 2020). The estimation objective (4) is from (Dikkala et al., 2020); the formulations in (Muandet et al., 2020; Singh et al., 2019) are slightly different. All of these works have only provided nonparametric error rates in the norm $\|E(\cdot)\|_2$. Among them, Dikkala et al. (2020) provide the best rate of $\max\{n^{-\frac{b}{2(b+1)}}, \delta_n\}$. As discussed in Section 4.1, the optimal choice of \mathcal{I} should yield $\delta_n \asymp n^{-\frac{b+2p}{2(b+2p+1)}}$, so the rate in (Dikkala et al., 2020) can only be optimal if $p = 0$. Unfortunately, the $p = 0$ case is uninteresting as it excludes the challenge of ill-posedness. We complete the theoretical picture, by improving the $\|E(\cdot)\|_2$ rate to δ_n , and providing the first minimax rates for L_2 and Sobolev norms.

7.3 Classical Nonparametric Methods

In the setting of Chen and Reiss (2011), minimax rates have been established for classical methods. It is thus interesting to compare the kernelized IV method with them. Smoothing-based methods also attain optimal L_2 rates (Horowitz, 2012), but it is unclear if optimal recovery of f_0 and its derivatives can be achieved simultaneously, i.e., with the same hyperparameter (Chen and Christensen, 2015). This is different from our estimator, and the sieve estimators (Chen and Christensen, 2015), where optimal L_2 and Sobolev rates are achieved by the same choice of hyperparameter.

Sieve estimators (Newey and Powell, 2003; Blundell et al., 2007; Chen and Pouzo, 2012) model f_0 , and possibly also \hat{E}_n , with orthogonal series. The kernelized IV estimator is thus similar to a sieve estimator using the Mercer bases $\{\bar{\varphi}_j\}$. One difference is that we include the term $\bar{\nu}\|g\|_{\mathcal{I}}^2 = \bar{\nu}\|\hat{E}_n(f - f_0)\|_{\mathcal{I}}^2$ in the objective for f_0 . More importantly, the classical sieve estimators require the basis functions to be determined *a priori*, as their construction involves explicit truncation of the series model. This prevents adaptation to regularity properties of the data distribution. In our case, however, the series $\{\bar{\varphi}_j\}$ is implicitly determined by the data distribution, and thus allows for some adaptation to the regularity properties. E.g., if \mathbf{x} or \mathbf{z} is supported on a low-dimensional subspace of \mathbb{R}^d , the kernelized estimators automatically “construct” the bases according to that subspace. On the other hand, the classical estimators have been studied extensively, with a wider range of theoretical results established in literature (e.g., recovery of nonlinear functional evaluations, validity of specification tests).

7.4 Other Related Work

Other recent work applying ML methods to nonlinear IV include (Hartford et al., 2017; Zhang et al., 2020; Xu et al., 2020). They focused on estimation methodology as opposed to uncertainty quantification, and did not provide results for nonparametric convergence.¹³ Among them, Zhang et al. (2020) also discussed a connection between a GP (quasi-)posterior

12. Note that Zhang et al. (2020) also studied RKHS methods for IV, with a different use of the kernel.

13. Bennett and Kallus (2020) also analyzed parametric models. While Liao et al. (2020) provided an L_2 error bound, it is in the *infinite sample* setting, and describes the dependency on computational budgets.

and a leave-one-out validation statistic, but the GP is used for hyperparameter selection and its frequentist properties (e.g., contraction rates, validity of credible sets) remain unclear. For the closely related problem of causal effect estimation with proxy variables (Miao et al., 2018), which also has a CMR structure, Mastouri et al. (2021) establish an RKHS-norm rate for the structural function, under source conditions similar to Florens and Simoni (2012). Their rate is also lower bounded by $O(n^{-1/4})$, although note the stronger norm.

Alternative approaches to uncertainty quantification include Bayesian inference and bootstrap. We have discussed the limitations of Bayesian IV in Section 1. Here we note that while the closely related *control function approach* is not less general than CMR (Horowitz, 2011), standard Bayesian approaches additionally assume independent errors, making their assumption strictly stronger than CMR. Nonetheless, the quasi-Bayesian approach is connected to standard Bayesian modeling; Florens and Simoni (2021) shows that for unconditional moment restriction (MR) problems, the quasi-posterior can be recovered as a non-informative limit of a sequence of standard Bayesian posteriors, where a prior on the joint data distribution becomes diffuse. However, computation of the Bayesian posteriors therein is expensive, and generalization to nonparametric CMR problems appears nontrivial.

For the classical sieve estimator, bootstrap enjoys a variety of theoretical guarantees, but non-asymptotic justification is relatively lacking. The quasi-Bayesian approach could be more appealing in this aspect, due to results such as (7) and (18), although there is a similar lack of complete non-asymptotic analysis. The need for bootstrap alternatives is also justified through analyses in the parametric regime, where nonparametric bootstrap inference for the classical two stage least squares (2SLS) method is known to be unreliable when instrument strength is weak (Moreira et al., 2004; Flores-Lagunes, 2007; Davidson and Mackinnon, 2010).

8. Synthetic Experiments

In this section we evaluate the proposed method. We first study the asymptotic and pre-asymptotic behavior of the quasi-posterior in a controlled setting; then, we compare its predictive performance with various baselines.¹⁴

8.1 Experiment in a Controlled Setting

We first experiment in a setting where all assumptions hold with known parameters, and the models are correctly specified. This setting allows us to validate the asymptotic theory, but also provides a first glimpse at the pre-asymptotic behaviors.

The setup follows Example 1: we set \mathcal{H}, \mathcal{I} as the Sobolev spaces on \mathbb{T}^1 with the appropriate orders. Points on \mathbb{T}^1 are represented with a coordinate in $[0, 1]$. We sample f_0 from the GP prior, and define the joint density f_{XZ} as

$$f_{XZ}(x, z) := 1 + \sum_{j=2}^{\infty} 0.2 \cdot (j-1)^{-p} \bar{\varphi}_j(x) \bar{\varphi}_j(z),$$

where $\bar{\varphi}_j(x) := \cos(2\pi[j/2](x) + (j - [j/2])\pi)$ constitutes the Mercer basis of k_x and k_z . It can be verified that f_{XZ} is a valid density, and the marginal distributions of x and z are

14. Code for the experiments can be found at <https://github.com/meta-inf/qbdiv>.

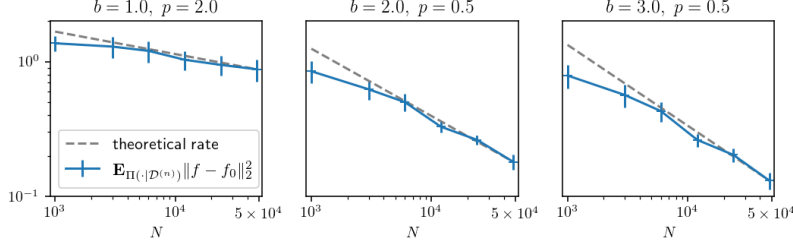


Figure 1: Average L_2 error $\mathbb{E}_{\Pi(df|\mathcal{D}(n))}\|f - f_0\|_2^2$ vs the theoretical rate $O(\epsilon_n^2)$, for varying choices of (b, p) . Error bars indicate standard deviations estimated from 10 independent trials. The theoretical rate is scaled for clarity.

both the uniform distribution. We introduce confounding by generating the observations as

$$(z_i, u_i) \stackrel{i.i.d.}{\sim} \mathcal{U}[0, 1], \quad x_i := F_{x|z=z_i}^{-1}(u_i), \quad y_i = f_0(x_i) + \tilde{\sigma} \cos(2\pi u_i),$$

where $F_{x|z=z_0}^{-1}(\cdot)$ denotes the inverse CDF transform of the conditional distribution, and $\tilde{\sigma}$ is chosen so that $\text{Var}[u] = \sigma^2$. We approximate f_{XZ} and the kernels by truncating the series sum at $J = 400$, and further approximate f_{XZ} with linear interpolation on a 500×500 grid. We vary $(b, p) \in \{(2, 0.5), (3, 0.5), (1, 2)\}$, and $n \in \{1, 3, 6, 12, 24, 48\} \times 10^3$. The hyperparameters are set as $\lambda := \sigma^2 = 1$, $\bar{\nu} := 20(\frac{n}{1000})^{-\frac{b+2p}{b+2p+1}}$.

When n is large, we find the closed-form expressions (11)-(13) to be numerically unstable, likely due to the need to invert the $n \times n$ matrix $\lambda I + LK_{xx}$, whose eigenvalues may have a decay rate of $\lambda_i \asymp i^{-b-2p+1}$. We find Nyström approximation for L to be an effective workaround; see Appendix D.3 for a description of the algorithm. As shown Appendix A.8.1, the approximation will not affect the asymptotic rates when the number of inducing points reaches $O(n^{\frac{1}{b+2p+1}})$. We use 50 inducing points.

Figure 1 plots the expected L_2 error averaged over the posterior measure, $\int \|f - f_0\|_2^2 \Pi(df | \mathcal{D}(n))$, which upper bounds the squared contraction rate. As we can see, the observations validate the asymptotic theory.

Figure 2 visualizes the uncertainty estimates from the quasi-posterior. We can see that the quasi-posterior has reliable coverage in the pre-asymptotic regime. Note that we plot credible intervals for illustrative purposes only; recall our theory does not provide guarantee

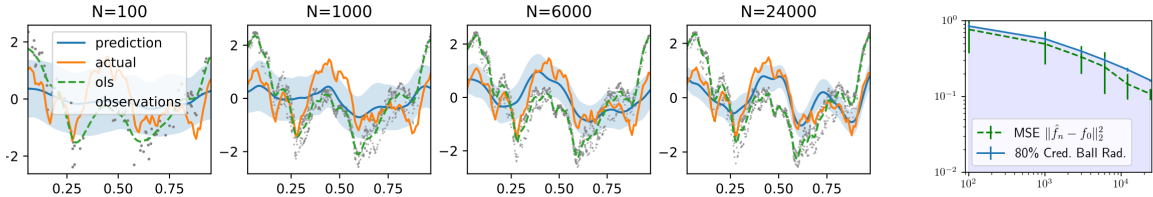


Figure 2: Visualizations of the quasi-posterior, with $b = 2, p = 0.5$. Left: sample runs; shade indicates pointwise 80% credible interval, dots indicate training data, and “ols” denotes a (biased) KRR estimator for reference. Right: comparison of the radius of the 80% L_2 credible ball with the error of the posterior mean estimator.

for its coverage, even though the discussion in Section 5 suggests that good coverage may be achieved, for “benign” f_0 as in this setting.

Additional results are provided in Appendix D.4. In brief, we find that

1. Across all settings, the posterior spread $\int \|f - \hat{f}_n\|_2^2 \Pi(df \mid \mathcal{D}^{(n)})$ is approximately as large as the L_2 error of the point estimator, $\|\hat{f}_n - f_0\|_2^2$; this further suggests the L_2 credible balls are consistently informative and reliable, as its radius is an upper percentile of the random variable $\|f - \hat{f}_n\|_2$.
2. The L_2 contraction rate for the derivative f' (i.e., the $W^{1,2}$ rate for f) also appears consistent with the theory, although convergence to the asymptotic regime is slower.

8.2 Predictive Performance: 1D Simulation

We now evaluate the predictive performance of the proposed method on a variety of 1D synthetic datasets adapted from Lewis and Syrgkanis (2018). We modify their setup to incorporate a nonlinear first stage, in a way similar to Singh et al. (2019); Chen and Christensen (2015):

$$z := \text{sigmoid}(w), \quad x := \text{sigmoid}\left(\frac{\alpha w + (1 - \alpha)u'}{\sqrt{\alpha^2 + (1 - \alpha)^2}}\right), \quad y_i \sim \mathcal{N}(f_0(2x - 1) + 2u, 0.1),$$

where (u, u') are normal random variables with unit variance and a correlation of 0.5, $w \sim \mathcal{N}(0, 1)$ is independent of (u, u') , α is a parameter controlling the instrument strength, and f_0 is constructed from the **sine**, **step**, **abs** or a **linear** function. We choose $N \in \{200, 1000\}$ and $\alpha \in \{0.05, 0.5\}$.

Our baselines include BayesIV (Wiesenfarth et al., 2014), a flexible Bayesian model based on B-splines and Dirichlet process mixture; we also include bootstrap on 2SLS with ridge regularization, either applied directly to the input features (Linear), on their polynomial expansion (Poly), or on the same kernelized models (KIV) as ours.¹⁵ Hyperparameter for the kernelized IV methods are selected by cross validation based on the observable first-stage and second-stage losses as in previous work (Singh et al., 2019; Muandet et al., 2020); see Appendix D.1. For kernels, we choose the RBF and Matérn kernels, but defer the results for Matérn kernels to appendix for brevity. See Appendix D.5 for the detailed setup.

We report MSE, coverage rate of 95% credible intervals (CIs) and CI width in this experiment. While there is no theoretical guarantee for CI coverage, our discussion in Section 5 and the last experiment suggest reliable coverage can be possible in practice. Besides, it can be much easier to provide pointwise CIs with good coverage *when averaged* over the input space, than to provide reliable CIs for the worst-case input; the former is still useful in many applications.

Normalized MSE and CI coverage on the **sine** datasets are plotted in Figure 3. We report results on 20 independently generated datasets. As we can see, quasi-Bayesian inference provides the most reliable uncertainty estimates, especially in the $\alpha = 0.05$ setting. The CIs are typically conservative (the larger variation when $\alpha = 0.05$ is partly due to the

15. We do not compare with Florens and Simoni (2012) since their source code is unavailable.

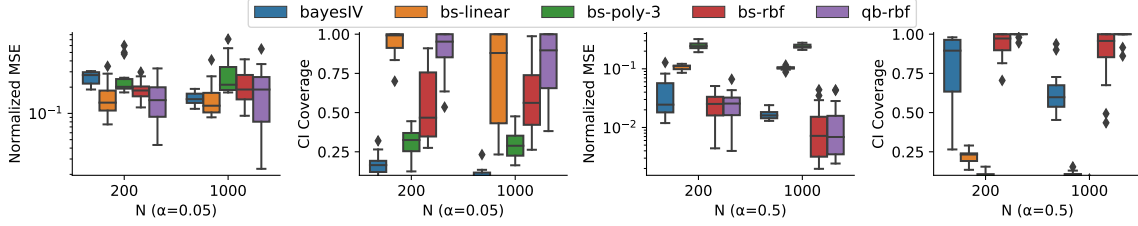


Figure 3: Test MSE and CI coverage on the `sine` dataset. The left two plots correspond to $\alpha = 0.05$, while the right two correspond to $\alpha = 0.5$. `bs` denotes bootstrap, `qb` denotes quasi-Bayesian. We report the average CI coverage over the data distribution.

instability of the hyperparameter selection procedure). However, as shown in Appendix D.6, it is still informative, and properly reflects the sample size and instrument strength.

Full results on all datasets, visualizations and additional experiments are deferred to Appendix D.6. As a summary, (i) on the `abs` and `linear` datasets where the kernel choices are more justified, the results are qualitatively similar to the `sin` dataset. Moreover, the over-smoothed RBF kernel appears to have similar coverage comparing with the optimal kernel, and follow a similar contraction rate. (ii) All methods have deteriorated performance on the `step` dataset, although the quasi-posterior still provides more coverage. (iii) Uncertainty estimates produced by the approximate inference algorithm are similar to that from the exact quasi-posterior. The first two findings above may be attributed to the fact that all three datasets, especially `abs` and `linear`, are “regular” in most regions of the input space.

8.3 Predictive Performance: Airline Demand

Finally, we consider the more challenging demand simulation proposed in Hartford et al. (2017). The dataset simulates a scenario where we need to predict the demand of airline tickets y , as a function of the price x , and two observed confounders: customer type s , and time of year t . The data generating process is

$$x := (z + 3)\psi(t) + 25 + u', \quad y := f_0(x, t, s) + u, \quad f_0(x, t, s) := 100 + (10 + x) \cdot s \cdot \psi(t) - 2x$$

where (u, u') are standard normal variables with correlation ρ , $z \sim \mathcal{N}(0, 1)$ is independent of (u, u') , and ψ is a nonlinear function whose shape is given in Figure 4. The variable s either varies across $\{0, \dots, 6\}$ (the lower-dimensional setting), or is observed as an MNIST image representing the corresponding digit; the latter case emulates the real-world scenario where only high-dimensional surrogates of the true confounder is observed. We only report results for $\rho = 0.5$, noting that results using other choices of ρ have been similar. We use $n \in \{10^3, 10^4\}$ for the lower-dimensional setting, and use $n = 5 \times 10^4$ for the image setting.

We compare our method with bootstrap on the same model, BayesIV, and bootstrap on linear or polynomial models. Performance of other point estimators on this dataset has been reported in Singh et al. (2019); Muandet et al. (2020); Xu et al. (2020), compared with which our method is generally competitive. We implement the dual IV model using both an RBF kernel and DNN models. See Appendix D.7 for details.

We report the test MSE and CI coverage for $N = 1000$ in Table 1, and visualize all approximate quasi-posteriors for the NN models in Figure 4. As we can see, when imple-

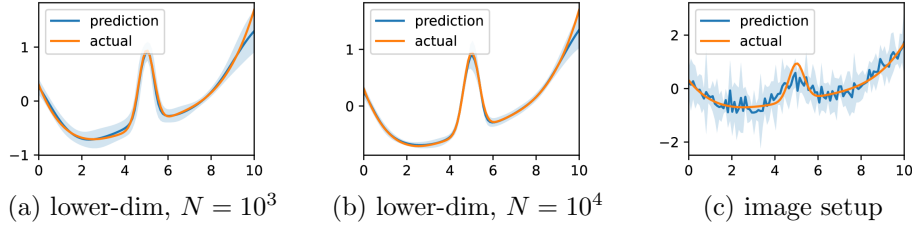


Figure 4: Approximate quasi-posteriors in the demand simulation. We plot a cross-section by fixing s, x to their mean values and varying t . Shade indicates pointwise 95% credible interval.

mented with DNNs, our method produces uncertainty estimates with excellent coverage, which also correctly reflects the information available in the dataset: the CI is wider when N is smaller, or in the high-dimensional experiment where estimation is harder. Bootstrap has a noticeably worse performance when $N = 1000$. Still, it performs well in the (arguably less interesting) large-sample setting, with a CI coverage similar to our method; see Appendix D.8. This is because on this dataset, the total instrument strength is stronger due to the presence of observed confounders, and the NN model is a good fit. Consequently, the asymptotic behavior of bootstrap can be observed when N is large.

Both methods have poorer performances when we switch to the RBF kernel, although the quasi-posterior is still more reliable. Given the discussion in Section 5, we hypothesize that both \mathcal{I} and \mathcal{H} are misspecified in this case, which seems reasonable as the magnitude of f_0 varies greatly as s, x varies (not shown in Figure 4). In this case the quasi-posterior could only reflect the uncertainty within the model. These results show that NN models can be advantageous, which our inference algorithm supports.

The other baselines perform poorly due to their inflexibility; in particular, note that BayesIV uses additive models for both stages (e.g., $f(x, t, s) = f_1(x) + f_2(t) + f_3(s)$) which do not approximate this data generating process well. Full results and visualizations are deferred to Appendix D.8.

Method	BS-Linear	BS-Poly	BayesIV	BS-RBF	QB-RBF	BS-NN	QB-NN
NMSE	.37 ± .01	.31 ± .06	.28 ± .04	.17 ± .01	.17 ± .01	.06 ± .03	.04 ± .00
CI Cvg.	.09 ± .01	.15 ± .03	.27 ± .06	.45 ± .02	.77 ± .02	.86 ± .02	.94 ± .01
CI Wid.	.09 ± .01	.16 ± .04	.08 ± .06	.18 ± .02	.37 ± .01	.14 ± .01	.26 ± .04

Table 1: Test normalized MSE, average CI coverage and CI width on the demand dataset, with $N = 1000$, averaged over 20 trials.

9. Conclusion

In this work we present a quasi-Bayesian procedure for kernelized and NN-based IV models. We analyze the frequentist behavior of the proposed quasi-posterior, and derive an approximate inference algorithm that can be applied to neural network models. Empirical evaluations show that the proposed method scales to large and high-dimensional datasets,

and can be advantageous in the finite-sample setting, or when the instrument strength is weak.

Appendix A. Proof of the Asymptotic Results

This section contains all proofs for the asymptotic results in Section 4.

A.1 Additional Notations and Conventions

We recall the following notations. $\bar{\mathcal{H}}, \bar{\varphi}_i, \lambda_i$ are defined in Section 4.1. $\mathcal{D}^{(n)} = (\mathbf{X}, \mathbf{Y}, \mathbf{Z})$ denotes the observed data. Π denotes the GP prior, and $\Pi_n(df \mid \mathcal{D}^{(n)})$ denotes the quasi-posterior.

Denote by $\|\cdot\|_n$ the L_2 norm w.r.t. the empirical data distribution. For any $x \in \mathbb{R}$, define $[x]$ as the maximum integer not exceeding x . Define

$$\ell_n(f) := \|\hat{E}(f(\mathbf{x}) - \mathbf{y})\|_n^2 + \bar{\nu} \|\hat{E}(f(\mathbf{x}) - \mathbf{y})\|_{\mathcal{I}}^2,$$

so that $\frac{d\Pi_n(\cdot \mid \mathcal{D}^{(n)})}{d\Pi}(f) \propto \exp(-\frac{n}{2\lambda} \ell_n(f))$. We overload notations and define the constant B as

$$B := \max\{\|f_0\|, \|Ef_0\|_{\mathcal{I}}, \max |\mathbf{y} - f_0(\mathbf{x})|\}$$

where the last term denotes the bound of the random variable (which is bounded by Assumption 1.)

Throughout this section, the denotation of the constants introduced in the proof (C_1, \dots, c_1, \dots) may change by each line. The constants hidden in $\lesssim, \gtrsim, \asymp$ will be uniformly bounded, across all possible data distributions and model choices satisfying the assumptions in Section 4.1. Therefore, the asymptotic results will hold uniformly across these distributions.

A.2 Background and Auxiliary Results

A.2.1 BACKGROUND ON POWER SPACES

Recall the definition of power space in Definition 2.

Lemma 10 *Let \mathcal{H} satisfy Assumption 2 and 3. Then, for any $\alpha \in \left[\frac{b_{emb}}{b+1}, \infty\right) \supset \left[\frac{b}{b+1}, \infty\right)$, we have (i) the function space \mathcal{H}^α given by*

$$\mathcal{H}^\alpha = \left\{ \sum_{j=1}^{\infty} a_j \bar{\varphi}_j : \sum_{j=1}^{\infty} \lambda_j^{-\alpha} a_j^2 < \infty \right\} \quad (22)$$

(and the norm defined accordingly) is an RKHS, with the reproducing kernel

$$k_\alpha(x, x') := \sum_{j=1}^{\infty} \lambda_j^\alpha \bar{\varphi}_j(x) \bar{\varphi}_j(x').$$

(ii) k_α is bounded. (iii) The RKHS \mathcal{H}^α satisfies Assumption 3 (ii), with the exponent $\frac{b_{emb}}{b+1}$ replaced by $\frac{b_{emb}}{\alpha(b+1)}$.

Proof (i)-(ii): As the kernel k_x is bounded, by Steinwart and Scovel (2012, Lemma 2.3, Definition 4.1, Proposition 4.2), (i) will be true if for all $x \in \mathcal{X}$, we have

$$\sum_{j=1}^{\infty} \lambda_j^\alpha \bar{\varphi}_j^2(x) < \infty.$$

This will also imply (ii). The above display will hold if we can apply Theorem 5.5 in Steinwart (2019),¹⁶ which requires that their Assumptions K and CK hold, and that $[\mathcal{H}]^\alpha$ can be continuously embedded into $L_\infty(P(dx))$. Under our Assumption 2, most requirements in Assumptions K and CK can be verified immediately from the discussions therein, with the only possible exception of separability of $L_2(P(dx))$, which follows because $\{\bar{\varphi}_i\}$ form an ONB; see the discussion around Assumption 2. The embedding property follows from our Assumption 3 (ii), and the fact that the property is stronger when α is smaller (see e.g., Fischer and Steinwart, 2020, Eq. (7)).

Now, (iii) follows from the assumption, and the observation that $[\mathcal{H}^\alpha]^{\alpha'} = [\mathcal{H}]^{\alpha\alpha'}$. \blacksquare

Observe that the \mathcal{H}^α -norm defined in (22) coincides with the definition of the $[\mathcal{H}]^\alpha$ norm. Technically the two spaces are different, since $[\mathcal{H}]^\alpha$ is a normed subspace of $L_2(P(dx))$ and consists of equivalence classes of functions. But the above lemma shows that when α is sufficiently large, \mathcal{H}^α can be continuously embedded into $[\mathcal{H}]^\alpha$. Conversely, each equivalence class in $[\mathcal{H}]^\alpha$ consists of functions with the same generalized Fourier coefficients $\{\langle f, \bar{\varphi}_i \rangle_2\}$ (and thus the same $[\mathcal{H}]^\alpha$ -norm), and corresponds to a unique function in \mathcal{H}^α with an equal \mathcal{H}^α -norm. Therefore, we do not distinguish between them in the text, and refer to $\bar{\mathcal{H}} = [\mathcal{H}]^{\frac{b}{b+1}}$ as having an RKHS structure.

Lemma 11 *Let \mathcal{H} satisfy Assumptions 2, 3. Then for any $f \in \mathcal{H}$, we have*

$$\begin{aligned} \|f\|_{\bar{\mathcal{H}}}^2 &\lesssim (\|f\|_{\mathcal{H}}^2)^{\frac{b}{b+1}} (\|f\|_2^2)^{\frac{1}{b+1}}, \\ \|f\|^2 &\lesssim (\|f\|_{\mathcal{H}}^2)^{\frac{b}{b+1}} (\|f\|_2^2)^{\frac{1}{b+1}}. \end{aligned} \quad (23)$$

Proof For the $\bar{\mathcal{H}}$ norm, observe that for the Mercer basis $\{\bar{\varphi}_i\}$, $(\|\bar{\varphi}_i\|_{\bar{\mathcal{H}}}^2)^{\frac{b}{b+1}} \asymp (i^{b+1})^{\frac{b}{b+1}} \asymp \|\bar{\varphi}_i\|_{\mathcal{H}}^2$, and thus $\|\bar{\varphi}_i\|_{\bar{\mathcal{H}}}^2 \lesssim (\|\bar{\varphi}_i\|_{\mathcal{H}}^2)^{\frac{b}{b+1}} (\|\bar{\varphi}_i\|_2^2)^{\frac{1}{b+1}}$, and for general f the claim follows from Hölder's inequality $\langle \cdot, \cdot \rangle \leq \|\cdot\|_{\frac{b+1}{b}} \|\cdot\|_{b+1}$.

(23) now follows from the $\bar{\mathcal{H}}$ norm bound, and Lemma 10 (ii). \blacksquare

A.2.2 PRELIMINARY RESULTS FOR THE GP PRIOR

In the posterior contraction framework, we need to construct a sequence of parameter subsets $\{\Theta_m\}$, *sieves* (Ghosal et al., 2000), such that their prior mass approaches 1 sufficiently fast, yet the complexity of Θ_m grows slowly. See van der Vaart and van Zanten (2008a, 2011) for a standard construction for GP priors. In this subsection, we construct Θ_m by adapting the result in Steinwart (2019). (26) is the main result.

16. While their theorem only state the result for $\alpha \leq 1$, the $\alpha > 1$ case follows since $\sum_j \lambda_j^\alpha \bar{\varphi}_j^2(x) \leq \sum_j \lambda_j \bar{\varphi}_j^2(x)$. The definitions in Steinwart and Scovel (2012) allow for any $\alpha > 0$.

Lemma 12 *Let $W \sim \Pi$ be a Gaussian process with covariance kernel k_x , where k_x satisfies our Assumptions 2, 3 (i). Then for all $b' \in [0, b)$, $m > 0$, we have, for some constant $C_1, C_2, C_3 > 0$ and $\tau_m'^2 = m^{-\frac{b-b'}{b+1}}$,*

$$\Pi(\{\|W\|_{[\mathcal{H}]^{\frac{b'}{b+1}}}^2 \leq \tau_m'^2\}) \geq e^{-C_1 m^{\frac{1}{b+1}}}, \quad (24)$$

$$\Pi(\Theta'_m) := \Pi(\{W = f_h + f_e : \|f_h\|_{\mathcal{H}} \leq C_2 m^{\frac{1}{2(b+1)}}, \|f_e\|_{[\mathcal{H}]^{\frac{b'}{b+1}}} \leq \tau_m'\}) \geq 1 - e^{-C_3 m^{\frac{1}{b+1}}}. \quad (25)$$

Proof By Steinwart (2019, Corollary 4.9), we have $-\log \Pi(\{\|W\|_{[\mathcal{H}]^{\frac{b'}{b+1}}}^2 \leq \epsilon^2\}) \asymp \epsilon^{-\frac{2}{b-b'}}$ which implies (24). (25) then follows from Borell's inequality (see, e.g. Ghosal and Van der Vaart, 2017, Proposition 11.17). \blacksquare

Corollary 13 *Let Π, W, k_x be defined as in the above lemma. Then (i) for any $b' \in [0, b)$, there exists constant $C_{b'}, C'_{b'} > 0$ such that for all $m \in \mathbb{N}$ and $\tau_m := m^{-\frac{b/2}{b+1}}$,*

$$\begin{aligned} \Pi(\Theta_{m,b'}) &:= \Pi(\{f = f_h + f_e : \|f_h\|_{\mathcal{H}}^2 \leq C_{b'} m \tau_m^2, \|f_e\|_2^2 \leq C_{b'} \tau_m^2, \|f_e\|_{[\mathcal{H}]^{\frac{b'}{b+1}}}^2 \leq C_{b'} m^{-\frac{b-b'}{b+1}}\}) \\ &\geq 1 - e^{-C'_{b'} m \tau_m^2}. \end{aligned}$$

(ii) *If additionally Assumption 3 (ii) holds, there will exist constants $C, C' > 0$ such that for all $m \in \mathbb{N}$,*

$$\Pi(\Theta_m) := \Pi(\{f = f_h + f_e : \|f_h\|_{\mathcal{H}}^2 \leq C m \tau_m^2, \|f_e\|_2^2 \leq C \tau_m^2, \|f_e\|^2 \leq C\}) \geq 1 - e^{-C' m \tau_m^2}. \quad (26)$$

Proof (i): We claim that Θ'_m defined in the above lemma satisfies the definition of $\Theta_{m,b'}$. To see this, for any $f \in \Theta'_m$ let f_h, f_e be defined as in (25). Let

$$j := \lceil m^{\frac{1}{b+1}} \rceil, \quad \tilde{f}_h := f_h + \text{Proj}_j f_e, \quad \tilde{f}_e := \text{Proj}_{>j} f_e.$$

Then by Lemma 15 below applied to $[\tilde{\mathcal{H}}] := [\mathcal{H}]^{\frac{b'}{b+1}}$, we have

$$\max\{\|\text{Proj}_j f_e\|_{[\tilde{\mathcal{H}}]}, \|\tilde{f}_e\|_{[\tilde{\mathcal{H}}]}\} \leq \|f_e\|_{[\tilde{\mathcal{H}}]}, \quad \|\tilde{f}_e\|_2^2 \leq \|f_e\|_{[\tilde{\mathcal{H}}]}^2 j^{-b'} \lesssim m^{-\frac{b-b'}{b+1}} m^{-\frac{b'}{b+1}} = m^{-\frac{b}{b+1}}.$$

And

$$\begin{aligned} \|\text{Proj}_j f_e\|_{\mathcal{H}}^2 &\asymp \sum_{i=1}^j \langle f_e, \bar{\varphi}_i \rangle_2^2 i^{b-b'+b'+1} \leq j^{b-b'+1} \sum_{i=1}^j \langle f_e, \bar{\varphi}_i \rangle_2^2 i^{b'} = j^{b-b'+1} \|\text{Proj}_j f_e\|_{[\tilde{\mathcal{H}}]}^2 \\ &\leq m^{\frac{b-b'+1}{b+1}} \|f_e\|_{[\tilde{\mathcal{H}}]}^2 = m^{\frac{1}{b+1}}, \end{aligned}$$

Thus, $\|\tilde{f}_h\|_{\mathcal{H}}^2 \leq 2(\|f_h\|_{\mathcal{H}}^2 + \|\text{Proj}_j f_e\|_{\mathcal{H}}^2) \lesssim m^{\frac{1}{b+1}}$. (ii): Pick any $b' \in (b_{emb}, b)$. Then $[\tilde{\mathcal{H}}]$ is equivalent to an RKHS with a bounded reproducing kernel (Lemma 10), so $\|f_e\| \lesssim \|f_e\|_{[\tilde{\mathcal{H}}]} \lesssim$

1, and $\Theta_{m,b'}$ defined above satisfies (26). ■

Finally, the $b' = 0$ case of Lemma 12 will be used separately, so we list it below:

Corollary 14 *Let \tilde{k} satisfy Assumptions 2, and the eigenvalues of its integral operator decay at $\tilde{\lambda}_i \asymp i^{-\tilde{b}}$. Let \tilde{W} be a GP with covariance kernel \tilde{k} . Then there exists $C_1, C_2 > 0$ such that for all $m > 0$, we have*

$$\Pi\left(\left\{\|\tilde{W}\|_2^2 \leq C_1 m^{-\frac{\tilde{b}}{\tilde{b}+1}}\right\}\right) \geq e^{-C_2 m^{\frac{1}{\tilde{b}+1}}}.$$

A.2.3 TECHNICAL LEMMAS

It is helpful to keep the following quantities in mind: the squared critical radius $\delta_n^2 \asymp n^{-\frac{b+2p}{b+2p+1}}$, for our GP prior $\tau_n^2 = n^{-\frac{b}{b+1}}$, and for $m = \lfloor n^{\frac{b+1}{b+2p+1}} \rfloor$, we have $\tau_m^2 \asymp n^{-\frac{b}{b+2p+1}} \asymp \epsilon_n^2$, $m\tau_m^2 = n^{\frac{1}{b+2p+1}} \asymp n\delta_n^2$.

In the following lemma, recall the definitions

$$\text{Proj}_j f := \sum_{i=1}^j \langle f, \bar{\varphi}_i \rangle_2 \bar{\varphi}_i, \text{Proj}_{>j} f := f - \text{Proj}_j f.$$

And by Lemma 10, $\{\bar{\varphi}_i\}$ also corresponds to the Mercer representation of k_α when $\alpha \geq \frac{b_{emb}}{b+1}$.

Lemma 15 *Let \mathcal{H} satisfy Assumptions 2, 3, $[\tilde{\mathcal{H}}] = [\mathcal{H}]^\alpha$ for some $\alpha \in [0, 1]$, $\tilde{b} := (b+1)\alpha$, and $\tilde{\lambda}_i := \lambda_i^\alpha \asymp i^{-\tilde{b}}$. Then for any $f \in [\tilde{\mathcal{H}}]$, we have (i) $\text{Proj}_j f = \sum_{i=1}^j \langle f, \sqrt{\tilde{\lambda}_i} \bar{\varphi}_i \rangle_{[\tilde{\mathcal{H}}]} \sqrt{\tilde{\lambda}_i} \bar{\varphi}_i$, (ii) $\text{Proj}_j \cdot$ equals the orthogonal projection onto the subspace spanned by $\{\tilde{\lambda}_i^{1/2} \bar{\varphi}_i : i \leq j\}$, the top j scaled orthonormal basis functions of $[\tilde{\mathcal{H}}]$, (iii)*

$$\|\text{Proj}_{>j} f\|_2 \lesssim \|f\|_{[\tilde{\mathcal{H}}]} j^{-\frac{\tilde{b}}{2}}.$$

Proof (i) follows by the definition of the $[\mathcal{H}]^\alpha$ norm, and the fact that $\{\bar{\varphi}_i\}$ is an ONB in $L_2(P(dx))$. (ii) follows from (i) and the fact that $\{\sqrt{\tilde{\lambda}_i} \bar{\varphi}_i\}$ forms an ONB in $[\tilde{\mathcal{H}}]$. Now (iii) follows because

$$\|f - \text{Proj}_j f\|_2^2 = \sum_{i \geq j} \langle f, \sqrt{\tilde{\lambda}_i} \bar{\varphi}_i \rangle_{[\tilde{\mathcal{H}}]}^2 \|\sqrt{\tilde{\lambda}_i} \bar{\varphi}_i\|_2^2 \leq \|\text{Proj}_{>j} f\|_{[\tilde{\mathcal{H}}]}^2 \cdot \tilde{\lambda}_j \|\bar{\varphi}_j\|_2^2 \lesssim \|f\|_{[\tilde{\mathcal{H}}]}^2 j^{-\tilde{b}}.$$
■

The following lemma applies to, e.g., $f \in \Theta_m$, and $f - f_0$ by Assumption 4.

Lemma 16 *For $m = \lfloor n^{\frac{b+1}{b+2p+1}} \rfloor$ and any $f = \tilde{f}_h + \tilde{f}_e$ where*

$$\|\tilde{f}_h\|_{\mathcal{H}}^2 \leq m\tau_m^2, \quad \|\tilde{f}_e\|_2^2 \leq \tau_m^2, \quad \|\tilde{f}_e\| \leq 1, \quad (27)$$

we have the decomposition $f = f_h + f_e$ where

$$\|f_h\|_{\mathcal{H}}^2 \lesssim m\tau_m^2, \quad \|f_e\|_2^2 \leq \tau_m^2, \quad \|Ef_e\|_2^2 \lesssim \delta_n^2, \quad \|f_e\| \lesssim 1, \quad (28)$$

where the constants in \lesssim only depend on k_x and the constant in Assumption 6.

Proof As $\tilde{f}_e \in L_2(P(dx))$, for any finite j , $\text{Proj}_j \tilde{f}_e$ is well-defined and in \mathcal{H} , and for $m' = \lceil m^{\frac{1}{b+1}} \rceil \asymp n^{\frac{1}{b+2p+1}}$, we have

$$\|\text{Proj}_{m'} \tilde{f}_e\|_{\mathcal{H}}^2 = \sum_{i=1}^{m'} \lambda_i^{-1} |\langle \tilde{f}_e, \tilde{\varphi}_i \rangle_2|^2 \leq \lambda_{m'}^{-1} \|\tilde{f}_e\|_2^2 \lesssim (m')^{b+1} \tau_m^2 \asymp m \tau_m^2,$$

where the last inequality follows from $b > 1$. Thus, for

$$f_h := \tilde{f}_h + \text{Proj}_{m'} \tilde{f}_e, \quad f_e := \tilde{f}_e - \text{Proj}_{m'} \tilde{f}_e,$$

we have $\|f_h\|_{\mathcal{H}}^2 \lesssim m \tau_m^2$ as advertised. By definition of Proj_j we have

$$\|f_e\|_2 \leq \|\tilde{f}_e\|_2 \leq \tau_m, \quad \|Ef_e\|_2^2 \stackrel{(a)}{\lesssim} (m')^{-2p} \|f_e\|_2^2 \lesssim n^{-\frac{2p}{b+2p+1}} n^{-\frac{b}{b+2p+1}} = n^{-\frac{b+2p}{b+2p+1}}.$$

where (a) follows from Assumption 6. Finally, by (23),

$$\|f_e\| \leq \|\tilde{f}_e\| + \|\text{Proj}_{m'} \tilde{f}_e\| \lesssim \|\text{Proj}_{m'} \tilde{f}_e\|_{\mathcal{H}}^{\frac{b}{b+1}} \|\text{Proj}_{m'} \tilde{f}_e\|_2^{\frac{1}{b+1}} \lesssim m^{\frac{1/2}{b+1} \cdot \frac{b}{b+1}} \cdot m^{\frac{-b/2}{b+1} \cdot \frac{1}{b+1}} = 1. \quad \blacksquare$$

We provide the following form of Bernstein's inequality (e.g., Steinwart and Christmann, 2008, Theorem 6.12) for reference.

Lemma 17 *Let the random variable \mathbf{l} be bounded by B_l and have variance $\text{Var}(\mathbf{l}) \leq \sigma_l^2$. Let l_1, \dots, l_n be i.i.d. copies of \mathbf{l} . Then for all $\eta > 0$,*

$$\mathbb{P} \left(\left| \frac{1}{n} \sum_{i=1}^n l_i - \mathbb{E} \mathbf{l} \right| \geq \left(\sqrt{2\eta} + \frac{2\eta}{3} \right) \frac{\sigma_l^2}{B_l} \right) \leq \exp \left(-\frac{n\sigma_l^2}{B_l^2} \cdot \eta \right).$$

A.3 Marginal Quasi-Likelihood Bound

We now bound the marginal likelihood, which will appear as a denominator in the decomposition of the posterior mass. We proceed in three steps:

1. Lemma 18 creates a “small-ellipsoid” subset of the parameter space, on which $\|E(f - f_0)\|_2$ can be controlled. $\|E(f - f_0)\|_2$ connects to the log quasi-likelihood ℓ_n , so this is similar to the (shifted) small-ball subset $\{\|W - f_0\| \leq \tau_n\}$ in the analysis of GPR.
2. Lemma 19 refines the subset so that other quantities needed in Step 3 are bounded.
3. Proposition 20 further refines the subset in a data-dependent way. On the final subset we can control the estimation error of ℓ_n , and thus the marginal likelihood can be lower bounded.

Lemma 18 *Let $W \sim \Pi$ be a draw from the prior Gaussian measure, $f_h \in \mathcal{H}$ be an arbitrary function. Then*

$$\log \Pi(\{\|E(W - f_h)\|_2^2 \leq n^{-\frac{b+2p}{b+2p+1}}\}) \lesssim -n^{\frac{1}{b+2p+1}}, \quad (29)$$

Moreover, if we have $\|f_h\|_{\mathcal{H}}^2 \lesssim n^{\frac{1}{b+2p+1}}$, then

$$\log \Pi(\{\|E(W - f_h)\|_2^2 \leq n^{-\frac{b+2p}{b+2p+1}}, \|W - f_h\|_2^2 \leq n^{-\frac{b}{b+2p+1}}\}) \gtrsim -n^{\frac{1}{b+2p+1}}. \quad (30)$$

Proof Let $W = \sum_{i=1}^{\infty} \lambda_i^{1/2} \epsilon_i \varphi_i$ be the Karhunen-Loève expansion, where (λ_i, φ_i) are the Mercer decomposition of k_x . We restrict ourselves to the probability-1 event that the series converge in $L_2(P(dx))$ (Steinwart, 2019, Theorem 3.1). For any $l \in \mathbb{N}$, by Assumption 6 (L) we have

$$\begin{aligned} \|E\text{Proj}_l(W - f_h)\|_2^2 &\leq C_2 \sum_{j=1}^l j^{-2p} \langle W - f_h, \bar{\varphi}_j \rangle_2^2 = C_2 \sum_{j=1}^l j^{-2p} (\epsilon_j \lambda_j^{1/2} - \langle f_h, \bar{\varphi}_j \rangle_2)^2, \\ \|E\text{Proj}_{>l}(W - f_h)\|_2^2 &\leq C_2 (l+1)^{-2p} \|\text{Proj}_{>l}(W - f_h)\|_2^2, \\ \|E(W - f_h)\|_2 &\leq \|E\text{Proj}_l(W - f_h)\|_2 + \|E\text{Proj}_{>l}(W - f_h)\|_2. \end{aligned}$$

In light of the second display above, the term $\|E\text{Proj}_{>l}(W - f_h)\|_2$ vanishes as $l \rightarrow \infty$, for any fixed W in the Π -probability 1 subset, and

$$\begin{aligned} \|E(W - f_h)\|_2^2 &\leq \lim_{l \rightarrow \infty} \|E\text{Proj}_l(W - f_h)\|_2^2 \leq C_2 \sum_{j=1}^{\infty} j^{-2p} (\epsilon_j \lambda_j^{1/2} - \langle f_h, \bar{\varphi}_j \rangle_2)^2 \\ &= C_2 \sum_{j=1}^{\infty} (\epsilon_j j^{-p} \lambda_j^{1/2} - \langle \tilde{f}_h, \bar{\varphi}_j \rangle_2)^2, \end{aligned}$$

where $\tilde{f}_h := \sum_{j=1}^{\infty} j^{-p} \langle f_h, \bar{\varphi}_j \rangle_2 \bar{\varphi}_j$. Consider the kernel $\tilde{k}(x, x') = \sum_{j=1}^{\infty} j^{-2p} \lambda_j \bar{\varphi}_j(x) \bar{\varphi}_j(x')$, and the induced RKHS $\tilde{\mathcal{H}}$. Then the process $\tilde{W} := \sum_{j=1}^{\infty} j^{-p} \lambda_j^{1/2} \epsilon_j \bar{\varphi}_j$ is a standard Gaussian process defined with \tilde{k}_x , where the series in the RHS converges in L_2 a.s. (Steinwart, 2019); and the RHS in the last display equals $C_2 \|\tilde{W} - \tilde{f}_h\|_2^2$. Thus we have, for any $\epsilon > 0$, $\{\|E(W - f_h)\|_2 \leq \epsilon\} \supset \{C_2 \|\tilde{W} - \tilde{f}_h\|_2 \leq \epsilon\}$. Similarly, by Assumption 6 (RL), we can reverse the inequalities above with a different C'_2 . Combining the two results we have, for any $\epsilon > 0$ and *all* $\|f_h\|_{\mathcal{H}}^2 \lesssim n\delta_n^2$,

$$\{C_2 \|\tilde{W} - \tilde{f}_h\|_2 \leq \epsilon\} \subset \{\|E(W - f_h)\|_2 \leq \epsilon\} \subset \{C'_2 \|\tilde{W} - \tilde{f}_h\|_2 \leq \epsilon\}. \quad (31)$$

For $\delta_n^2 \asymp n^{-\frac{b+2p}{b+2p+1}}$, we have

$$\Pi(\{\|\tilde{W} - \tilde{f}_h\|_2 \leq \delta_n\}) \stackrel{(a)}{\geq} e^{-\frac{1}{2} \|\tilde{f}_h\|_{\tilde{\mathcal{H}}}^2} \Pi(\{\|\tilde{W}\|_2 \leq \delta_n/C\}) \stackrel{(b)}{\geq} e^{-C' n \delta_n^2}. \quad (32)$$

where (a) can be found in, e.g., Ghosal and Van der Vaart (2017, Lemma I.28), and (b) holds because $\|\tilde{f}_h\|_{\tilde{\mathcal{H}}}^2 = \|f_h\|_{\mathcal{H}}^2 \asymp n^{\frac{1}{b+2p+1}}$, and Corollary 14 applied to $(\tilde{\mathcal{H}}, b+2p)$.¹⁷ By the same argument we have, *for all* $f_h \in \mathcal{H}$,

$$\Pi(\{\|\tilde{W} - \tilde{f}_h\|_2 \leq \delta_n\}) \leq e^{-\frac{1}{2} \|\tilde{f}_h\|_{\tilde{\mathcal{H}}}^2} \Pi(\{\|\tilde{W}\|_2 \leq \delta_n/C\}) \leq \Pi(\{\|\tilde{W}\|_2 \leq \delta_n/C\}) \leq e^{-C'' n \delta_n^2}. \quad (33)$$

Now (29) is proved by combining the above display and the second relation in (31).

¹⁷ The application is valid since \tilde{k}_x is obviously L_2 universal, although technically this is not necessary for the small-ball probability bound to hold.

It now remains to prove (30). Fix $m = \lceil n^{\frac{b+1}{b+2p+1}} \rceil$, $m' = \lceil n^{\frac{1}{b+2p+1}} \rceil$. Then by (32),

$$\begin{aligned} \log \Pi(\Theta_{dz}) &:= \log \Pi(\Theta_{dzl} \cap \Theta_{dzh}) \\ &:= \log \Pi(\{\|\text{Proj}_{m'}(\tilde{W} - \tilde{f}_h)\|_2 \leq \delta_n/(2C_2), \|\text{Proj}_{>m'}(\tilde{W} - \tilde{f}_h)\|_2 \leq \delta_n/(2C_2)\}) \\ &\geq \log \Pi(\{\|\tilde{W} - \tilde{f}_h\|_2 \leq \delta_n/(2C_2)\}) \gtrsim -n\delta_n^2. \end{aligned}$$

And by (31), on Θ_{dz} we have

$$\max\{\|E(\text{Proj}_{m'}(W - f_h))\|_2, \|E(W - f_h)\|_2\} \leq \delta_n.$$

By Assumption 6 (RL), this implies that

$$\|\text{Proj}_{m'}(W - f_h)\|_2^2 \leq (m')^{2p}\delta_n^2 = n^{-\frac{b}{b+2p+1}} \asymp \tau_m^2.$$

Moreover,

$$\log \Pi(\Theta_{dh}) := \log \Pi(\|\text{Proj}_{>m'}(W - f_h)\|_2 \leq \tau_m) \geq \log \Pi(\|W - f_h\|_2 \leq \tau_m) \stackrel{(a)}{\gtrsim} -n^{\frac{1}{b+2p+1}},$$

where (a) follows the same reasoning as (32). Combining the last three displays, we can see that the event in (30) is implied by $\Theta_{dh} \cap \Theta_{dz}$, after an inconsequential scaling. So it remains to lower bound $\Pi(\Theta_{dh} \cap \Theta_{dz})$.

On Θ_{dh} we have

$$\begin{aligned} \|\text{Proj}_{>m'}(\tilde{W} - \tilde{f}_h)\|_2^2 &= \sum_{j>m'} j^{-2p} (\epsilon_j \lambda_j^{1/2} - \langle f_h, \varphi_j \rangle_2)^2 \leq (m')^{-2p} \sum_{j>m'} (\epsilon_j \lambda_j^{1/2} - \langle f_h, \varphi_j \rangle_2)^2 \\ &= (m')^{-2p} \|\text{Proj}_{>m'}(W - f_h)\|_2^2 \leq m'^{-2p} \tau_m^2 \lesssim n^{-\frac{2p}{b+2p+1} - \frac{b}{b+2p+1}} \asymp \delta_n^2. \end{aligned}$$

Thus, after a trivial rescaling we have $\Theta_{dh} \subset \Theta_{dzh}$ (recall W and \tilde{W} are coupled). Moreover, both Θ_{dzh} and Θ_{dh} only depend on $\{\epsilon_j : j > m'\}$ and are independent of Θ_{dzl} . Therefore,

$$\log \mathbb{P}(\Theta_{dh} \cap \Theta_{dz}) = \log \mathbb{P}(\Theta_{dzl}) + \log \mathbb{P}(\Theta_{dh}) \gtrsim -n\delta_n^2$$

which concludes the proof. \blacksquare

Lemma 19 *Let $\delta_n^2 := n^{-\frac{b+2p}{b+2p+1}}$, $\epsilon_n^2 := n^{-\frac{b}{b+2p+1}}$. There exist constants $C_1, C_2, C_3, C_4 > 0$ s.t.*

$$\Pi(\Theta_{d0}) := \Pi(\{\|E(f - f_0)\|_2 \leq C_1\delta_n, \|f - f_0\|_2 \leq C_2\epsilon_n, \|f - f_0\| \leq C_3\}) \geq \exp(-C_4n\delta_n^2).$$

Proof For $m' = \lceil n^{\frac{1}{b+2p+1}} \rceil$, by Assumption 4 we can decompose $f_0 = \tilde{f}_h + \tilde{f}_e$ where \tilde{f}_h, \tilde{f}_e satisfies (27). Invoking Lemma 16 we obtain $f_h + f_e = f_0$ where $\|f_h\|_{\mathcal{H}} \lesssim \|\tilde{f}_h\|_{\mathcal{H}}$, $\|Ef_e\|_2 \lesssim \delta_n$, $\|f_e\|_2 \lesssim \epsilon_n$. Thus, by the triangle inequality, the parameter subset created by applying Lemma 18 to f_h satisfies

$$\|E(f - f_0)\|_2 \leq C_1\delta_n, \|f - f_0\|_2 \leq C_2\epsilon_n$$

and has the advertised prior probability. It remains to deal with $\|f - f_0\|$.

Let $m = \lceil n^{\frac{b+1}{b+2p+1}} \rceil$ and Θ_{d0} be the intersection of the aforementioned subset with $C\Theta_m := \{f : C^{-1}f \in \Theta_m\}$, where $C, C' \geq 1$ are large constants, and \mathbb{B}_1 denotes the L_2 unit norm ball. Since $1 - \Pi(C\Theta_m) \leq e^{-C''n\delta_n^2}$, we can choose C so that Θ_{d0} still has the advertised prior probability. Now, by Corollary 13, for any $f \in \Theta_{d0} \subset C\Theta_m$, we have

$$f = \bar{f}_h + \bar{f}_e, \quad \text{where} \quad \|\bar{f}_h\|_{\mathcal{H}}^2 \lesssim n^{\frac{1}{b+2p+1}}, \quad \|\bar{f}_e\|_2^2 \lesssim n^{-\frac{b}{b+2p+1}}, \quad \|\bar{f}_e\|^2 \lesssim 1.$$

As by assumption f_0 admits a similar decomposition (14), we have $f - f_0 = f'_h + f'_e$, where $\|f'_h\|_{\mathcal{H}}^2 \lesssim n^{\frac{1}{b+2p+1}}, \|f'_e\|_2^2 \lesssim n^{-\frac{b}{b+2p+1}} \asymp \epsilon_n^2, \|f'_e\| \lesssim 1$. We also have $\|f'_h\|_2 \leq \|f - f_0\|_2 + \|f'_e\|_2 \lesssim \epsilon_n$. Thus, by Lemma 11,

$$\|f - f_0\|^2 \lesssim \|f'_h\|^2 + \|f'_e\|^2 \lesssim \|f'_h\|_{\mathcal{H}}^{\frac{2b}{b+1}} \|f'_h\|_2^{\frac{2}{b+1}} + \|f'_e\|^2 \lesssim n^{\frac{1}{b+2p+1} \cdot \frac{b}{b+1}} n^{\frac{-b}{b+2p+1} \cdot \frac{1}{b+1}} + 1 \leq 2.$$

■

Proposition 20 (marginal likelihood bound) *Let $\lambda = 1, \bar{\nu} \geq 2C\delta_n^2$ where $C > 0$ is a sufficiently large constant. Then there exists constants $C_{1,\dots,5} > 0$, and a $\mathcal{D}^{(n)}$ -measurable event E_{den} with probability $\rightarrow 1$, on which*

$$\Pi(\{f \in \Theta_{d0} : \ell_n(f) \leq C_1\|E(f - f_0)\|_2^2 + C_2\delta_n^2\}) \geq \frac{1}{2}\Pi(\Theta_{d0}). \quad (34)$$

Consequently, on E_{den} we have $\Pi(\{f : \ell_n(f) \leq C_3\delta_n^2\}) \geq e^{-C_4n\delta_n^2}$, and

$$\int \exp\left(-\frac{n}{\lambda}\ell_n(f)\right) \Pi(df) \geq \exp(-C_5n\delta_n^2). \quad (35)$$

In the above, $C_2, C_3, C_5 \lesssim B^2$.

Proof We proceed in two steps.

(Step 1) In Step 2 below we will show that there exists $C_1, C_2 > 0$ and a sequence $\eta_n \rightarrow 0$ s.t. for any fixed $f \in \Theta_{d0}$,

$$\mathbb{P}(I(f, \mathcal{D}^{(n)})) := \mathbb{P}(\{\ell_n(f) \leq C_1\|E(f - f_0)\|_2^2 + C_2\delta_n^2\}) \geq 1 - \eta_n. \quad (36)$$

We claim that if (36) is true, (34) will hold with $\mathcal{D}^{(n)}$ -probability greater than $1 - 4\eta_n$, and (35) by the definition of Θ_{d0} in Lemma 19; hence the proof will complete. To prove this claim, suppose by contrary that (36) holds, yet

$$\mathbb{P}(\{(34) \text{ holds}\}) \leq 1 - 4\eta_n. \quad (37)$$

Define $\Pi_{dr}(df) := \Pi(df \cap \Theta_{d0})/\Pi(\Theta_{d0})$. By Fubini's theorem and (36),

$$\mathbb{P}(\Pi_{dr}(I(f, \mathcal{D}^{(n)}))) = \Pi_{dr}(\mathbb{P}(I(f, \mathcal{D}^{(n)}))) \geq 1 - \eta_n.$$

Yet (37) would imply

$$\begin{aligned} \mathbb{P}(\Pi_{dr}(I(f, \mathcal{D}^{(n)}))) &= \mathbb{P}(\Pi_{dr}(I(f, \mathcal{D}^{(n)})) \cdot \mathbf{1}_{\{(34) \text{ holds}\}}) + \mathbb{P}(\Pi_{dr}(I(f, \mathcal{D}^{(n)})) \cdot \mathbf{1}_{\{(34) \text{ does not hold}\}}) \\ &\leq 1 \cdot (1 - 4\eta_n) + \frac{1}{2} \cdot 4\eta_n = 1 - 2\eta_n, \end{aligned}$$

a contradiction.

(Step 2) It remains to prove (36). We follow the argument in Dikkala et al. (2020).

Denote by $\hat{\delta}_n$ the critical radius of the empirical local Radamacher complexity of $3\mathcal{I}_1$. Then for some universal $c > 0$, $\mathbb{P}_{\mathcal{D}^{(n)}}(\hat{\delta}_n \leq c\delta_n) \rightarrow 1$ (Wainwright, 2019, p. 455). And by Wainwright (2019, Theorem 14.1 and 14.20) applied to $g/\|g\|_{\mathcal{I}}$, there exists $c' > 0$ such that with probability greater than $1 - c'e^{-c'n\delta_n^2} =: 1 - \eta_n \rightarrow 1$, we have, for fixed $f \in \Theta_{d0}$ and all $g \in \mathcal{I}$,

$$\begin{aligned} \|g\|_{2,n}^2 &\geq \frac{1}{2}\|g\|_2^2 - C\delta_n^2(1 + \|g\|_{\mathcal{I}}^2), \\ \Psi_n(f, g) &\leq \Psi(f, g) + 10LC\delta_n(\|g\|_2 + \delta_n(1 + \|g\|_{\mathcal{I}})). \end{aligned}$$

where $L = \|f - f_0\| + \max_{i=1}^n |y_i - f_0(x_i)| \lesssim 1 + B$, $\Psi_n(f, g) := \sum_{i=1}^n g(z_i)(f(x_i) - y_i)$, $\Psi(f, g) := \mathbb{E}(g(\mathbf{z})(f(\mathbf{x}) - \mathbf{y}))$, and $C = \sup_{\|g\|_{\mathcal{I}}=1} \|g\|$. Define $C_n := (20L + 2)C$. Define E_{den} as the event when the above displays hold. On this event we have, for $\bar{\nu} > 2C\delta_n^2$,

$$\begin{aligned} \ell_n(f) &= \sup_{g \in \mathcal{I}} 2\Psi_n(f, g) - \|g\|_{n,2} - \bar{\nu}\|g\|_{\mathcal{I}}^2 \\ &\leq \sup_g 2\Psi(f, g) + 20L(\delta_n\|g\|_2 + \delta_n^2(1 + \|g\|_{\mathcal{I}})) - \frac{1}{2}\|g\|_2^2 + C\delta_n^2(1 + \|g\|_{\mathcal{I}}^2) - \bar{\nu}\|g\|_{\mathcal{I}}^2 \\ &= \sup_g 2\Psi(f, g) - \frac{1}{4}\|g\|_2^2 + C_n\delta^2 + (C_n\delta^2\|g\|_{\mathcal{I}} - (\bar{\nu} - C\delta_n^2)\|g\|_{\mathcal{I}}^2) + \left(C_n\delta\|g\|_2 - \frac{1}{4}\|g\|_2^2\right) \\ &\stackrel{(a)}{\leq} \sup_{g \in \mathcal{I}} \Psi(f, g) - \frac{1}{4}\|g\|_2^2 + C_n'\delta^2 \leq \sup_{g \in L_2} \Psi(f, g) - \frac{1}{4}\|g\|_2^2 + C_n''\delta^2 \\ &\stackrel{(b)}{=} 2\|E(f - f_0)\|_2^2 + C_n''\delta^2. \end{aligned}$$

In the above (a) follows from the inequality $a\|x\|_s - b\|x\|_s^2 \leq \frac{a^2}{4b}$, where $\|\cdot\|_s$ is an arbitrary norm; and (b) by definition of Ψ and properties of the conditional expectation. Finally, we note that $C_n'^2 = C_n + C_n^2(1 + 1/4C) \lesssim B^2$. \blacksquare

A.4 Proof of Theorem 3

At a high level, we will follow the posterior contraction framework and bound the expectation of the posterior mass

$$\mathbb{P}_{\mathcal{D}^{(n)}}\Pi(\text{err}_{n,f} \mid \mathcal{D}^{(n)}) = \mathbb{P}_{\mathcal{D}^{(n)}} \frac{\int_{\text{err}_{n,f}} \exp(-\lambda^{-1}n\ell_n(f))\Pi(df)}{\int \exp(-\lambda^{-1}n\ell_n(f))\Pi(df)},$$

where $\text{err}_{n,f}$ denotes the parameter set in the theorem, that is, either $\{\|f - f_0\|_2 \geq M\epsilon_n\}$ or $\{\|E(f - f_0)\|_2 \geq M\delta_n\}$. The denominator has been bounded in Appendix A.3, where

we sketch the proof at the beginning of the subsection; the numerator will be addressed in this subsection. For this purpose,

1. We first decompose the posterior mass further, in (45)-(47) below, where we pick out some events on which estimation of the quasi-likelihood fails, and a small parameter set Θ_m^c consisting of “bad” parameters. As we show below, these events have vanishing contribution to the above display, and will not affect the final result.
2. Lemma 21 below shows that on Θ_m , a large error in the $L_2(P(dx))$ norm is equivalent to a large error in the $\|E(\cdot)\|_{L_2(P(dz))}$ norm. This shows the equivalence of (15) and (16), and enables us to lower bound the quasi-likelihood which (for the most part) estimates $\|E(f - f_0)\|_2$.
3. The proof proceeds by bounding various estimation errors.

Throughout the proof we rely on the *sieve set* Θ_m consisting of “well-behaved” functions in the prior support; its properties have been established in Appendix A.2.2. We also refer readers to the additional notations and conventions in Appendix A.1.

Lemma 21 *There exists $M_0, C > 0$ such that for all $n \in \mathbb{N}$, $m = \lfloor n^{\frac{b+1}{b+2p+1}} \rfloor$, and $f \in \Theta_m$,*

$$\|f - f_0\|_2 \geq M_0 \epsilon_n \quad \text{only if} \quad \|E(f - f_0)\|_2 \geq \frac{\|f - f_0\|_2}{C \epsilon_n} \delta_n. \quad (38)$$

$$\|E(f - f_0)\|_2 \geq M_0 \delta_n \quad \text{only if} \quad \|f - f_0\|_2 \geq \frac{\|E(f - f_0)\|_2}{C \delta_n} \epsilon_n. \quad (39)$$

The constant C is determined by Assumption 6.

Proof Since $f \in \Theta_m$ and f_0 satisfies (14), we can invoke Lemma 16 on $\Delta f := f - f_0$, showing that there exists $\widetilde{\Delta f} \in \mathcal{H}$ such that

$$\|\widetilde{\Delta f}\|_{\mathcal{H}}^2 \lesssim n \delta_n^2, \quad \|E(\Delta f - \widetilde{\Delta f})\|_2^2 \lesssim \delta_n^2, \quad \|\Delta f - \widetilde{\Delta f}\|_2^2 \leq C \epsilon_n^2, \quad \|\Delta f - \widetilde{\Delta f}\|^2 \leq C, \quad (40)$$

where $C > 0$ is a constant. Introduce the notations

$$j := \lfloor n^{\frac{1}{b+2p+1}} \rfloor, \quad g := E \Delta f, \quad \widetilde{g} := E(\widetilde{\Delta f}), \quad g_j := E(\text{Proj}_j \widetilde{\Delta f}). \quad (41)$$

From (40) we can see that for sufficiently large M_0 and $\|f - f_0\|_2 \geq M_0 \epsilon_n$,

$$\|\widetilde{\Delta f}\|_2 \geq \|\Delta f\|_2 - \|\Delta f - \widetilde{\Delta f}\|_2 \geq \|\Delta f\|_2 - \sqrt{C} \epsilon_n \geq \frac{1}{2} \|\Delta f\|_2,$$

$$\|\text{Proj}_j \widetilde{\Delta f}\|_2^2 = \|\widetilde{\Delta f}\|_2^2 - \|\text{Proj}_{>j} \widetilde{\Delta f}\|_2^2 \stackrel{(a)}{\geq} \frac{1}{4} \|\Delta f\|_2^2 - \|\widetilde{\Delta f}\|_{\mathcal{H}}^2 j^{-(b+1)} \geq \frac{1}{5} \|\Delta f\|_2^2,$$

where (a) follows from Lemma 15 with $\tilde{b} = b + 1$. And

$$\begin{aligned} \|E(\Delta f)\|_2^2 &\geq \frac{1}{2} \|E(\widetilde{\Delta f})\|_2^2 - \|E(\Delta f - \widetilde{\Delta f})\|_2^2 \\ &\stackrel{(a)}{\geq} C'_1 j^{-2p} \|\text{Proj}_j \widetilde{\Delta f}\|_2^2 - \|E(\Delta f - \widetilde{\Delta f})\|_2^2 \\ &\geq \frac{1}{5} C'_1 j^{-2p} \|\Delta f\|_2^2 - \|E(\Delta f - \widetilde{\Delta f})\|_2^2 \\ &= C''_1 \epsilon_n^{-2} \|\Delta f\|_2^2 \delta_n^2 - C_2 n^{-\frac{b+2p}{b+2p+1}} \gtrsim \epsilon_n^{-2} \|\Delta f\|_2^2 \delta_n^2. \end{aligned}$$

In the above, (a) follows from Assumption 6, the last inequality holds for $M \geq 2C_2/C_1''$, and we recall C_2 is from (40). This concludes the proof of (38).

It remains to prove (39). First, for any $f \in \Theta_m$, we have

$$\begin{aligned} \|g - g_j\|_2^2 &\leq 2\|g - \tilde{g}\|_2^2 + 2\|\tilde{g} - g_j\|_2^2 \stackrel{(a)}{\lesssim} \cancel{\delta_n^2} \|\tilde{g} - g_j\|_2^2 = \|E(\text{Proj}_{>j} \widetilde{\Delta} f)\|_2^2 \\ &\stackrel{(b)}{\leq} j^{-2p} \|\text{Proj}_{>j} \widetilde{\Delta} f\|_2^2 \stackrel{(c)}{\leq} j^{-2p} \|\widetilde{\Delta} f\|_{\mathcal{H}}^2 j^{-(b+1)} \lesssim n^{\frac{-2p+1-(b+1)}{b+2p+1}} = \delta_n^2. \end{aligned} \quad (42)$$

where (a) follows by (40), (b) by Assumption 6, and (c) by Lemma 15 with $\tilde{b} = b + 1$. Thus, for M_0 sufficiently large and $f \in \Theta_m$ s.t. $\|g\|_2 = \|E\Delta f\|_2 \geq M_0\delta_n$, we have, by Assumption 6,

$$\begin{aligned} \|\widetilde{\Delta} f\|_2 &\gtrsim j^p \|g_j\|_2 \geq j^p (\|g\|_2 - \|g - g_j\|_2) \geq \frac{\|g\|_2}{2\delta_n} \epsilon_n, \\ \|\Delta f\|_2 &\geq \|\widetilde{\Delta} f\|_2 - \|\Delta f - \widetilde{\Delta} f\|_2 \stackrel{(a)}{\gtrsim} \left(\frac{\|g\|_2}{2\delta_n} - \sqrt{C} \right) \epsilon_n \geq \frac{\|g\|_2}{3\delta_n} \epsilon_n, \end{aligned}$$

where (a) also follows from (40). This completes the proof. \blacksquare

We now complete the proof of the theorem, which we restate below with minor changes in notations.

Theorem 3 Fix $\lambda = 1$, $\bar{\nu} = C\delta_n^2 \asymp n^{-\frac{b+2p}{b+2p+1}}$ where $C > 0$ is a large constant. Then there exists $M > 0$ such that for $\epsilon_n^2 = n^{-\frac{b}{b+2p+1}}$, we have

$$\mathbb{P}_{\mathcal{D}^{(n)}} \Pi \left(\{f : \|f - f_0\|_2^2 \geq M\epsilon_n^2\} \mid \mathcal{D}^{(n)} \right) \rightarrow 0. \quad (43)$$

$$\mathbb{P}_{\mathcal{D}^{(n)}} \Pi \left(\{f : \|E(f - f_0)\|_2^2 \geq M\delta_n^2\} \mid \mathcal{D}^{(n)} \right) \rightarrow 0. \quad (44)$$

Furthermore, if Assumption 1 is relaxed so that only $\mathbf{y} - f_0(\mathbf{x})$ is subgaussian will hold, the above two equations will hold with M replaced by M_n , where M_n is any slowly growing sequence such that $\lim_{n \rightarrow \infty} \frac{M_n}{\log n} = \infty$.

A.4.1 PROOF OF THEOREM 3, BOUNDED NOISE CASE

Before we start, note that throughout the proof the constants hidden in $\lesssim, \asymp, \gtrsim$ will not depend on M or B . We use $\text{err}_{n,f}$ to denote the function set in either (43) or (44).

(Step 1) Let $E_n(\mathcal{D}^{(n)}) := E_{den}$ which is defined in Proposition 20. Consider the decomposition

$$\mathbb{P}_{\mathcal{D}^{(n)}} \Pi \left(\text{err}_{n,f} \mid \mathcal{D}^{(n)} \right) \leq \mathbb{P}_{\mathcal{D}^{(n)}}(E_n^c) + \mathbb{P}_{\mathcal{D}^{(n)}} \left[\mathbf{1}_{E_n} \cdot \frac{\tilde{\Pi}(\text{err}_{n,f} \mid \mathcal{D}^{(n)})}{\tilde{\Pi}(\Theta \mid \mathcal{D}^{(n)})} \right], \quad (45)$$

where $\tilde{\Pi}(A \mid \mathcal{D}^{(n)}) := \int_A \exp(-\lambda^{-1} n \ell_n(f)) \Pi(df)$ is the unnormalized posterior measure. By Proposition 20, on E_n the denominator above is greater than $\exp(-C_{den} n \delta_n^2)$, for some

$0 < C_{den} \lesssim B^2$. So it remains to show that, there exists some $C_{num} > C_{den}$ such that when M is sufficiently large,

$$\mathbb{P}_{\mathcal{D}^{(n)}} \left[\mathbf{1}_{E_n} \tilde{\Pi}(\text{err}_{n,f} \mid \mathcal{D}^{(n)}) \right] \leq \exp(-C_{num} n \delta_n^2). \quad (46)$$

Fix $m := \lfloor n^{\frac{b+1}{b+2p+1}} \rfloor$. We decompose the LHS above as

$$\begin{aligned} & \mathbb{P}_{\mathcal{D}^{(n)}} \left[\mathbf{1}_{E_n} \int_{\text{err}_{n,f}} \Pi(df) \exp(-\lambda n \ell_n(f)) \right] \\ & \leq \Pi(\Theta_m^c) + \int_{\Theta_m \cap \text{err}_{n,f}} \Pi(df) \left(\mathbb{P}_{\mathcal{D}^{(n)}} A(f, \mathcal{D}^{(n)})^c + \mathbb{P}_{\mathcal{D}^{(n)}} (\mathbf{1}_{A(f, \mathcal{D}^{(n)})} e^{-n \ell_n(f)}) \right), \end{aligned} \quad (47)$$

where the event A will be defined in Step 2. Since $\Pi(\Theta_m^c) \leq \exp(-C_{gp'} n \delta_n^2)$, where the constant $C_{gp'}$ can be chosen to be smaller than C_{num} ,¹⁸ it suffices to deal with the integral term. For its former half involving $A(f, \mathcal{D}^{(n)})^c$, we will specify A so that it has the required probability. For the latter half, observe that by Lemma 21, for sufficiently large M , the function sets $\{\|f - f_0\|_2 \geq M \epsilon_n\}$ and $\{\|E(f - f_0)\|_2 \geq M \delta_n\}$ are equivalent (up to an inconsequential scaling) after intersecting with Θ_m . Therefore, it suffices to prove one of (43) or (44), and the other will follow; and in the following, we can consider $f \in \text{err}_{n,f} \cap \Theta_m$ as satisfying

$$\|f - f_0\|_2^2 \geq M \epsilon_n^2, \quad \|E(f - f_0)\|_2^2 \geq C \delta_n^2 \frac{\|f - f_0\|_2^2}{\epsilon_n^2}, \quad (48)$$

which is valid for sufficiently large M ; and we recall C is determined by Assumption 6. In the remainder of the proof, we lower bound $\ell_n(f)$ using the above display.

(Step 2) We use an argument inspired by Dikkala et al. (2020). Introduce the notations

$$\Psi_n(f, g) := \frac{1}{n} \sum_{i=1}^n (f(x_i) - y_i) g(z_i), \quad \Psi(f, g) = \mathbb{E}_{\mathcal{D}^{(n)}} \Psi_n(f, g),$$

so that $\ell_n(f) = \sup_{g \in \mathcal{I}} 2\Psi_n(f, g) - \|g\|_n^2 - \bar{\nu} \|g\|_{\mathcal{I}}^2$. Recall the notations from Lemma 21: $g := E(f - f_0)$, $\tilde{g} := E(\tilde{\Delta} f)$, $g_j := E(\text{Proj}_j \tilde{\Delta} f) \in \mathcal{I}$, $j := \lfloor n^{\frac{1}{b+2p+1}} \rfloor$; and $\tilde{\Delta} f$ defined in (40).

Let $\mathbf{l} := (f(\mathbf{x}) - \mathbf{y}) g_j(\mathbf{z}) - g_j(\mathbf{z})^2$, and l_1, \dots, l_n be its realizations using x_i, y_i, z_i . Then

$$\begin{aligned} \|\mathbf{l}\| & \leq (\|f - f_0\| + B + \|g_j\|)^2, \quad \text{Var} \mathbf{l} \leq \mathbb{E}_{\mathcal{D}^{(n)}} \mathbf{l}^2 \leq (\|f - f_0\| + B + \|g_j\|)^2 \|g_j\|_2^2, \\ \Psi_n(f, g_j) - \|g_j\|_n^2 & = \frac{1}{n} \sum_{i=1}^n l_i, \quad \Psi(f, g_j) - \|g_j\|_2^2 = \mathbb{E}_{\mathcal{D}^{(n)}} \mathbf{l}. \end{aligned}$$

(In the first inequality above, observe $\mathbf{l} = (f(\mathbf{x}) - f_0(\mathbf{x}) + f_0(\mathbf{x}) - \mathbf{y} - g_j(\mathbf{z})) g_j(\mathbf{z})$, and recall $|y_i - f_0(x_i)| \leq B$ by assumption.) By Lemma 17, we have, for any fixed $f \in \Theta_m$,

$$\mathbb{P} \left(\Psi_n(f, g_j) - \|g_j\|_n^2 \geq \Psi(f, g_j) - \frac{3}{2} \|g_j\|_2^2 \right) \geq 1 - \exp \left(- \frac{n \|g_j\|_2^2}{16 (\|f - f_0\| + B + \|g_j\|)^2} \right). \quad (49)$$

18. We can replace Θ_m with $\Theta_{\lfloor m/C \rfloor}$ at the cost of inflating τ_m by a constant, which can be absorbed into M .

We define $A(f, \mathcal{D}^{(n)})$ as the event above; its required probability bound from Step 1 will be verified shortly. On this event we have,

$$\begin{aligned}
 \ell_n(f) &= \sup_{g \in \mathcal{I}} 2\Psi_n(f, g) - \|g\|_n^2 - \bar{\nu}\|g\|_{\mathcal{I}}^2 \\
 &\stackrel{(a)}{\geq} 2\Psi_n(f, g_j) - \|g_j\|_n^2 - \bar{\nu}\|g_j\|_{\mathcal{I}}^2 \stackrel{(b)}{\geq} 2\Psi(f, g_j) - \frac{3}{2}\|g_j\|_2^2 - \bar{\nu}\|g_j\|_{\mathcal{I}}^2 \\
 &= 2\mathbb{E}((f(\mathbf{x}) - \mathbf{y})(g(\mathbf{z}) - g(\mathbf{z}) + g_j(\mathbf{z}))) - \frac{3}{2}\|g_j - g + g\|_2^2 - \bar{\nu}\|g_j\|_{\mathcal{I}}^2 \\
 &\stackrel{(c)}{=} 2\|g\|_2^2 - 2\|g\|_2\|g - g_j\|_2 - \frac{3}{2}(\|g\|_2^2 + \|g_j - g\|_2^2 + 2\|g\|\|g_j - g\|) - \bar{\nu}\|g_j\|_{\mathcal{I}}^2 \\
 &\stackrel{(d)}{\geq} c_1\|g\|_2^2 - c_2\|g - g_j\|_2^2 - \bar{\nu}\|g_j\|_{\mathcal{I}}^2 \stackrel{(e)}{\geq} c_1\|g\|_2^2 - C_2\delta_n^2 - \bar{\nu}\|g_j\|_{\mathcal{I}}^2. \tag{50}
 \end{aligned}$$

In the above, (a) follows because $g_j \in \mathcal{I}$, (b) by definition of $A(f, \mathcal{D}^{(n)})$, (c) by the tower property, (d) follows from the inequality $2\|g\|_2\|g - g_j\|_2 \leq \epsilon^2\|g\|_2^2 + \epsilon^{-2}\|g - g_j\|_2^2$ for any $\epsilon > 0$, c_1, c_2 are universal constants, and (e) follows from (42).

It remains to bound $\|g_j\|_{\mathcal{I}}$ and $\mathbb{P}(A^c(f, \mathcal{D}^{(n)}))$. Let $U := \|f - f_0\|_2/\epsilon_n$, so that $U \geq \sqrt{M}$ on $\text{err}_{n,f}$. When M is sufficiently large, we have $U > 1$, and

$$U\delta_n \stackrel{(a)}{\lesssim} \|g\|_2 \leq \|f - f_0\|_2 = U\epsilon_n \leq U, \tag{51}$$

$$\|\widetilde{\Delta f}\|_2 \leq \|f - f_0 - \widetilde{\Delta f}\|_2 + \|f - f_0\|_2 \stackrel{(b)}{\leq} 2U\epsilon_n, \tag{52}$$

where (a) is by (48), and (b) is by (40). Now,

$$\begin{aligned}
 \|f - f_0\|^2 &\leq 2\|\widetilde{\Delta f}\|^2 + 2\|f - f_0 - \widetilde{\Delta f}\|^2 \stackrel{(a)}{\lesssim} \|\widetilde{\Delta f}\|^2 + 1 \\
 &\stackrel{(b)}{\lesssim} (\|\widetilde{\Delta f}\|_{\mathcal{H}}^2)^{\frac{b}{b+1}} (\|\widetilde{\Delta f}\|_2^2)^{\frac{1}{b+1}} + 1 \stackrel{(c)}{\lesssim} n^{\frac{1}{b+2p+1} \cdot \frac{b}{b+1}} (U^2 n^{\frac{-b}{b+2p+1}})^{\frac{1}{b+1}} + 1 \leq 2U^{\frac{2}{b+1}}, \tag{53} \\
 \|g_j\|_{\mathcal{I}}^2 &= \|E(\text{Proj}_j \widetilde{\Delta f})\|_{\mathcal{I}}^2 \stackrel{(d)}{\lesssim} \|\text{Proj}_j \widetilde{\Delta f}\|_{\mathcal{H}}^2 \\
 &\stackrel{(b)}{\lesssim} \|\text{Proj}_j \widetilde{\Delta f}\|_{\mathcal{H}}^{\frac{2b}{b+1}} \|\text{Proj}_j \widetilde{\Delta f}\|_2^{\frac{2}{b+1}} \stackrel{(c')}{\lesssim} n^{\frac{1}{b+2p+1} \cdot \frac{b}{b+1}} (U^2 n^{\frac{-b}{b+2p+1}})^{\frac{1}{b+1}} = U^{\frac{2}{b+1}}. \tag{54}
 \end{aligned}$$

In the above, (a) follows from (40), (b) from Lemma 11, (c) from (40) and (52), (c') additionally from the fact that Proj_j is an orthogonal projection in both L_2 and \mathcal{H} , and (d) by Assumption 7 (ii).

It now follows that $\|g_j\| \lesssim \|g_j\|_{\mathcal{I}} \lesssim U^{\frac{2}{b+1}}$. Plugging this inequality, (51) and (53) into (49), we have

$$-\log \mathbb{P}_{\mathcal{D}^{(n)}}(A^c(f, \mathcal{D}^{(n)})) \geq \frac{n\|g_j\|_2^2}{16(\|f - f_0\| + B + \|g_j\|)^2} \gtrsim \frac{U^2}{(U^{\frac{1}{b+1}} + B)^2} n\delta_n^2.$$

Therefore, when $U \gtrsim B$ is sufficiently large, we have

$$\sup_{f \in \Theta_m \cap \text{err}_{n,f}} \mathbb{P}_{\mathcal{D}^{(n)}}(A^c(f, \mathcal{D}^{(n)})) \leq e^{-2C_{\text{num}} n\delta_n^2},$$

which fulfills the requirement in Step 1.

Plugging (51), (54) and $\bar{\nu} \asymp \delta_n^2$ into (50), we have

$$\ell_n(f) \geq C_1 U^2 \delta_n^2 - C_2 \delta_n^2 - C_3 U^{\frac{2}{b+1}} \delta_n^2.$$

As $b > 1$, there exists $C, C' > 0$ such that when $M = U^2$ is sufficiently large, we have, for all $f \in \Theta_m \cap \text{err}_{n,f}$,

$$\ell_n(f) \geq C U^2 \delta_n^2 = C' M \delta_n^2.$$

This completes the proof for (46), and by Step 1, the proof for (43) and (44).

A.4.2 GENERAL SUBGAUSSIAN CASE

In this case we replace B with $B_n := \gamma_n \sqrt{\log n}$, where γ_n is any slowly growing sequence $\rightarrow \infty$, so that $\mathbb{P}_{\mathcal{D}(n)}(\max_i |\mathbf{y}_i - f_0(\mathbf{x}_i)| \leq B_n) \rightarrow 1$. We add this event to the definition of E_{den} . Then the proof follows, with all occurrences of B replaced by B_n . As mentioned above, it suffices to have $M_n \gtrsim B_n^2$.

Now the proof for Theorem 3 is complete. \blacksquare

A.5 Proof of Corollary 4

The proof is also based on reduction to Theorem 3, but requires a specific sieve. In particular, we choose $\Theta_m = \Theta_{m,b''}$ defined in Corollary 13, where $\max\{b_{emb}, b'\} < b'' < b$. Recall it also satisfies (26). We also need to derive some additional properties for Θ_m .

Below we denote the norm $\|\cdot\|_{\mathcal{H}^{\frac{b'}{b+1}}}$ as $\|\cdot\|_{b'}$ for $b' \in [0, b)$.

Lemma 22 *Let $m = \lceil n^{\frac{b+1}{b+2p+1}} \rceil$, Θ_m be defined as above. Let $f \in \Theta_m$. Then (i) For the decomposition $f = \tilde{f}_h + \tilde{f}_e$ as defined in (26), it additionally holds that $\|\tilde{f}_e\|_{b'}^2 \lesssim m^{-\frac{b-b'}{b+1}}$. (ii) Suppose f additionally satisfies $\|f - f_0\|_{b'}^2 > M n^{-\frac{b-b'}{b+2p+1}}$, where $M > 0$ is sufficiently large. Then*

$$\|f - f_0\|_2^2 \gtrsim M n^{-\frac{b}{b+2p+1}}.$$

Proof (i): Recall the construction in Corollary 13: $\tilde{f}_e = \text{Proj}_{>j} f_e$ for $j = \lceil m \rceil^{\frac{1}{b+1}}$. By a similar argument as in Corollary 13 and Lemma 15 (iii), we find $\|\tilde{f}_e\|_{b'}^2 \lesssim m^{-\frac{b-b'}{b+1}}$.

(ii): Using a similar argument to Lemma 23, the condition $f_0 \in \bar{\mathcal{H}}$ implies that f_m^\dagger defined in Assumption 4 also satisfy

$$\|f_0 - f_m^\dagger\|_{b'}^2 \leq m^{-\frac{b-b'}{b+1}}. \quad (55)$$

By Assumption 4, (55) and the definition of Θ'_m , we have $f - f_0 = \tilde{f}'_h + \tilde{f}'_e$, where

$$\|\tilde{f}'_h\|_{\mathcal{H}}^2 \lesssim n^{\frac{1}{b+2p+1}}, \quad \|\tilde{f}'_e\|_2^2 \lesssim n^{-\frac{b}{b+2p+1}}, \quad \|\tilde{f}'_e\|_{b'}^2 \lesssim n^{-\frac{b-b'}{b+2p+1}}.$$

Let $m' = \lfloor n^{\frac{1}{b+2p+1}} \rfloor$, $f'_h = \text{Proj}_{m'} \tilde{f}'_h$, $f'_e = f - f_0 - f'_h$. Then by Lemma 15 and a similar argument for the $\|\cdot\|_{b'}$ norm, we can show that f'_e satisfies the same norm inequalities as above. And since f'_h is a truncation,

$$\|f'_h\|_2^2 \geq \lambda_{m'}^{-\frac{b'}{b+1}} \|f'_h\|_{b'}^2 \asymp n^{-\frac{b'}{b+2p+1}} \|f'_h\|_{b'}^2 \gtrsim n^{-\frac{b'}{b+2p+1}} (\|f - f_0\|_{b'}^2 - \|f'_e\|_{b'}^2) \gtrsim Mn^{-\frac{b}{b+2p+1}}.$$

And $\|f - f_0\|_2^2 \geq (\|f'_h\|_2 - \|f'_e\|_2)^2 \gtrsim Mn^{-\frac{b}{b+2p+1}}$ as claimed. \blacksquare

Proof [Proof of Corollary 4] Lemma 22 shows the intersection of Θ_m and the parameter region defined in Theorem 4 is a subset of $\text{err}_{n,f}$ in Theorem 3. Thus, we can follow the proof in Appendix A.4.1 and obtain Corollary 4. \blacksquare

A.6 Proof for Theorem 6

Consider the inequality

$$\begin{aligned} \mathbb{P}(\Pi(\{\|f - \hat{f}_n\|_{b'} \leq \rho\epsilon_{n,b'}\} \mid \mathcal{D}^{(n)})) &\leq \mathbb{P}(E_{den}^c) + \mathbb{P}\left(\mathbf{1}_{E_{den}} \frac{\Pi(\{\|f - \hat{f}_n\|_{b'} \leq \rho\epsilon_{n,b'}\})}{\int \exp(-\lambda^{-1}n\ell_n(f))\Pi(df)}\right), \\ &\stackrel{(a)}{\leq} o(1) + e^{C_1 n^{\frac{1}{b+2p+1}}} \Pi(\{\|f - \hat{f}_n\|_{b'} \leq \rho\epsilon_{n,b'}\}) \\ &\stackrel{(b)}{\leq} o(1) + e^{C_1 n^{\frac{1}{b+2p+1}}} \Pi(\{\|f\|_{b'} \leq \rho\epsilon_{n,b'}\}), \end{aligned}$$

where (a) holds by Proposition 20, and (b) by Ghosal and Van der Vaart (2017, Lemma I.28).

Recall that by Lemma 12 we have, for sufficiently small ϵ ,

$$\log \Pi(\{\|f\|_{b'} \leq \epsilon\}) \leq -C_{b'}\epsilon^{-\frac{2}{b}} \quad (56)$$

where $C_{b'}$ is also determined by k_x . Thus, for $\rho \leq (2C_1/C_{b'})^{-\frac{b}{2}}$, we have

$$\log \Pi(\{\|f\|_{b'} \leq \rho\epsilon_{n,b'}\}) \leq -2C_1\epsilon_n^{-\frac{2}{b}} = -2C_1n^{\frac{1}{b+2p+1}},$$

leading to

$$e^{C_1 n^{\frac{1}{b+2p+1}}} \Pi(\{\|f\|_{b'} \leq \rho\epsilon_{n,b'}\}) \leq e^{-C_1 n^{\frac{1}{b+2p+1}}} \rightarrow 0,$$

which completes the proof. \blacksquare

Note that a similar result hold for the $\|E(\cdot)\|_2$ norm as well, if we replace Lemma 12 with (29). But $\|E(\cdot)\|_2$ -norm balls cannot be constructed with finite samples.

A.7 Proof of Theorem 5

Recall that in the GPR setting, we have $p = 0$, $m = \lceil n^{\frac{b+1}{b+2p+1}} \rceil = n$, $\Theta_m = \Theta_n$, and $\delta_n = \epsilon_n$. The posterior is $\frac{d\Pi(\cdot|\mathcal{D}^{(n)})}{d\Pi}(f) \propto e^{-n\ell_n(f)}$, where

$$\ell_n(f) = \frac{1}{n} \sum_{i=1}^n (f(x_i) - y_i)^2 \equiv \frac{1}{n} \sum_{i=1}^n (f(x_i) - f_0(x_i))^2 - 2(y_i - f_0(x_i))(f(x_i) - f_0(x_i)).$$

In the second equality above we dropped the term $\frac{1}{n} \sum_i e_i^2$, which is independent of f ; and we recall $\mathbf{e} := \mathbf{y} - f_0(\mathbf{x})$ now satisfies $\mathbb{E}(\mathbf{e} \mid \mathbf{x}) = 0$, $|\mathbf{e}| \leq B$.

Let $\mathbf{l} := (f(\mathbf{x}) - f_0(\mathbf{x}))^2 - 2(\mathbf{y} - f_0(\mathbf{x}))(f(\mathbf{x}) - f_0(\mathbf{x}))$, and l_1, \dots, l_n be its n i.i.d. realizations using x_i, y_i . Then $\frac{1}{n} \sum_{i=1}^n l_i = \ell_n(f)$, $\mathbb{E}\mathbf{l} = \|f - f_0\|_2^2$, $\text{Var}(\mathbf{l}) \leq \mathbb{E}\mathbf{l}^2 \leq \mathbb{E}(f(\mathbf{x}) - f_0(\mathbf{x}))^2 (\|f - f_0\| + 2B)^2 =: \sigma_l^2$, and is bounded by $(\|f - f_0\| + 2B)^2 =: B_l$. By Bernstein's inequality as in Lemma 17, we have, for any fixed f ,

$$\mathbb{P}_{\mathcal{D}^{(n)}}(\ell_n(f) \geq 2\|f - f_0\|_2^2) \leq \exp\left(-\frac{n\|f - f_0\|_2^2}{5(\|f - f_0\| + 2B)^2}\right), \quad (57)$$

$$\mathbb{P}_{\mathcal{D}^{(n)}}\left(\ell_n(f) \leq \frac{1}{3}\|f - f_0\|_2^2\right) \leq \exp\left(-\frac{n\|f - f_0\|_2^2}{10(\|f - f_0\| + 2B)^2}\right). \quad (58)$$

Now we can prove the theorem. It suffices to prove the L_2 case, as the $b' > 0$ case follows by reduction as in Corollary 4. We follow the strategy in Theorem 3, in particular the decomposition in Step 1. All we need are

1. a new bound for the denominator,
2. a new event $A(f, \mathcal{D}^{(n)})$ with probability $\mathbb{P}_{\mathcal{D}^{(n)}}(A^c(f, \mathcal{D}^{(n)})) \leq \exp(-C_{num}n^{\frac{1}{b+1}})$, and a lower bound for $\ell_n(f)$ on the event $A(f, \mathcal{D}^{(n)}) \cap E_{den}$, for any $f \in \Theta_m \cap \text{err}_{n,f}$.

We address them in turn:

1. As all assumptions in Section 4.1 hold, Lemma 20 will still hold, leading to

$$\Pi(\Theta_{d0}) := \Pi(\{\|f - f_0\|_2 \leq C_1\epsilon_n, \|f - f_0\| \leq C_2\}) \geq \exp(-C_3n\epsilon_n^2).$$

By (57) and the definition of Θ_{d0} above, we have

$$\inf_{f \in \Theta_{d0}} \mathbb{P}_{\mathcal{D}^{(n)}}(\{\ell_n(f) \leq 2\|f - f_0\|_2^2\}) \geq 1 - \exp\left(-\frac{nC_1^2\epsilon_n^2}{5(C_2 + 2B)^2}\right) \rightarrow 1. \quad (59)$$

Therefore, by the argument of Step 1 in Proposition 20, we have

$$\int e^{-n\ell_n(f)} \Pi(df) \geq e^{-C'_3n\epsilon_n^2}. \quad (60)$$

2. Let $A(f, \mathcal{D}^{(n)}) := \{\ell_n(f) \geq \frac{1}{3}\|f - f_0\|_2^2\}$ be the complement of the event in (58). As all assumptions in Theorem 3 hold, (53) holds, which says that for all $f \in \Theta_m \cap \text{err}_{n,f}$,

$$\|f - f_0\|^2 \lesssim U^{\frac{2}{b+1}} = \left(\frac{\|f - f_0\|_2^2}{\epsilon_n^2}\right)^{\frac{1}{b+1}}.$$

Plugging back to (58), we have, for some fixed constant $C > 0$,

$$\mathbb{P}_{\mathcal{D}^{(n)}} A^c(f, \mathcal{D}^{(n)}) \leq \exp \left(-Cn(\|f - f_0\|_2^2)^{\frac{b}{b+1}} (\epsilon_n^2)^{\frac{1}{b+1}} \right) \leq \exp \left(-CM^{\frac{b}{b+1}} n \epsilon_n^2 \right),$$

where the last inequality holds because $\|f - f_0\|_2^2 \geq M\epsilon_n^2$. On the event $E_{den} \cap A(f, \mathcal{D}^{(n)})$ we have, for all $f \in \text{err}_{n,f} \cap \Theta_m$,

$$\ell_n(f) \geq \frac{1}{4} \|f - f_0\|_2^2 - 3Bn^{-1} \gtrsim M\epsilon_n^2.$$

Plugging the two displays above to (47), we can establish (46) with $C_{num} \gtrsim M^{\frac{b}{b+1}}$.

Now the proof for Theorem 5 is complete. \blacksquare

A.8 Additional Discussion on the Assumptions

We prove the following claim referenced in the main text.

Lemma 23 *In Assumption 4, (a) implies (b).*

Proof Let $j_n = \lfloor n^{\frac{1}{b+1}} \rfloor$ and $f_n^\dagger := \text{Proj}_{j_n} f_0$. By Lemma 15 with $\tilde{b} = b$, f_n^\dagger satisfies the L_2 approximation condition, and $\|f_n^\dagger\|_{\bar{\mathcal{H}}} \leq \|f_0\|_{\bar{\mathcal{H}}}$ which implies $\|f_0 - f_n^\dagger\| \lesssim 1$ (recall $\bar{\mathcal{H}}$ has a bounded kernel, Lemma 10). Finally, $\|f_n^\dagger\|_{\mathcal{H}}^2 \lesssim \sum_{j=1}^{j_n} j^{b+1} \langle f_n^\dagger, \bar{\varphi}_j \rangle_2 \leq j_n \cdot \sum_{j=1}^{j_n} j^b \langle f_n^\dagger, \bar{\varphi}_j \rangle_2 = j_n \|f_n^\dagger\|_{\mathcal{H}}^2 \leq j_n \|f_0\|_{\mathcal{H}}^2 \lesssim n^{\frac{1}{b+1}}$. \blacksquare

A.8.1 RELAXATION OF ASSUMPTION 7

Consider the following relaxation of Assumption 7 (ii), in which we keep the choice of norm for g unchanged, but relax the inner optimization problem (8) to allow an approximation error of $O(\delta_n)$:

Assumption 7 (ii') *For any $n \in \mathbb{N}$, let $\tilde{\mathcal{I}}_n \subset \mathcal{I}$ be a possibly random subset, and $\{M_n\}$ be a sequence of positive numbers. Then with $\mathbb{P}_{\mathcal{D}^{(n)}}$ probability $\rightarrow 1$, it holds that for any $g \in \mathcal{I}_1$, there exists $g_n \in \tilde{\mathcal{I}}_n$ s.t.*

$$\|g_n - g\|_2 \leq M_n \delta_n, \quad \|g_n\|_{\mathcal{I}} \leq M_n. \quad (61)$$

The definition of the (scaled log) quasi-likelihood (8) is changed into

$$d_n^2(\hat{E}_n f - \hat{b}) := \max_{g \in \tilde{\mathcal{I}}_n} \frac{1}{n} \sum_{j=1}^n \left((f(x_j) - y_j)g(z_j) - \frac{g(z_j)^2}{2} \right) - \frac{\bar{\nu}}{2} \|g\|_{\mathcal{I}}^2.$$

Now Theorem 3 will hold, if we multiply the rates ϵ_n, δ_n by M_n , as its proof follows with minimal modifications: we add the event defined by (61) to the test event E_{den} (and thus E_n) in the proof. Now the denominator bound (Proposition 20) will hold, because the

sup term to be upper bounded is now defined with a smaller scope. For the denominator bound, we replace g_j with its approximation defined in (61), and account for their difference in (50). The subtracted terms will be inflated by a factor of M_n^2 , which can be accounted by multiplying the large constant M in the theorem by M_n^2 . Then the proof follows, and the theorem will hold with M modified accordingly, i.e., with the rate inflated by M_n .

Now we verify the relaxed assumption allows for Nyström approximation for \hat{E}_n , where $\tilde{\mathcal{I}}_n := \text{span}\{k(z_{i_j}, \cdot) : j \in [m]\}$, and z_{i_1}, \dots, z_{i_m} are sampled from the training data. We verify (61) using $g_n := \min_{g_n \in \tilde{\mathcal{I}}_n} \|g_n - g\|_n^2 + \tilde{\nu}_n \|g_n\|_{\mathcal{I}}$, by adapting the analysis of Rudi et al. (2016).¹⁹ Theorem 1 therein shows that for their choice of m , we have, for any $\|g\|_{\mathcal{I}} \leq 1$,

$$\mathbb{P}_{\mathcal{D}^{(n)}}(\|g_n - g\|_2 \lesssim \log \eta^{-1} \delta_n) \geq 1 - \eta. \quad (62)$$

From their proof (in particular, the last display on p. 24) we can see that, in our noiseless setting, the event defined above is independent of g , so the first half of (61) holds. To show $\|g_n\|_{\mathcal{I}} \lesssim 1$, we modify their argument in the proof of Theorem 2 on p. 24.

We now switch to the notations in Rudi et al. (2016), under which we need to show $\|\hat{f}_{\lambda, m}\|_{\mathcal{I}} \lesssim 1$, or equivalently $\|\hat{f}_{\lambda, m} - f_{\mathcal{H}}\|_{\mathcal{I}} \lesssim 1$ for all $\|f_{\mathcal{H}}\|_{\mathcal{H}} \leq 1$.²⁰ It has a similar decomposition as the L_2 error they analyzed: $\|\hat{f}_{\lambda, m} - f_{\mathcal{H}}\|_{\mathcal{H}} \leq \|(I - g_{\lambda, m}(C_n)C_n)f\|_{\mathcal{H}}$. (Note we have dropped their term \mathbf{A} , because we are in the noiseless regime.) Following the last display on their p. 24, with the leading $C^{1/2}$ removed on the first two lines, we find $\|\hat{f}_{\lambda, m} - f_{\mathcal{H}}\|_{\mathcal{H}} \leq R\lambda^{-1/2}(1 + \theta) \cdot \mathbf{B}.1 + R\lambda^{-1/2} \cdot \mathbf{B}.2$. Following the remainder of their proof, and subsequently the proof for their Proposition 2, we find that on the event defined by (62), the RHS above is $O(\lambda^{-1/2} \delta_n \log \eta^{-1})$, where δ_n denotes the L_2 error rate, and $\lambda \asymp \delta_n^2$ is their ridge regularization hyperparameter. Therefore, *switching back to our notations*, we have, on the event (62),

$$\sup_{\|g\|_{\mathcal{I}} \leq 1} \|g_n - g\|_{\mathcal{I}} \lesssim \log \eta^{-1}.$$

Thus, we can set M_n as any slowly increasing sequence, so that $\eta = e^{-M_n} \rightarrow 0$, and the assumption will hold. It may be possible to replace the increasing $\{M_n\}$ with a fixed M , using a more sophisticated choice of g_n and/or a slightly larger m , but such a discussion is beyond the scope for this work.

Appendix B. Deferred Derivations in Section 5

B.1 Proof of Proposition 7

Define

$$\hat{\mathcal{V}} := \hat{C}_{xz} \hat{C}_{zz, \bar{\nu}}^{-1} \hat{C}_{zx}, \quad A := (\hat{\mathcal{V}} + \bar{\lambda} I)^{-1} \hat{C}_{xz} \hat{C}_{zz, \bar{\nu}}^{-1} \frac{S_z^*}{n}, \quad P := AS_x = (\hat{\mathcal{V}} + \bar{\lambda} I)^{-1} \hat{\mathcal{V}}, \quad E := Y - f(X),$$

so that AY maps the observed data $Y \in \mathbb{R}^n$ to the IV mean prediction, i.e., $\hat{f}_n = A(f(X) + E)$. By (70) below we can see that

$$\mathcal{C} = I - P.$$

¹⁹. This is noiseless KRR, so their analysis applies; recall that our definition of g_n does not have to match \hat{E}_n in any sense. We also note that we use the extended version of Rudi et al. (2016) on arXiv.

²⁰. Our notations $g_n, g, \bar{\nu}, \mathcal{I}$ corresponds to their $\hat{f}_{\lambda, m}, f_{\mathcal{H}}, \lambda, \mathcal{H}$, respectively.

For (18), we have

$$\begin{aligned}
 \sup_{\|f\|_{\mathcal{H}}=1} \mathbb{E} \langle \hat{f}_n - f_0, k_* \rangle_{\mathcal{H}}^2 &= \sup_{\|f\|_{\mathcal{H}}=1} \mathbb{E} (\langle A(f(X) + E), k_* \rangle_{\mathcal{H}} - \langle f, k_* \rangle_{\mathcal{H}})^2 \\
 &= \sup_{\|f\|_{\mathcal{H}}=1} \langle Af(X), k_* \rangle_{\mathcal{H}} - f(x_*)^2 + \lambda k_*^\top A A^\top k_* \\
 &= \sup_{\|f\|_{\mathcal{H}}=1} (\langle f, \tilde{h} \rangle_{\mathcal{H}})^2 + \lambda k_*^\top A A^\top k_* = \|\tilde{h}\|_{\mathcal{H}}^2 + \lambda k_*^\top A A^\top k_*,
 \end{aligned}$$

where $\tilde{h} := k_*^\top A k(X, \cdot) - k(x_*, \cdot)$. Plugging back, we have

$$\sup_{\|f\|_{\mathcal{H}}=1} \mathbb{E} \langle \hat{f}_n - f_0, k_* \rangle_{\mathcal{H}}^2 = k_{**} - 2k_*^\top A k_{X*} + k_*^\top A k(X, X) A^\top k_* + \lambda k_*^\top A A^\top k_* =: k_*^\top \tilde{\mathcal{C}} k_*,$$

where

$$\begin{aligned}
 \tilde{\mathcal{C}} &= I - 2AS_x + A(S_x S_x^* + \lambda I) A^\top \\
 &= I - 2(\hat{\mathcal{V}} + \bar{\lambda} I)^{-1} \hat{\mathcal{V}} + (\hat{\mathcal{V}} + \bar{\lambda} I)^{-1} \hat{C}_{xz} \hat{C}_{zz, \bar{\nu}}^{-1} \frac{S_z^*}{n} (S_x S_x^* + n \bar{\lambda} I) \frac{S_z}{n} \hat{C}_{zz, \bar{\nu}}^{-1} \hat{C}_{zx} (\hat{\mathcal{V}} + \bar{\lambda} I)^{-1} \\
 &\stackrel{(a)}{=} I - 2(\hat{\mathcal{V}} + \bar{\lambda} I)^{-1} \hat{\mathcal{V}} + (\hat{\mathcal{V}} + \bar{\lambda} I)^{-1} (\hat{\mathcal{V}} \hat{\mathcal{V}} + \bar{\lambda} \hat{\mathcal{V}} - \hat{C}_{xz} \hat{C}_{zz, \bar{\nu}}^{-1} \cdot \bar{\lambda} \bar{\nu} I \cdot \hat{C}_{zz, \bar{\nu}}^{-1} \hat{C}_{zx}) (\hat{\mathcal{V}} + \bar{\lambda} I)^{-1} \\
 &= I - (\hat{\mathcal{V}} + \bar{\lambda} I)^{-1} \hat{\mathcal{V}} - (\hat{\mathcal{V}} + \bar{\lambda} I)^{-1} \hat{C}_{xz} \hat{C}_{zz, \bar{\nu}}^{-1} \cdot \bar{\lambda} \bar{\nu} I \cdot \hat{C}_{zz, \bar{\nu}}^{-1} \hat{C}_{zx} (\hat{\mathcal{V}} + \bar{\lambda} I)^{-1} \\
 &\stackrel{(b)}{=} \mathcal{C} - \Delta \mathcal{C}.
 \end{aligned}$$

In the above, (a) holds because we can replace the $\hat{\mathcal{V}}$ term in RHS with $\hat{C}_{xz} \hat{C}_{zz, \bar{\nu}}^{-1} \hat{C}_{zz, \bar{\nu}} \hat{C}_{zz, \bar{\nu}}^{-1} \hat{C}_{zx}$, and (b) since $\mathcal{C} = I - (\hat{\mathcal{V}} + \bar{\lambda} I)^{-1} \hat{\mathcal{V}}$. The last equality shows that (18) holds, and

$$\Delta \mathcal{C} = (\hat{\mathcal{V}} + \bar{\lambda} I)^{-1} \hat{C}_{xz} \hat{C}_{zz, \bar{\nu}}^{-1} \cdot \bar{\lambda} \bar{\nu} I \cdot \hat{C}_{zz, \bar{\nu}}^{-1} \hat{C}_{zx} (\hat{\mathcal{V}} + \bar{\lambda} I)^{-1} \quad (63)$$

is non-negative.

For (19), we have

$$\mathbb{E}_f \mathbb{E}_E (\langle A(f(X) + E), k_* \rangle_{\mathcal{H}} - \langle f, k_* \rangle_{\mathcal{H}})^2 = k_*^\top A(k(X, X) + \lambda I) A^\top k_* + k_{**} - 2k_*^\top A k_{X*},$$

so the proof follows (18). ■

B.2 Additional Discussion

Consider the *stochastic* estimator

$$\hat{f}_{sn} := \bar{A}Y := \min_{f \in \mathcal{H}} \max_{g \in \mathcal{I}} \frac{1}{n} \sum_{i=1}^n \left((f(x_i) - y_i)g(z_i) - \frac{g(z_i)^2}{2} \right) - \frac{\bar{\nu}}{2} \|g - g_{rp}\|_{\mathcal{I}}^2 + \frac{\bar{\lambda}}{2} \|f\|_{\mathcal{H}}^2,$$

where $g_{rp} \sim \mathcal{GP}(0, \lambda \nu^{-1} k_z)$. With direct calculations similar to the above, we can show that, in the unconfounded setting as Proposition 7,

$$\langle k_*, \mathcal{C} k_* \rangle_{\mathcal{H}} = \sup_{\|f_0\|_{\mathcal{H}}=1} \mathbb{E}_{Y|X, Z} \langle k_*, \hat{f}_{sn} - f_0 \rangle_{\mathcal{H}}^2 = \mathbb{E}_{f_0 \sim \mathcal{GP}(0, k_x)} \mathbb{E}_{Y|X, Z} \langle k_*, \hat{f}_{sn} - f_0 \rangle_{\mathcal{H}}^2, \quad (64)$$

i.e., the marginal variance actually represents the estimation error using the stochastic estimator, due to the additional term $\Delta\mathcal{C}$.

We now discuss the behavior of \hat{f}_{sn} . Clearly we have $\mathbb{E}_{g_{rp}}\hat{f}_{sn} = \hat{f}_n$ (in the sense that evaluations of any bounded linear functional equal). Conditioned on $\mathcal{D}^{(n)}$, \hat{f}_{sn} has a non-zero variance, but the variance is smaller than the posterior draw (65). We can verify that it replaced the conditional expectation estimate $\hat{E}_n(f - f_0)$, which is the inner loop optima in (4), with a draw from the GPR posterior constructed from the problem of conditional expectation estimation. It thus accounts for the uncertainty in the first-stage estimation, and one may hope that it has a more stable behavior in the presence of confounding, in which case the estimation error may be higher.

Readers may find it counterintuitive that the marginal variance of the quasi-posterior represents estimation error of a different estimator \hat{f}_{sn} , as opposed to the posterior mean \hat{f}_n , which is different from the GPR setting. Fundamentally, the reason is that the quasi-likelihood involves the regularization term $\bar{\nu}\|g\|_{\tilde{\mathcal{I}}}^2$. Also, recall that contrary to the GPR setting, the unconfounded data generating process considered in Proposition 7 is not fully representative of the typical scenario; hence, the difference may be reasonable.

Appendix C. Analysis of the Approximate Inference Algorithm

C.1 Proof of the Double Randomized Prior Trick

C.1.1 A FUNCTION-SPACE EQUIVALENT TO PROPOSITION 8

We first claim that Proposition 8 is equivalent to the following function-space version, the proof of which is deferred to Section C.1.3:

Proposition 24 *Let $\tilde{\mathcal{H}}, \tilde{\mathcal{I}}$ be finite-dimensional RKHSes with kernels k_x, k_z , respectively,*

$$g_0 \sim \mathcal{GP}(0, \lambda\nu^{-1}\tilde{k}_z), \quad f_0 \sim \mathcal{GP}(0, \tilde{k}_x), \quad \tilde{y}_i \sim \mathcal{N}(y_i, \lambda).$$

Then the optima f^ of*

$$\min_{f \in \tilde{\mathcal{H}}} \max_{g \in \tilde{\mathcal{I}}} \mathcal{L}(f, g) := \sum_{i=1}^n \left((f(x_i) - \tilde{y}_i)g(z_i) - \frac{g(z_i)^2}{2} \right) - \frac{\nu}{2}\|g - g_0\|_{\tilde{\mathcal{I}}}^2 + \frac{\lambda}{2}\|f - f_0\|_{\tilde{\mathcal{H}}}^2 \quad (65)$$

follows the posterior distribution (10), with the kernels replaced by \tilde{k}_x, \tilde{k}_z .

Proof [Proof of the equivalence] Observe that (65) is exactly the same as (20) when the random feature parameterization $\phi \mapsto g(z; \phi)$ is injective,²¹ in which case we have $\|\phi\|_2 = \|g(\cdot; \phi)\|_{\tilde{\mathcal{I}}}$. Otherwise, observe that on the subspace

$$\Phi_s := \text{span}\{\phi_{z,m}(z') : z' \in \mathcal{Z}\},$$

$\|\phi\|_2 = \|g(\cdot; \phi)\|_{\tilde{\mathcal{I}}}$ always holds: this follows by definition of \tilde{k}_z when ϕ is a finite linear combination of the ϕ 's, and the general case follows by continuity (note that $\tilde{\mathcal{I}}$ is already defined by \tilde{k}_z). Clearly any $g - g_0 \in \tilde{\mathcal{I}}$ can be parameterized with some ϕ in this subspace, so

21. Most random feature models, such as the random Fourier feature model, satisfies this property almost surely.

the optima of (65) is a valid candidate solution for (20). On the other hand, for any $\phi - \phi_0$ outside the aforementioned subspace, we have $\|\phi - \phi_0\|_2 > \|g(\cdot; \phi) - g(\cdot; \phi_0)\|_{\tilde{\mathcal{X}}}$. Therefore, the optimal ϕ of (20) must satisfy $\|\phi - \phi_0\|_2 = \|g(\cdot; \phi) - g(\cdot; \phi_0)\|_{\tilde{\mathcal{X}}}$, and thus solves (65). As a similar result also holds for f , we conclude that the two objectives are equivalent. ■

Remark 25 *The non-injective setting above justifies the formal analysis of (21) in the main text. We also remark that any parameter θ, ϕ visited by the SGDA algorithm on (20) or (21) (starting from θ_0, ϕ_0) satisfies*

$$\theta - \theta_0 \in \Theta_s, \quad \phi - \phi_0 \in \Phi_s.$$

Thus $\|\phi - \phi_0\|_2 = \|g(\cdot; \phi) - g(\cdot; \phi_0)\|_{\tilde{\mathcal{X}}}$ (and similarly for θ), and from the perspective of the SGDA algorithm, the objectives (65) and (20) are always the same. This can be proved by induction. Take ϕ for example; clearly $\phi = \phi_0$ satisfies the above. For ϕ_ℓ obtained at the ℓ -th step of SGDA, we have

$$\phi_\ell - \phi_0 = (1 - \nu)(\phi_{\ell-1} - \phi_0) + V_\ell^\top \phi_{z,m}(Z),$$

where $V_\ell \in \mathbb{R}^n$ is independent of ϕ_ℓ . Thus $\phi_\ell - \phi_0 \in \Phi_s$ by definition of Φ_s and the inductive hypothesis.

C.1.2 MATRIX IDENTITIES

We list two identities here that will be used in the derivations.

Lemma 26 *Let U, C, V, S be operators between appropriate Banach spaces, $\lambda \in \mathbb{R} \setminus \{0\}$, then*

$$(\lambda I + UCV)^{-1} = \lambda^{-1}(I - U(\lambda C^{-1} + VU)^{-1}V), \quad (66)$$

$$S(S^*S + \lambda I)^{-1} = (SS^* + \lambda I)^{-1}S. \quad (67)$$

Proof Recall the Woodbury identity:

$$(A + UCV)^{-1} = A^{-1} - A^{-1}U(C^{-1} + VA^{-1}U)^{-1}VA^{-1}.$$

Then, we have

$$\begin{aligned} (\lambda I + UCV)^{-1} &= \lambda^{-1}I - \lambda^{-2}U(C^{-1} + \lambda^{-1}VU)^{-1}V = \lambda^{-1}(I - U(\lambda C^{-1} + VU)^{-1}V). \\ S(S^*S + \lambda I)^{-1} &= S(\lambda^{-1}I - \lambda^{-2}S^*(\lambda^{-1}SS^* + I)^{-1}S) = \lambda^{-1}(S - SS^*(SS^* + \lambda I)^{-1}S) \\ &= (SS^* + \lambda I)^{-1}S. \end{aligned}$$

■

C.1.3 PROOF OF PROPOSITION 24

Define $Y = (y_1, \dots, y_n)$, $\tilde{Y} = (\tilde{y}_1, \dots, \tilde{y}_n)$. We rewrite the objective as

$$\begin{aligned}\mathcal{L}(f, g) &= \left(\langle n\hat{C}_{zx}f - S_z^*\tilde{Y}, g \rangle_{\tilde{\mathcal{I}}} - \frac{1}{2} \langle n\hat{C}_{zz}g, g \rangle_{\tilde{\mathcal{I}}} - \frac{\nu}{2} \|g - g_0\|_{\tilde{\mathcal{I}}}^2 \right) + \frac{\lambda}{2} \|f - f_0\|_{\mathcal{H}}^2 \\ &= n \left(\langle \hat{C}_{zx}f - n^{-1}S_z^*\tilde{Y}, g \rangle_{\tilde{\mathcal{I}}} - \frac{1}{2} \langle \hat{C}_{zz,\bar{\nu}}g, g \rangle_{\tilde{\mathcal{I}}} + \bar{\nu} \langle g, g_0 \rangle_{\tilde{\mathcal{I}}} - \frac{\bar{\nu}}{2} \|g_0\|_{\tilde{\mathcal{I}}}^2 \right) + \frac{\lambda}{2} \|f - f_0\|_{\mathcal{H}}^2,\end{aligned}$$

where $S_z, \hat{C}_{zx}, \hat{C}_{zz}$ are now defined w.r.t. the approximate kernels. The optimal g^* for fixed f is

$$g^*(f) = \hat{C}_{zz,\bar{\nu}}^{-1}(\hat{C}_{zx}f - n^{-1}S_z^*\tilde{Y} + \bar{\nu}g_0). \quad (68)$$

Plugging g^* back to the objective, we have

$$\begin{aligned}\mathcal{L}(f, g^*(f)) &= \frac{n}{2} \langle g^*, \hat{C}_{zz,\bar{\nu}}g^* \rangle_{\tilde{\mathcal{I}}} + \frac{\lambda}{2} \|f - f_0\|_{\mathcal{H}}^2 - \frac{n\bar{\nu}}{2} \|g_0\|_{\tilde{\mathcal{I}}}^2, \\ \partial_f \mathcal{L} &= n\hat{C}_{xz}\hat{C}_{zz,\bar{\nu}}^{-1}\hat{C}_{zz,\bar{\nu}}g^* + \lambda(f - f_0) = n\hat{C}_{xz}\hat{C}_{zz,\bar{\nu}}^{-1}(\hat{C}_{zx}f - n^{-1}S_z^*\tilde{Y} + \bar{\nu}g_0) + \lambda(f - f_0).\end{aligned}$$

Setting $\partial_f \mathcal{L}$ to zero, we obtain

$$f^* = (n\hat{C}_{xz}\hat{C}_{zz,\bar{\nu}}^{-1}\hat{C}_{zx} + \lambda I)^{-1}(n\hat{C}_{xz}\hat{C}_{zz,\bar{\nu}}^{-1}(n^{-1}S_z^*\tilde{Y} - \bar{\nu}g_0) + \lambda f_0). \quad (69)$$

Since

$$\begin{aligned}(n\hat{C}_{xz}\hat{C}_{zz,\bar{\nu}}^{-1}\hat{C}_{zx} + \lambda I)^{-1} &= (n^{-1}S_x^*S_z\hat{C}_{zz,\bar{\nu}}^{-1}S_z^*S_x + \lambda I)^{-1} = (S_x^*LS_x + \lambda I)^{-1} \\ &\stackrel{(66)}{=} \lambda^{-1} \underbrace{(I - S_x^*(\lambda L^{-1} + S_xS_x^*)^{-1}S_x)}_{\text{defined as } \mathcal{C}},\end{aligned} \quad (70)$$

we can rewrite f^* as

$$f^* = \lambda^{-1}\mathcal{C}(\hat{C}_{xz}\hat{C}_{zz,\bar{\nu}}^{-1}(S_z^*\tilde{Y} - \nu g_0) + \lambda f_0).$$

Clearly, f^* is a Gaussian process. Suppose $f^*(x_*) \sim \mathcal{N}(S_*\mu', S_*C'S_*^*)$, then

$$\begin{aligned}\mu' &= \lambda^{-1}\mathcal{C}n\hat{C}_{xz}\hat{C}_{zz,\bar{\nu}}^{-1}(n^{-1}S_z^*Y) = \lambda^{-1}(I - S_x^*(\lambda L^{-1} + S_xS_x^*)^{-1}S_x)S_x^*LY \\ &= \lambda^{-1}S_x^*(I - (\lambda L^{-1} + S_xS_x^*)^{-1}S_xS_x^*)LY = S_x^*(\lambda L^{-1} + S_xS_x^*)^{-1}Y.\end{aligned}$$

The RHS above matches the posterior mean (11) (with k_x, k_z replaced by their random feature approximations) since $S_xS_x^* = K_{xx}$ and

$$S_*\mu' = S_*S_x^*(\lambda L^{-1} + S_xS_x^*)^{-1}Y = K_{*x}(\lambda L^{-1} + K_{xx})^{-1}Y = K_{*x}(\lambda + LK_{xx})^{-1}LY.$$

As $\tilde{Y} - Y, g_0$ and f_0 are independent, the covariance operator of f^* is

$$\begin{aligned}C' &= \lambda^{-1}\mathcal{C}(\hat{C}_{xz}\hat{C}_{zz,\bar{\nu}}^{-1}(n\lambda\hat{C}_{zz} + \lambda\nu I)\hat{C}_{zz,\bar{\nu}}^{-1}\hat{C}_{zx} + \lambda^2 I)\lambda^{-1}\mathcal{C} \\ &= \lambda^{-1}\mathcal{C}(\lambda n\hat{C}_{xz}\hat{C}_{zz,\bar{\nu}}^{-1}\hat{C}_{zx} + \lambda^2 I)\lambda^{-1}\mathcal{C} \stackrel{(70)}{=} \mathcal{C}.\end{aligned}$$

In view of (70), we know

$$S_*C'S_*^* = S_*S_x^* - S_*S_x^*(\lambda L^{-1} + S_xS_x^*)^{-1}S_xS_x^* = K_{**} - K_{*x}(\lambda L^{-1} + K_{xx})^{-1}K_{x*},$$

which matches the posterior covariance matrix (12) with replaced kernels.

Remark 27 For the discussion in Section 5, observe that (69) implies the posterior mean estimator \hat{f}_n satisfies

$$\hat{f}_n = (n\hat{C}_{xz}\hat{C}_{zz,\bar{\nu}}^{-1}\hat{C}_{zx} + \lambda I)^{-1}n\hat{C}_{xz}\hat{C}_{zz,\bar{\nu}}^{-1}\left(\hat{C}_{zx}f_0 + \frac{S_z^*(Y - f_0(X))}{n}\right), \quad (71)$$

The derivations do not rely on the RKHSes being finite-dimensional.

C.2 Assumptions in Proposition 9

The subsequent analysis will rely on the following assumptions on the random feature expansion. We only state them for x for conciseness; the requirements for z are similar.

The following assumption holds for, e.g., random Fourier features Rahimi et al. (2007).

Assumption 8 As $m \rightarrow \infty$, it holds that $\sup_{x,x' \in \mathcal{X}} |k_x(x, x') - \tilde{k}_{x,m}(x, x')| \xrightarrow{p} 0$.

Assumption 9 There exists a constant $\tilde{\kappa} > 0$ such that $\max_{m \in \mathbb{N}} \sup_{x \in \mathcal{X}} \tilde{k}_{x,m}(x, x) \leq \tilde{\kappa}$.

C.3 Analysis of Random Feature Approximation

We recall the following facts: for $A, B \in \mathbb{R}^{n \times n}$,

$$\|A\| \leq \|A\|_F \leq \sqrt{n}\|A\|, \quad A^{-1} - B^{-1} = A^{-1}(B - A)B^{-1}.$$

Lemma 28 For all $m \in \mathbb{N}$, let $k_{x,m}$ be a random feature approximation to k_x such that Assumption 8 holds, and let $\tilde{k}_{z,m}$ be an approximation to k_z satisfying a similar requirement as above. Then the random feature-approximated posterior $\Pi_m(f(x_*) \mid \mathcal{D}^{(n)}) = \mathcal{N}(\tilde{\mu}, \tilde{S})$ satisfies

$$\lim_{m \rightarrow \infty} \sup_{x^* \in \mathcal{X}^l} \|\mu - \tilde{\mu}\|_2 = 0, \quad \lim_{m \rightarrow \infty} \sup_{x^* \in \mathcal{X}^l} \|\tilde{S} - S\|_F = 0,$$

for any fixed training data (X, Y, Z) , $l \in \mathbb{N}$, and $\lambda, \nu > 0$. In the above, $\tilde{\mu}$ and \tilde{S} are defined as in (11)-(12), but with the Gram matrices redefined using $\tilde{k}_{x,m}$ and $\tilde{k}_{z,m}$.

Proof Define

$$\epsilon_m := \max \left(\sup_{x,x' \in \mathcal{X}} |k(x, x') - \tilde{k}_{x,m}(x, x')|, \sup_{z,z' \in \mathcal{Z}} |k(z, z') - \tilde{k}_{z,m}(z, z')| \right).$$

By assumption $\epsilon_m \xrightarrow{p} 0$. For \tilde{S} we consider the decomposition

$$\begin{aligned} \|\tilde{S} - S\| &\leq \|\tilde{K}_{**} - K_{**}\| \\ &\quad + \|\tilde{K}_{*x} - K_{*x}\| \|\tilde{L}\| \|(\lambda I + \tilde{K}_{xx}\tilde{L})^{-1}\tilde{K}_{x*}\| \\ &\quad + \|K_{*x}\| \|\tilde{L} - L\| \|(\lambda I + \tilde{K}_{xx}\tilde{L})^{-1}\tilde{K}_{x*}\| \\ &\quad + \|K_{*x}L\| \|(\lambda I + \tilde{K}_{xx}\tilde{L})^{-1} - (\lambda I + K_{xx}L)^{-1}\| \|\tilde{K}_{x*}\| \\ &\quad + \|K_{*x}L(\lambda I + K_{xx}L)^{-1}\| \|\tilde{K}_{x*} - K_{x*}\| \\ &=: \text{(I)} + \text{(II)} + \text{(III)} + \text{(IV)} + \text{(V)}. \end{aligned}$$

In the following, we use $O(\cdot)$ and $O_p(\cdot)$ to represent the asymptotic behaviour when $m \rightarrow \infty$. Since n and l are fixed, the operator norms of the matrices K_{*x}, L, K_{xx} are $O(1)$. Observe that $\|K_{zz} - \tilde{K}_{zz}\| \leq \sqrt{n}\epsilon_m$. By the triangle inequality, the inequality $\|\cdot\| \leq \|\cdot\|_F$ and the boundedness of $\tilde{k}_{x,m}$ and $\tilde{k}_{z,m}$, we have $\|\tilde{K}_{*x}\| = O(1)$. Both $O(\cdot)$ terms above are independent of x^* . Finally, recall that $\|L\| = \|K_{zz}(K_{zz} + \nu I)^{-1}\| \leq 1$ and similarly $\|\tilde{L}\| \leq 1$. Using these facts, we have

$$\begin{aligned}
\text{(I)} &\leq \|\tilde{K}_{**} - K_{**}\|_F \leq l\epsilon_m \rightarrow 0. \\
\text{(II)} &\leq \sqrt{ln}\epsilon_m \cdot 1 \cdot \lambda^{-1} \cdot O(1) \rightarrow 0. \\
\|\tilde{L} - L\| &= \|K_{zz}(K_{zz} + \nu I)^{-1} - \tilde{K}_{zz}(\tilde{K}_{zz} + \nu I)^{-1}\| \rightarrow 0. \\
&\leq \|K_{zz} - \tilde{K}_{zz}\| \cdot \nu^{-1} + \|\tilde{K}_{zz}(\tilde{K}_{zz} + \nu I)^{-1}\| \|(K_{zz} - \tilde{K}_{zz})(K_{zz} + \nu I)^{-1}\| \\
&\leq 2\sqrt{n}\epsilon_m \cdot \nu^{-1} \rightarrow 0. \\
\text{(III)} &\leq O(1) \cdot \|\tilde{L} - L\| \cdot \lambda^{-1} O(1) \rightarrow 0 \\
\text{(IV)} &= O(1) \cdot \|(\lambda I + \tilde{K}_{xx}\tilde{L})^{-1}\| \|\tilde{K}_{xx}\tilde{L} - K_{xx}L\| \|(\lambda I + K_{xx}L)^{-1}\| \\
&\leq O(1) \cdot \lambda^{-2} \cdot (\|\tilde{K}_{xx} - K_{xx}\| \|\tilde{L}\| + \|K_{xx}\| \|\tilde{L} - L\|) \rightarrow 0. \\
\text{(V)} &= O(1) \cdot \sqrt{ln}\epsilon_m \rightarrow 0.
\end{aligned}$$

Moreover, the converges above are all independent of the choice of x^* . Thus we have

$$\sup_{x^* \in \mathcal{X}^l} \|\tilde{S} - S\|_F \leq l \sup_{x^* \in \mathcal{X}^l} \|\tilde{S} - S\| \rightarrow 0.$$

Using a similar argument we have $\sup_{x^* \in \mathcal{X}^l} \|\tilde{\mu} - \mu\|_2 \rightarrow 0$. ■

C.4 Analysis of the Optimization Algorithm

Algorithm 1: Modified randomized prior algorithm for approximate inference.

Input: Hyperparameters $\nu, \lambda \in \mathbb{R}$. Random feature models $\theta \mapsto f(\cdot; \theta)$,

$\varphi \mapsto g(\cdot; \varphi)$.

Result: A single sample from the approximate posterior

Initialize: draw $\theta_0 \sim \mathcal{N}(0, I)$, $\varphi_0 \sim \mathcal{N}(0, \lambda\nu^{-1}I)$, $\tilde{Y} \sim \mathcal{N}(Y, \lambda I)$;

for $\ell \leftarrow 1, \dots, L-1$ **do**

$\hat{\theta}_\ell \leftarrow \theta_{\ell-1} - \eta_\ell \hat{\nabla}_\theta \mathcal{L}_{\text{rf}}(\theta_{\ell-1}, \varphi_{\ell-1}, \theta_0, \varphi_0);$
 $\hat{\varphi}_\ell \leftarrow \varphi_{\ell-1} + \eta_\ell \hat{\nabla}_\varphi \mathcal{L}_{\text{rf}}(\theta_{\ell-1}, \varphi_{\ell-1}, \theta_0, \varphi_0);$
 $\theta_{\ell+1} \leftarrow \text{Proj}_{B_f}(\hat{\theta}_\ell);$
 $\varphi_{\ell+1} \leftarrow \text{Proj}_{B_g}(\hat{\varphi}_\ell);$

end

return $f(\cdot; \theta_L)$

For the purpose of the analysis we consider the standard SGDA algorithm as outlined in Algorithm 1. In the algorithm \mathcal{L}_{rf} denotes the objective in (20), and Proj_B denotes the

projection into the ℓ_2 -norm ball with radius B , and $\hat{\nabla}\mathcal{L}_{\text{rf}}$ represents a stochastic (unbiased) approximation of the gradient $\nabla\mathcal{L}_{\text{rf}}$. In the following, we will suppress the dependency of \mathcal{L}_{rf} on θ_0, φ_0 for simplicity.

Concretely, we introduce the notations

$$\Phi_f := \frac{1}{\sqrt{m}} \begin{bmatrix} \phi_{x,m}(x_1)^\top \\ \vdots \\ \phi_{x,m}(x_n)^\top \end{bmatrix} \in \mathbb{R}^{n \times m}, \quad \Phi_g := \frac{1}{\sqrt{m}} \begin{bmatrix} \phi_{z,m}(z_1)^\top \\ \vdots \\ \phi_{z,m}(z_n)^\top \end{bmatrix} \in \mathbb{R}^{n \times m},$$

where we recall $X := (x_1, \dots, x_n)$ and $Z := (z_1, \dots, z_n)$ are the training data.

Observe that $\Phi_f \theta = f(X; \theta)$, $\Phi_g \varphi = g(Z; \varphi)$, we can rewrite the objective (20) as

$$\mathcal{L}_{\text{rf}}(\theta, \varphi) = \theta^\top \Phi_f^\top \Phi_g \varphi - \tilde{Y}^\top \Phi_g \varphi - \frac{1}{2} \varphi^\top \Phi_g^\top \Phi_g \varphi - \frac{\nu}{2} \|\varphi - \varphi_0\|_2^2 + \frac{\lambda}{2} \|\theta - \theta_0\|_2^2. \quad (72)$$

We additionally define

$$\mathcal{L}_i(\theta, \varphi) = n \left(\theta^\top \Phi_f^\top E_i \Phi_g \varphi - \tilde{Y}^\top E_i \Phi_g \varphi - \frac{1}{2} \varphi^\top \Phi_g^\top E_i \Phi_g \varphi \right) - \frac{\nu}{2} \|\varphi - \varphi_0\|_2^2 + \frac{\lambda}{2} \|\theta - \theta_0\|_2^2,$$

where $E_i := e_i e_i^\top$ and $\{e_i\}_{i \in [n]}$ is the standard orthogonal basis of \mathbb{R}^n . We can see that $\mathcal{L}_{\text{rf}}(\theta, \varphi) = \frac{1}{n} \sum_{i \in [n]} \mathcal{L}_i(\theta, \varphi)$. Therefore, the stochastic gradient in Algorithm 1 can be defined as

$$\hat{\nabla}\mathcal{L}_{\text{rf}}(\theta, \varphi) := \nabla\mathcal{L}_{\mathcal{I}}(\theta, \varphi) = \sum_{i \in [n]} \nabla\mathcal{L}_i(\theta, \varphi) \mathbf{1}_{i=\mathcal{I}}, \quad (73)$$

where \mathcal{I} is a random variable sampled from the uniform distribution of the set $[n]$.

In practice we run the algorithm concurrently on J sets of parameters, starting from independent draws of initial conditions $\{\theta_0^{(j)}, \varphi_0^{(j)}\}$; moreover, the projection is not implemented, and there are various other modifications to further improve stability, as described in Appendix D.2.

The following lemma is a convergence theorem of Algorithm 1 under the choice of stochastic gradient defined in (73).

Lemma 29 *Fix an $m \in \mathbb{N}$. Denote by θ^* the optima of (20) and take $\eta_\ell := \frac{1}{\mu(\ell+1)}$ with $\mu = \min\{\lambda, \nu\}$. Then for any $\epsilon, B_1, B_2, B_3 > 0$, there exist $B_f, B_g > 0$ such that when $L = \Omega(\delta^{-1}\epsilon^{-2})$, the approximate optima θ_L returned by Algorithm 1 satisfies*

$$\mathbb{P}(\{\|\theta_L - \theta^*\|_2 > \epsilon\} \cap E_n) \leq \delta,$$

where

$$E_n := \left\{ \|\theta_0\|_2 + \|\varphi_0\|_2 \leq B_1, \|\tilde{Y}\|_2 \leq B_2, \sup_{z \in \mathcal{Z}} \tilde{k}_{z,m}(z, z) + \sup_{x \in \mathcal{X}} \tilde{k}_{x,m}(x, x) \leq B_3 \right\},$$

and $\tilde{k}_{\cdot,m}$ denotes the random feature-approximated kernel. The randomness in the statement above is from the sampling of the initial values θ_0, φ_0 , the gradient noise.

Proof Recall from (69) that θ^* is a sum of bounded linear transforms of θ_0, φ_0 and \tilde{Y}_0 . Thus on the event E_n , $\|\theta^*\|_2$ is bounded. Similarly, $\|\varphi^*\|_2$ is also bounded on E_n by (68). We choose B_f and B_g to be their maximum values on the event E_n .

As \mathcal{L}_{rf} is strongly-convex in θ , and strongly-concave in φ , it has the unique stationary point (θ^*, φ^*) . We will then bound $\|\theta_\ell - \theta^*\|_2^2 + \|\varphi_\ell - \varphi^*\|_2^2$. Let σ_f, σ_g be the minimal constants such that $\|\nabla_\theta \mathcal{L}_i(\theta, \varphi)\|_2^2 \leq \sigma_f^2$, $\|\nabla_\varphi \mathcal{L}_i(\theta, \varphi)\|_2^2 \leq \sigma_g^2$ for all $i \in [n]$, $\|\theta\|_2 \leq B_f$ and $\|\varphi\|_2 \leq B_g$. Denote $B := \max\{B_f, B_g\}$, so we have $\|\theta\|_2, \|\varphi\|_2 \leq B$. Define

$$r_\ell = \mathbb{E} [\|\theta_\ell - \theta^*\|_2^2 + \|\varphi_\ell - \varphi^*\|_2^2].$$

We want to know how r_ℓ contracts. We first make a stochastic gradient step on θ_ℓ with step size η_ℓ , i.e., $\hat{\theta}_{\ell+1} := \theta_\ell - \eta_\ell \hat{\nabla}_\theta \mathcal{L}_{\text{rf}}(\theta_\ell, \varphi_\ell)$ with $\hat{\nabla}_\theta \mathcal{L}_{\text{rf}}$ defined in (73). Then,

$$\mathbb{E}[\|\hat{\theta}_{\ell+1} - \theta^*\|_2^2 \mid \theta_\ell, \varphi_\ell] \leq \|\theta_\ell - \theta^*\|_2^2 - 2\eta_\ell \langle \theta_\ell - \theta^*, \nabla_\theta \mathcal{L}(\theta_\ell, \varphi_\ell) \rangle + \eta_\ell^2 \sigma_f^2,$$

where the expectation is taken with respect to the randomness of the gradient. For the above inner product term, we have that

$$\begin{aligned} \langle \theta_\ell - \theta^*, \nabla_\theta \mathcal{L}_{\text{rf}}(\theta_\ell, \varphi_\ell) \rangle &= \langle \theta_\ell - \theta^*, \nabla_\theta \mathcal{L}_{\text{rf}}(\theta_\ell, \varphi_\ell) - \nabla_\theta \mathcal{L}_{\text{rf}}(\theta^*, \varphi^*) \rangle \\ &= \lambda \|\theta_\ell - \theta^*\|_2^2 + \langle \theta_\ell - \theta^*, \Phi_f^\top \Phi_g(\varphi_\ell - \varphi^*) \rangle. \end{aligned}$$

Next, we consider the gradient step on φ_ℓ with step size η_ℓ , i.e., $\hat{\varphi}_{\ell+1} := \varphi_\ell + \eta_\ell \hat{\nabla}_\varphi \mathcal{L}_{\text{rf}}(\theta_\ell, \varphi_\ell)$. Then, we have that

$$\mathbb{E}[\|\hat{\varphi}_{\ell+1} - \varphi^*\|_2^2 \mid \theta_\ell, \varphi_\ell] \leq \|\varphi_\ell - \varphi^*\|_2^2 + 2\eta_\ell \langle \varphi_\ell - \varphi^*, \nabla_\varphi \mathcal{L}_{\text{rf}}(\theta_\ell, \varphi_\ell) \rangle + \eta_\ell^2 \sigma_g^2.$$

We similarly deal with the inner product term:

$$\begin{aligned} \langle \varphi_\ell - \varphi^*, \nabla_\varphi \mathcal{L}_{\text{rf}}(\theta_\ell, \varphi_\ell) \rangle &= \langle \varphi_\ell - \varphi^*, \nabla_\varphi \mathcal{L}_{\text{rf}}(\theta_\ell, \varphi_\ell) - \nabla_\varphi \mathcal{L}_{\text{rf}}(\theta^*, \varphi^*) \rangle \\ &= -\langle \varphi_\ell - \varphi^*, (\Phi_g^\top \Phi_f + \nu I)(\varphi_\ell - \varphi^*) \rangle + \langle \varphi_\ell - \varphi^*, \Phi_g^\top \Phi_f(\theta_\ell - \theta^*) \rangle \\ &\leq -\nu \|\varphi_\ell - \varphi^*\|_2^2 + \langle \varphi_\ell - \varphi^*, \Phi_g^\top \Phi_f(\theta_\ell - \theta^*) \rangle, \end{aligned}$$

Combining the above results, we have

$$r_{\ell+1} \leq \mathbb{E}[\|\hat{\theta}_{\ell+1} - \theta^*\|_2^2 + \|\hat{\varphi}_{\ell+1} - \varphi^*\|_2^2 \mid \theta_\ell, \varphi_\ell] \leq (1 - 2\mu\eta_\ell)r_\ell + \eta_\ell^2(\sigma_f^2 + \sigma_g^2),$$

where we have set $\mu := \min\{\nu, \lambda\}$, and the first inequality follows from the fact that the projection onto a convex set is a contraction map, i.e., $\|\text{Proj}_B(x) - \text{Proj}_B(y)\| \leq \|x - y\|$.

Let $\sigma^2 = \sigma_f^2 + \sigma_g^2$ and $\eta_\ell = \frac{\xi}{\ell+1}$ for some $\xi > \frac{1}{2\mu}$, by induction we have

$$r_\ell \leq \frac{c_\xi}{\ell+1}, \quad \text{where } c_\xi = \max \left\{ r_0, \frac{2\xi^2\sigma^2}{2\mu\xi - 1} \right\}.$$

Specifically, taking $\xi = \mu^{-1}$, we have

$$r_\ell \leq \frac{1}{\ell+1} \max \left\{ r_0, \frac{2\sigma^2}{\mu^2} \right\}. \quad (74)$$

We now track the constants we have used in (74). Note that on the event E_n ,

$$r_0 \leq 2 (\|\theta_0\|_2^2 + \|\theta^*\|_2^2 + \|\varphi_0\|_2^2 + \|\varphi^*\|_2^2) \leq 4(B_1^2 + B^2).$$

Recall the definition of σ^2 :

$$\sigma^2 = \max_{i \in [n], \|\theta\|_2, \|\varphi\|_2 \leq B} \|\nabla_{\theta} \mathcal{L}_i(\theta, \varphi)\|_2^2 + \max_{i \in [n], \|\theta\|_2, \|\varphi\|_2 \leq B} \|\nabla_{\varphi} \mathcal{L}_i(\theta, \varphi)\|_2^2 =: \text{(I)} + \text{(II)}.$$

For the first term, we have

$$\begin{aligned} \text{(I)} &= \max_{i \in [n], \|\theta\|_2, \|\varphi\|_2 \leq B} \|\lambda(\theta - \theta_0) + n\Phi_f^{\top} E_i \Phi_g \varphi\|_2^2 \\ &\leq \max_{i \in [n], \|\theta\|_2, \|\varphi\|_2 \leq B} \left(2\lambda^2 \|\theta - \theta_0\|_2^2 + 2n^2 \|\Phi_f^{\top} E_i \Phi_g \varphi\|_2^2 \right) \leq 4\lambda^2(B^2 + B_1^2) + 2n^2 B_3^2 B^2. \end{aligned}$$

Similarly, for the second term, we have

$$\begin{aligned} \text{(II)} &= \max_{i \in [n], \|\theta\|_2, \|\varphi\|_2 \leq B} \|n(\theta^{\top} \Phi_f^{\top} E_i \Phi_g - \tilde{Y}^{\top} E_i \Phi_g - \Phi_g^{\top} E_i \Phi_g \varphi) - \nu(\varphi - \varphi_0)\|_2^2 \\ &\leq 4n^2 B_3^2 B^2 + 2n^2 B_2^2 B^2 + 4\nu^2(B^2 + B_1^2). \end{aligned}$$

Thus, we know that

$$\sigma^2 \leq 8(\lambda^2 + \nu^2)(B^2 + B_1^2) + 6n^2 B_3^2 B^2 + 2n^2 B_2^2 B^2 =: \tilde{C}.$$

Taking $L_{\delta} = \delta^{-1} \epsilon^{-2} \max\{4B_1^2 + 4B^2, \tilde{C}\mu^{-1}\}$ and $\eta_{\ell} = \frac{1}{\mu(\ell+1)}$, by (74), we know that

$$\mathbb{P}(\|\theta_L - \theta^*\|_2 > \epsilon) \leq \epsilon^{-2} \mathbb{E}\|\theta_L - \theta^*\|_2^2 \leq \epsilon^{-2} r_{\ell} \leq \delta.$$

■

C.5 Proof of Proposition 9

By Lemma 28, for any $\epsilon_1 > 0$ we have

$$\lim_{m \rightarrow \infty} \mathbb{P} \left(\left\{ \sup_{x^* \in \mathcal{X}^l} \|\tilde{\mu} - \mu\|_2 > \epsilon_1 \right\} \cup \left\{ \sup_{x^* \in \mathcal{X}^l} \|\tilde{S} - S\|_F > \epsilon_1 \right\} \right) = 0, \quad (75)$$

where the randomness is from the sampling of random feature bases.

Fix an arbitrary set of $\epsilon_1 > 0, \delta_0 > 0$. Then we can find $m \in \mathbb{N}$ such that the event in (75) has probability smaller than δ_0 . Combining Assumption 9 with the fact that $\theta_0, \phi_0, \tilde{Y}_0$ are now Gaussian random variables with fixed dimensionality, for any $\delta_1 > 0$, we can choose B_1, B_2, B_3 such that the event E_n defined in Lemma 29 has probability $1 - \delta_1$. Thus for any $\epsilon_2 > 0$, when the number of iteration steps exceeds $\Omega(\delta_1^{-1} \epsilon_2^{-2})$, we have

$$\mathbb{P}(\|\hat{\theta}_m - \theta_m^*\|_2 > \epsilon_2) \leq \mathbb{P}(\{\|\hat{\theta}_m - \theta_m^*\|_2 > \epsilon_2\} \cap E_n) + \mathbb{P}(E_n^c) \leq 2\delta_1, \quad (76)$$

where $\hat{\theta}_m$ denotes the approximate optima returned by Algorithm 1 after $\Omega(\delta_1^{-1}\epsilon_2^{-2})$ iterations, θ_m^* denotes the exact optima of the minimax objective, and the randomness is from the gradient noise as well as the perturbations f_0, g_0, Y . Thus we have

$$\mathbb{E}\|\hat{\theta}_m - \theta_m^*\|_2 \leq \epsilon_2 + 2\delta_1(\mathbb{E}\|\hat{\theta}_m\|_2 + \mathbb{E}\|\theta_m^*\|_2) \leq \epsilon_2 + 4\delta_1 B.$$

From the choice of B in Lemma 29, we can see that $\delta_1 B \leq \mathbb{E}(\|\theta_m^*\| \cdot (1 - \mathbf{1}_{E_n}))$, and thus converges to 0 as $\delta_1 \rightarrow 0$. Therefore, $\mathbb{E}\|\hat{\theta}_m - \theta_m^*\|_2$ converges to 0, and for any $x^* \in \mathcal{X}^l$,

$$\begin{aligned} \mathbb{E} \sup_{x^* \in \mathcal{X}^l} \|f(x^*; \hat{\theta}_m) - f(x^*; \theta_m^*)\|_2 &= \mathbb{E} \sup_{x^* \in \mathcal{X}^l} \|\phi_{x,m}(x^*)^\top (\hat{\theta}_m - \theta_m^*)\|_2 \\ &\leq l\sqrt{\tilde{\kappa}} \cdot \mathbb{E}\|\hat{\theta}_m - \theta_m^*\|_2 \rightarrow 0, \end{aligned}$$

where the expectation is taken with respect to the gradient noise, perturbations, and random feature draws. Hence, the mean and covariance of $f(x^*; \hat{\theta}_m)$ converges to that of $f(x^*; \theta_m^*)$ as intended, and we know that the following holds with probability at least $1 - \delta_0$

$$\sup_{x^* \in \mathcal{X}^l} \max \left\{ \|\mathbb{E}(f(x^*; \hat{\theta}_m)) - \mathbb{E}(f(x^*; \theta_m^*))\|_2, \|\text{Cov}(f(x^*; \hat{\theta}_m)) - \text{Cov}(f(x^*; \theta_m^*))\|_F \right\} \leq \epsilon_1$$

Combining this with (75) completes the proof.

Appendix D. Implementation Details, Experiment Setup and Additional Results

D.1 Hyperparameter Selection

We follow the strategy in previous work (e.g., Singh et al., 2019; Muandet et al., 2020) and select hyperparameters by minimizing the *observable* first or second stage loss, depending on which part they directly correspond to.

For the first stage, the loss is

$$\mathcal{L}_{v1} = \text{Tr}(K_{xx} - 2K_{x\tilde{x}}L + K_{\tilde{x}\tilde{x}}L^\top L) = \mathbb{E}_{f \sim \mathcal{GP}(0,k)} \|f(X) - Lf(\tilde{X})\|_2^2$$

where $L := K_{z\tilde{z}}(K_{\tilde{z}\tilde{z}} + \nu I)^{-1}$, and tilde indicates the held-out data. From the above equality we can see that a Monte-Carlo estimator for L_1 can be constructed with the following procedure:

- (i). Draw $f \sim \mathcal{GP}(0, k_x)$.
- (ii). Perform kernel ridge regression on the dataset $\{(\tilde{z}_i, f(\tilde{x}_i))\}$.
- (iii). Return the mean squared error on the dataset (X, Z) .

This procedure can also be implemented for the NN-based models.

For the second stage, the loss $\sum_{i=1}^n \hat{d}_n(\hat{E}_n f, \hat{b})$ can be computed directly, for both the closed-form quasi-posterior and the random feature approximation. For the approximate inference algorithm, as we can see from (65) that the dual functions $\{g(\cdot; \varphi^{(k)})\}$ are samples from Gaussian process posteriors centered at the needed point estimates $\hat{E}_n f(\cdot; \theta^{(k)})$,

instead of the point estimates themselves, we train separate validator models to approximate the latter. The validator models have the architecture to the dual functions used for training, and follow the same learning rate schedule. The validator models are trained before estimating the validation statistics, and we run SGD until convergence to ensure an accurate estimate.

D.2 Details in the Approximate Inference Algorithm

To draw multiple samples from the quasi-posterior efficiently, our algorithm runs J SGDA chains in parallel, with different perturbations $\{(\tilde{Y}^{(j)}, f_0^{(j)}, g_0^{(j)}) : j \in [J]\}$. While the convergence analysis works with the extremely simple Algorithm 1, in practice we extend it to improve stability and accelerate convergence:

- (i). we employ early stopping based on the validation statistics;
- (ii). before the main optimization loop we initialize the dual parameters at the approximate optima $\arg \min_{\varphi} L_{\text{rf}}(f^{(j)}, g(\cdot; \varphi))$, by running SGD until convergence;
- (iii). in each SGDA iteration, we use $K_1 > 1$ GD steps on g and one GA step for f ;
- (iv). after every K_2 epochs, we fix $\theta^{(j)}$ and train the dual parameters $\varphi^{(j)}$ for one epoch.

All the above choices are shown to improve the observable validation statistics. We fix $K_1 = 3, K_2 = 2$ which are determined on the 1D datasets using the validation statistics.

D.3 Nyström Approximation for the Closed-form Quasi-Posterior

Recall the definition of the Nyström-approximated quasi-posterior: we change the definition of the quasi-likelihood to Assumption 7 (ii'), where $\mathcal{I}_n := \text{span}\{k(z_{i_j}, \cdot) : j \in [m]\}$, and z_{i_1}, \dots, z_{i_m} are inducing points sampled from the training data. The new closed-form expressions are then

$$\Pi(f(x_*) \mid \mathcal{D}^{(n)}) = \mathcal{N}(K_{*x} \tilde{\Lambda} Y, K_{**} - K_{*x} \tilde{\Lambda} K_{x*}), \quad (77)$$

$$\text{where } \tilde{\Lambda} := (\lambda I + K_{xx} \tilde{L})^{-1} \tilde{L}, \quad (78)$$

$$\tilde{L} := K_{zz}(\nu K_{zz} + K_{zz} K_{zz})^{-1} K_{zz}, \quad (79)$$

and \tilde{z} denotes the inducing points. In the implementation, we compute a low-rank factorization $A^\top A := \tilde{L}$, defined through the Cholesky factorization of $\nu K_{zz} + K_{zz} K_{zz}$, and use the following equivalent expression of $\tilde{\Lambda}$ obtained from the Woodbury identity:

$$\tilde{\Lambda} = \lambda^{-1} A^\top (I - (\lambda I + A K_{xx} A^\top)^{-1} A K_{xx} A^\top) A = A^\top U \text{diag}((\lambda + \gamma_1)^{-1}, \dots, (\lambda + \gamma_n)^{-1}) U^\top A,$$

where $U \text{diag}(\gamma_1, \dots, \gamma_n) U^\top = A K_{xx} A^\top$ denotes the eigendecomposition. This ensures that matrix inversion is only performed on $m \times m$ matrices.

We use uniform sampling for inducing points, which is equivalent to the leverage score sampling scheme studied in Rudi et al. (2016) as we work on the symmetric $\mathcal{U}[\mathbb{S}^1]$.

D.4 Experiment in Section 8.1: Additional Results

Additional results are plotted in Figure 5. For the contraction rate of the derivative, observe the power space of $W^{s,2}(\mathbb{T})$ matches lower-order Sobolev spaces, so the contraction rate follows that of the power space, as in Section 4.2.2.

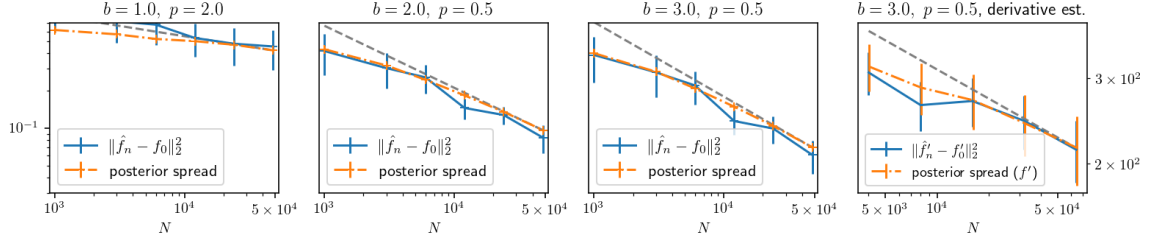


Figure 5: Additional results. The left three plots correspond to the estimation of f ; the rightmost plot corresponds to the estimation of f' . Dashed line indicates the theoretical rate.

D.5 1D Simulation: Experiment Setup Details

In constructing the datasets, let \tilde{f}_0 denote the sine, step, abs or linear ($\tilde{f}_0(x) = x$) function; we then set $f_0 = \tilde{f}_0(4 \cdot (2x - 1))$ if \tilde{f}_0 is sine, abs or linear, $\mathbf{1}_{\{2x-1 < 0\}} + 2.5 \cdot \mathbf{1}_{\{2x-1 \geq 0\}}$ otherwise. These choices are made to maintain consistency with previous work (Lewis and Syrgkanis, 2018; Bennett et al., 2019), which used the same transformed step function and defined \mathbf{x} so that it has a range of approximately $[-4, 4]$.

For 2SLS and the kernelized IV methods, we determine λ and ν following D.1. To improve stability, we repeat the procedures on 50 random partitions of the combined training and validation set, and choose the hyperparameters that minimize the average loss. The hyperparameters are chosen from a log-uniform grid consisting of 10 values in the range of $[0.1, 30]$. The occasional instability of hyperparameter selection is also reported in Muandet et al. (2020). For BayesIV, we run the MCMC sampler for 25000 iterations, discard the first 5000 iterations for burn in, and take one sample out of every 80 consecutive iterations to construct the approximate posterior. For bootstrap we use 20 samples. In both cases, further increasing the computational budget will not improve performance.

We normalize the dataset to have zero mean and unit variance. For all kernel methods we set the kernel bandwidth using the median trick.

D.6 1D Simulation: Full Results

Normalized MSE, average CI coverage and CI width on test set are provided in Table 2-3. We can see that the quasi-posterior consistently provides the most reliable coverage, and is most advantageous in the small-sample setting, or when instrument strength is weak. All methods suffer from lower coverage on the **step** design, due to its discontinuity, and in the weak IV setting, due to instabilities in the hyperparameter selection process.

We provide the following visualizations: (i) Figure 6 plots the quasi-posterior on the **abs** design, for the Matérn and RBF kernels; we also include the approximate inference

algorithm in the plot. (ii) Figure 7 compares the quasi-posterior and bootstrap in the weak instrument setting. The hyperparameters λ, ν are set to the median of all values selected in the repeated experiments, and hyperparameters in the approximate inference algorithm are set as in the demand experiment below. Additional visualizations are provided in the conference version of this work.

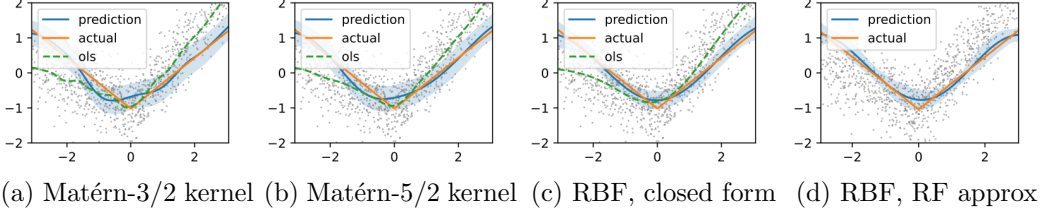


Figure 6: 1D datasets: visualization of the quasi-posterior on the **abs** design using various models. Dots indicate training data. We fix $N = 1000, \alpha = 0.5$.

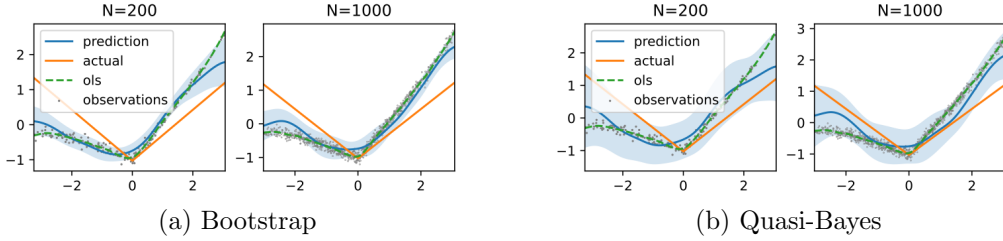


Figure 7: 1D datasets: visualization of the weak instrument setting, on the **abs** design with the Matérn-3/2 kernel. Results for other kernels are qualitatively similar.

D.7 Demand Simulation: Experiment Setup Details

All variables in the dataset are normalized to have zero mean and unit variance. For BayesIV, we run the MCMC sampler for 50000 iterations, discard the first 10000 samples as burn in, and take every 80th sample for inference. For the kernelized methods, hyperparameter selection follows the 1D experiments. For the NN-based methods, implementation details are discussed in Appendix D.2; for both our method and bootstrap, we draw $J = 10$ samples from the predictive distribution.

We select hyperparameters by applying the procedure in Appendix D.1 to a fixed train / validation split, since on this dataset we observe little variation in its results. Hyperparameters include λ, ν , and the learning rate schedule (initial learning rate η_0 and period of learning rate decay τ). The learning rate is adjusted by multiplying it by a factor of 0.8 every τ iterations. We fix the optimizer to Adam, and train until validation statistics no longer improves.

For the lower-dimensional setup, we select λ and ν from a log-linearly scaled grid of 10 values, with the range of $[5 \times 10^{-3}, 5]$ and $[0.05, 1]$, respectively. The ranges are chosen based on preliminary experiments using the range of $[0.1, 30]$. We determine η from $\{5 \times 10^{-4}, 10^{-3}, 5 \times 10^{-3}, 1 \times 10^{-2}, 5 \times 10^{-2}\}$, and τ from $\{80, 160, 320, 640\}$. We fix the batch

Method	bayesIV	bs-lin	qb-lin	bs-poly	qb-poly	bs-ma3	qb-ma3	bs-ma5	qb-ma5	bs-rbf	qb-rbf
$f_0 = \sin, N = 200, \alpha = 0.5$											
MSE	.024 (.038)	.111 (.011)	.109 (.010)	.243 (.037)	.243 (.034)	.023 (.010)	.025 (.014)	.022 (.011)	.021 (.015)	.025 (.013)	.026 (.015)
CI Cvg.	.895 (.252)	.232 (.039)	.110 (.019)	.077 (.032)	.045 (.017)	.965 (.065)	1.00 (.000)	.972 (.065)	1.00 (.000)	.972 (.079)	1.00 (.013)
CI Wid.	.188 (.035)	.143 (.028)	.072 (.004)	.078 (.025)	.041 (.006)	.283 (.031)	.661 (.066)	.288 (.032)	.569 (.067)	.293 (.040)	.408 (.063)
$f_0 = \sin, N = 1000, \alpha = 0.5$											
MSE	.016 (.003)	.103 (.006)	.103 (.006)	.237 (.020)	.239 (.020)	.009 (.011)	.008 (.014)	.008 (.012)	.007 (.015)	.007 (.012)	.007 (.013)
CI Cvg.	.598 (.155)	.097 (.020)	.049 (.006)	.036 (.012)	.017 (.004)	.962 (.113)	1.00 (.000)	.954 (.111)	1.00 (.000)	.957 (.168)	1.00 (.036)
CI Wid.	.085 (.006)	.061 (.011)	.032 (.001)	.038 (.009)	.019 (.002)	.186 (.032)	.602 (.037)	.173 (.029)	.509 (.037)	.164 (.029)	.326 (.041)
$f_0 = \text{abs}, N = 200, \alpha = 0.5$											
MSE	.042 (.038)	.454 (.052)	.456 (.053)	.478 (.085)	.477 (.089)	.033 (.026)	.035 (.025)	.032 (.024)	.031 (.025)	.031 (.019)	.031 (.021)
CI Cvg.	.863 (.184)	.190 (.039)	.085 (.198)	.055 (.027)	.020 (.072)	.945 (.110)	1.00 (.004)	.942 (.118)	1.00 (.004)	.920 (.125)	1.00 (.030)
CI Wid.	.207 (.027)	.214 (.035)	.077 (.220)	.110 (.038)	.043 (.091)	.316 (.037)	.676 (.072)	.317 (.034)	.599 (.079)	.277 (.037)	.462 (.082)
$f_0 = \text{abs}, N = 1000, \alpha = 0.5$											
MSE	.024 (.011)	.448 (.016)	.449 (.016)	.468 (.025)	.469 (.026)	.020 (.006)	.019 (.005)	.019 (.006)	.018 (.006)	.017 (.007)	.016 (.006)
CI Cvg.	.507 (.196)	.083 (.018)	.111 (.092)	.028 (.007)	.009 (.003)	.857 (.075)	1.00 (.000)	.823 (.079)	1.00 (.000)	.829 (.102)	1.00 (.016)
CI Wid.	.092 (.005)	.098 (.019)	.127 (.103)	.061 (.016)	.019 (.002)	.181 (.024)	.646 (.050)	.174 (.026)	.530 (.056)	.168 (.024)	.383 (.061)
$f_0 = \text{step}, N = 200, \alpha = 0.5$											
MSE	.045 (.026)	.075 (.010)	.075 (.010)	.179 (.025)	.180 (.023)	.041 (.013)	.047 (.017)	.043 (.012)	.046 (.015)	.046 (.011)	.048 (.013)
CI Cvg.	.845 (.176)	.347 (.069)	.220 (.045)	.110 (.048)	.067 (.022)	.797 (.101)	1.00 (.022)	.787 (.085)	.998 (.038)	.710 (.085)	.917 (.051)
CI Wid.	.194 (.018)	.139 (.023)	.072 (.004)	.068 (.022)	.041 (.006)	.300 (.047)	.665 (.083)	.285 (.041)	.593 (.082)	.252 (.035)	.453 (.061)
$f_0 = \text{step}, N = 1000, \alpha = 0.5$											
MSE	.023 (.009)	.070 (.004)	.069 (.004)	.178 (.012)	.176 (.011)	.035 (.012)	.038 (.015)	.038 (.011)	.040 (.014)	.039 (.012)	.040 (.014)
CI Cvg.	.616 (.116)	.185 (.042)	.098 (.014)	.053 (.021)	.030 (.005)	.784 (.153)	1.00 (.016)	.739 (.164)	.976 (.028)	.661 (.134)	.839 (.077)
CI Wid.	.086 (.004)	.060 (.011)	.032 (.001)	.032 (.010)	.019 (.002)	.206 (.062)	.565 (.053)	.196 (.073)	.483 (.065)	.168 (.031)	.312 (.054)
$f_0 = \text{linear}, N = 200, \alpha = 0.5$											
MSE	.009 (.011)	.002 (.002)	.001 (.002)	.128 (.019)	.128 (.017)	.012 (.008)	.017 (.013)	.011 (.009)	.014 (.014)	.011 (.011)	.013 (.016)
CI Cvg.	.948 (.091)	1.00 (.153)	1.00 (.130)	.087 (.026)	.060 (.018)	.995 (.044)	1.00 (.001)	.995 (.050)	1.00 (.003)	.990 (.060)	1.00 (.043)
CI Wid.	.129 (.025)	.088 (.012)	.072 (.004)	.055 (.017)	.041 (.006)	.269 (.031)	.520 (.049)	.261 (.031)	.438 (.058)	.239 (.034)	.298 (.041)
$f_0 = \text{linear}, N = 1000, \alpha = 0.5$											
MSE	.005 (.002)	.000 (.001)	.000 (.001)	.121 (.012)	.121 (.012)	.006 (.004)	.007 (.005)	.006 (.003)	.007 (.005)	.006 (.003)	.005 (.004)
CI Cvg.	.626 (.130)	1.00 (.174)	1.00 (.230)	.034 (.008)	.026 (.004)	.992 (.094)	1.00 (.000)	.990 (.095)	1.00 (.000)	.975 (.103)	1.00 (.000)
CI Wid.	.051 (.002)	.039 (.006)	.032 (.001)	.026 (.006)	.019 (.002)	.171 (.031)	.508 (.043)	.156 (.032)	.418 (.044)	.135 (.024)	.242 (.043)

Table 2: Full results in the 1D simulation, for $\alpha = 0.5$

Method	bayesIV	bs-lin	qb-lin	bs-poly	qb-poly	bs-ma3	qb-ma3	bs-ma5	qb-ma5	bs-rbf	qb-rbf
$f_0 = \sin, N = 200, \alpha = 0.05$											
MSE	.275 (.045)	.133 (.070)	.193 (.125)	.202 (.121)	.215 (.161)	.231 (.037)	.190 (.068)	.209 (.037)	.163 (.073)	.183 (.047)	.142 (.081)
CI Cvg.	.165 (.077)	.992 (.080)	1.00 (.134)	.325 (.092)	.425 (.080)	.270 (.082)	.960 (.084)	.332 (.121)	.955 (.086)	.468 (.219)	.952 (.134)
CI Wid.	.192 (.030)	.589 (.166)	.971 (.481)	.394 (.171)	.771 (.265)	.192 (.036)	.712 (.045)	.233 (.054)	.694 (.065)	.297 (.085)	.638 (.105)
$f_0 = \sin, N = 1000, \alpha = 0.05$											
MSE	.146 (.025)	.123 (.077)	.169 (.315)	.213 (.145)	.228 (.192)	.246 (.071)	.216 (.113)	.238 (.085)	.214 (.131)	.188 (.096)	.188 (.131)
CI Cvg.	.082 (.060)	.880 (.296)	.888 (.346)	.289 (.086)	.344 (.135)	.373 (.111)	.819 (.131)	.436 (.145)	.840 (.185)	.562 (.218)	.897 (.212)
CI Wid.	.095 (.018)	.552 (.367)	.852 (.568)	.405 (.294)	.588 (.400)	.254 (.036)	.605 (.049)	.298 (.042)	.568 (.050)	.373 (.086)	.536 (.055)
$f_0 = \text{abs}, N = 200, \alpha = 0.05$											
MSE	.806 (.478)	.487 (.259)	.500 (.505)	.489 (.233)	.472 (.453)	.392 (.064)	.349 (.156)	.368 (.074)	.350 (.180)	.336 (.094)	.393 (.221)
CI Cvg.	.122 (.197)	.435 (.167)	.775 (.201)	.247 (.119)	.545 (.122)	.217 (.102)	.795 (.137)	.287 (.130)	.832 (.163)	.352 (.243)	.805 (.250)
CI Wid.	.239 (.049)	.526 (.311)	1.30 (.473)	.303 (.152)	.895 (.279)	.294 (.047)	.712 (.045)	.351 (.065)	.694 (.065)	.424 (.103)	.638 (.105)
$f_0 = \text{abs}, N = 1000, \alpha = 0.05$											
MSE	1.45 (.250)	.479 (.105)	.500 (.083)	.472 (.159)	.472 (.111)	.376 (.090)	.390 (.144)	.374 (.109)	.367 (.181)	.304 (.134)	.265 (.214)
CI Cvg.	.019 (.014)	.464 (.179)	.742 (.249)	.332 (.165)	.562 (.191)	.306 (.109)	.665 (.207)	.374 (.165)	.667 (.248)	.505 (.269)	.625 (.308)
CI Wid.	.139 (.017)	.460 (.328)	1.24 (.576)	.340 (.238)	.923 (.384)	.339 (.044)	.605 (.049)	.367 (.056)	.561 (.049)	.504 (.114)	.536 (.061)
$f_0 = \text{step}, N = 200, \alpha = 0.05$											
MSE	.226 (.127)	.105 (.069)	.148 (.199)	.157 (.092)	.192 (.148)	.214 (.036)	.183 (.070)	.194 (.038)	.176 (.077)	.160 (.056)	.147 (.090)
CI Cvg.	.193 (.090)	.777 (.158)	.787 (.197)	.382 (.079)	.438 (.066)	.262 (.103)	.952 (.068)	.300 (.158)	.920 (.089)	.432 (.282)	.890 (.149)
CI Wid.	.184 (.032)	.621 (.297)	.767 (.452)	.456 (.179)	.652 (.292)	.262 (.051)	.712 (.045)	.310 (.070)	.694 (.065)	.365 (.103)	.638 (.112)
$f_0 = \text{step}, N = 1000, \alpha = 0.05$											
MSE	.079 (.444)	.083 (.044)	.131 (.207)	.152 (.105)	.236 (.120)	.231 (.059)	.214 (.107)	.224 (.070)	.208 (.127)	.192 (.082)	.170 (.130)
CI Cvg.	.149 (.231)	.715 (.171)	.696 (.201)	.366 (.087)	.390 (.120)	.290 (.075)	.841 (.165)	.353 (.144)	.853 (.212)	.515 (.229)	.800 (.189)
CI Wid.	.125 (.021)	.544 (.295)	.815 (.564)	.408 (.187)	.539 (.423)	.298 (.037)	.605 (.049)	.330 (.052)	.561 (.049)	.420 (.095)	.543 (.065)
$f_0 = \text{linear}, N = 200, \alpha = 0.05$											
MSE	.083 (.023)	.013 (.032)	.041 (.202)	.103 (.065)	.151 (.149)	.052 (.015)	.046 (.024)	.046 (.016)	.045 (.023)	.046 (.020)	.053 (.023)
CI Cvg.	.238 (.133)	1.00 (.284)	1.00 (.172)	.372 (.099)	.412 (.109)	.490 (.194)	1.00 (.000)	.750 (.219)	1.00 (.000)	.895 (.188)	1.00 (.026)
CI Wid.	.121 (.030)	.559 (.213)	.595 (.406)	.495 (.181)	.543 (.327)	.220 (.028)	.712 (.045)	.270 (.041)	.694 (.065)	.323 (.074)	.638 (.105)
$f_0 = \text{linear}, N = 1000, \alpha = 0.05$											
MSE	.051 (.007)	.018 (.034)	.022 (.165)	.125 (.092)	.188 (.411)	.070 (.023)	.069 (.041)	.070 (.028)	.070 (.047)	.057 (.031)	.066 (.043)
CI Cvg.	.094 (.041)	1.00 (.215)	1.00 (.200)	.338 (.113)	.298 (.122)	.455 (.107)	1.00 (.028)	.528 (.192)	1.00 (.066)	.684 (.237)	1.00 (.096)
CI Wid.	.058 (.007)	.535 (.289)	.423 (.470)	.435 (.309)	.406 (.365)	.205 (.020)	.605 (.049)	.230 (.033)	.561 (.049)	.297 (.089)	.530 (.061)

 Table 3: Full results in the 1D simulation, for $\alpha = 0.05$

size at 256. The NN architecture consists of two fully-connected layers, with 50 hidden units and the tanh activation. We also experimented with NNs with 3 hidden layers or with ReLU activation, and made this choice based on the validation statistics.

For the image-based setup, the range of λ and η follows the above. For ν, τ we consider $\nu \in [1, 100], \tau \in \{640, 1280, 2560, 5120\}$, based on preliminary experiments. We fix the batch size at 80. The network architecture is adapted from Hartford et al. (2017), and consists of two 3×3 convolutional layers with 64 filters, followed by max pooling, dropout, and three fully-connected layers with 64, 32 and 1 units.

Following the setup in all previous work, we use a uniform grid on $[5, 30] \times [0, 10] \times \{0, \dots, 6\}$ as the test set.

D.8 Demand Simulation: Full Results and Visualizations

Results in the large-sample settings are presented in Table 4, which are consistent with the discussion in the main text.

We plot the predictive distributions for all methods in Figure 9, on the same cross-section as in the main text, for $N = 1000$. (We omit the plot for $N = 10^4$ and the image experiment, since in those settings bootstrap and the quasi-posterior have similar behaviors.) As we can see, all non-NN baselines except BayesIV produce overly smooth predictions, presumably due to the lack of flexibility in these models. Note that the visualizations only correspond to an intersection of the true function $f(x_0, t_0, s)$, with x_0, t_0 fixed; the complete function has the form of $x \cdot s \cdot \psi(t)$, ignoring the less significant terms, and thus may incur a large norm penalty in the less flexible RKHSes. The issue is further exacerbated by the discrepancy between the training and test distributions: the former is non-uniform due to confounding. As we can see from Figure 8, in the region where t is close to 5, the data is scarce for most values of x , which may explain the reason that the closed-form kernels fail to provide good coverage around $t = 5$ (and $s = 3, x = 17.5$, as used in the visualizations), and the reason that both NN-based methods assign higher uncertainty around this location.

BayesIV has a different failure mode: as it employs additive regression models for both stages $p(\mathbf{x} \mid \mathbf{z}), p(\mathbf{y} \mid \mathbf{x})$, it approximates this cross-section relatively well. However, as the true structural function does not have an additive decomposition, its prediction in other regions can be grossly inaccurate; we plot one such cross-section in Figure 10(a).

When implemented with the NN model, bootstrap CIs are sharper in regions with more training data, although the difference is often insignificant. The difference in out-of-distribution regions is more significant, where bootstrap is often less robust. An example is shown in Figure 10.

Setting	Low-dimensional, $N = 10^4$			Image, $N = 5 \times 10^4$		
Method	BS-2SLS	BS-NN	QB-NN	BS-2SLS	BS-NN	QB-NN
NMSE	.371 \pm .003	.014 \pm .003	.020 \pm .002	.559 \pm .008	.168 \pm .027	.138 \pm .037
CI Cvg.	.024 \pm .005	.944 \pm .009	.957 \pm .008	.112 \pm .005	.892 \pm .022	.909 \pm .017
CI Wid.	.014 \pm .002	.136 \pm .015	.203 \pm .013	.132 \pm .039	.636 \pm .027	.597 \pm .024

Table 4: Deferred results on the demand design. Results are averaged over 20 trials for the low-dimensional experiment, and 10 trials for the image experiment.

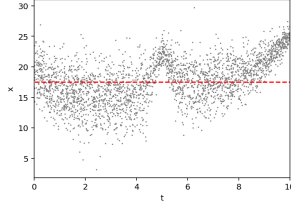


Figure 8: Demand experiment: scatter plot of 10^4 samples from the training data distribution $p(x, t \mid s = 4)$. The dashed line indicates the cross-section used in Figure 4.

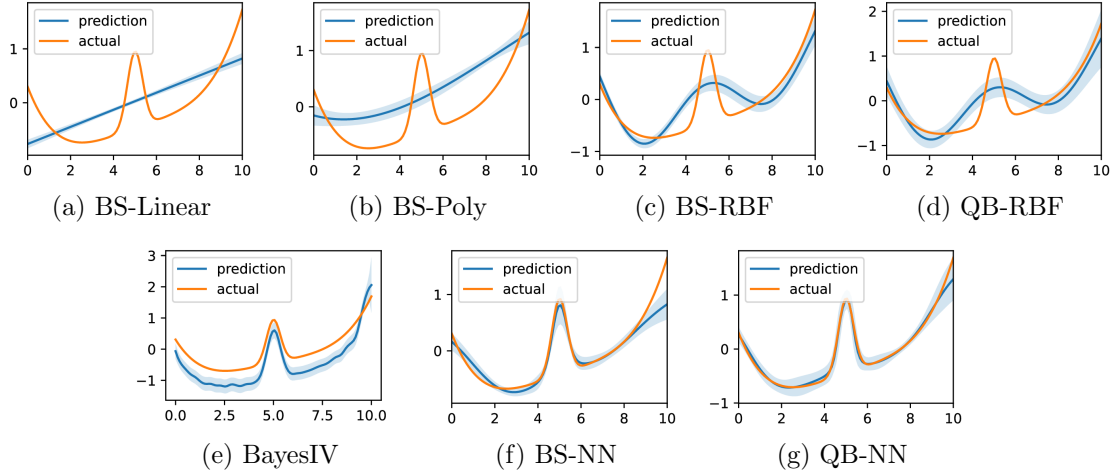


Figure 9: Demand experiment: visualizations of the predictive distributions for $N = 1000$, on the same cross-section as in Figure 4.

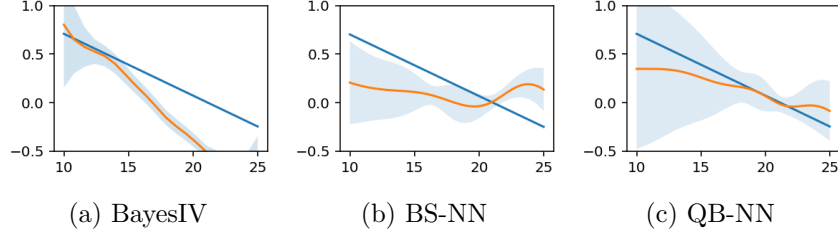


Figure 10: Demand experiment: visualizations of the predictive distributions for $N = 1000$ on a out-of-distribution cross-section, obtained by fixing $t = 9, s = 6$ and varying x .

D.8.1 COMPUTATIONAL COST

We report the typical training time for a single set of hyperparameters, excluding JIT compilation time, on a GeForce GTX 1080Ti GPU. In the lower-dimensional experiments, training takes around 25 minutes for a single set of hyperparameters when $N = 10^3$, or around 30 minutes when $N = 10^4$; in both cases 6 experiments can be carried out in parallel on a single GPU. In the image experiment, training takes around 7.5 hours.

The time cost above is for the optimal hyperparameter configuration; experiments using suboptimal hyperparameters usually take a shorter period of time due to early stopping. It can also be improved by switching to low-precision numerical operations, or with various heuristics in the hyperparameter search (e.g., using a smaller J in an initial search).

References

- Robert A Adams and John JF Fournier. *Sobolev Spaces*. Elsevier, 2003.
- Sergios Agapiou, Stig Larsson, and Andrew M Stuart. Posterior contraction rates for the bayesian approach to linear ill-posed inverse problems. *Stochastic Processes and their Applications*, 123(10):3828–3860, 2013.
- Joshua D Angrist and Jörn-Steffen Pischke. *Mostly Harmless Econometrics: An Empiricist’s Companion*. Princeton University Press, 2008.
- Andrew Bennett and Nathan Kallus. The variational method of moments. *arXiv preprint arXiv:2012.09422*, 2020.
- Andrew Bennett, Nathan Kallus, and Tobias Schnabel. Deep generalized method of moments for instrumental variable analysis. In *Advances in Neural Information Processing Systems*, 2019.
- Richard Blundell, Xiaohong Chen, and Dennis Kristensen. Semi-nonparametric IV estimation of shape-invariant Engel curves. *Econometrica*, 75(6):1613–1669, 2007.
- Viacheslav Borovitskiy, Alexander Terenin, Peter Mostowsky, and Marc Peter Deisenroth. Matérn Gaussian processes on Riemannian manifolds. In *Advances in Neural Information Processing Systems*, 2020.
- Laurent Cavalier. Nonparametric statistical inverse problems. *Inverse Problems*, 24(3):034004, 2008.
- Xiaohong Chen and Timothy M. Christensen. Optimal sup-norm rates and uniform inference on nonlinear functionals of nonparametric IV regression. *arXiv preprint arXiv:1508.03365*, 2015.
- Xiaohong Chen and Demian Pouzo. Estimation of nonparametric conditional moment models with possibly nonsmooth generalized residuals. *Econometrica*, 80(1):277–321, 2012.
- Xiaohong Chen and Markus Reiss. On rate optimality for ill-posed inverse problems in econometrics. *Econometric Theory*, pages 497–521, 2011.
- Victor Chernozhukov and Han Hong. An MCMC approach to classical estimation. *Journal of Econometrics*, 115(2):293–346, 2003.
- Timothy G Conley, Christian B Hansen, Robert E McCulloch, and Peter E Rossi. A semi-parametric Bayesian approach to the instrumental variable problem. *Journal of Econometrics*, 144(1):276–305, 2008.

- Jack Cuzick, Robert Edwards, and Nereo Segnan. Adjusting for non-compliance and contamination in randomized clinical trials. *Statistics in Medicine*, 16(9):1017–1029, 1997.
- Bo Dai, Niao He, Yunpeng Pan, Byron Boots, and Le Song. Learning from conditional distributions via dual embeddings. *arXiv preprint arXiv:1607.04579*, 2016.
- Russell Davidson and James G. Mackinnon. Wild bootstrap tests for IV regression. *Journal of Business & Economic Statistics*, 28(1):128–144, 2010.
- Nishanth Dikkala, Greg Lewis, Lester Mackey, and Vasilis Syrgkanis. Minimax estimation of conditional moment models. In *Advances in Neural Information Processing Systems*, volume 33, pages 12248–12262, 2020.
- Miroslav Dudík, Steven J Phillips, and Robert E Schapire. Maximum entropy density estimation with generalized regularization and an application to species distribution modeling. *Journal of Machine Learning Research*, 2007.
- Nathaniel Eldredge. Analysis and probability on infinite-dimensional spaces. *arXiv preprint arXiv:1607.03591*, 2016.
- Simon Fischer and Ingo Steinwart. Sobolev norm learning rates for regularized least-squares algorithms. *Journal of Machine Learning Research*, 21:205–1, 2020.
- Jean-Pierre Florens and Anna Simoni. Nonparametric estimation of an instrumental regression: A quasi-Bayesian approach based on regularized posterior. *Journal of Econometrics*, 170(2):458–475, 2012.
- Jean-Pierre Florens and Anna Simoni. Gaussian processes and Bayesian moment estimation. *Journal of Business & Economic Statistics*, 39(2):482–492, 2021.
- Alfonso Flores-Lagunes. Finite sample evidence of IV estimators under weak instruments. *Journal of Applied Econometrics*, 22(3):677–694, 2007.
- Subhashis Ghosal and Aad Van der Vaart. *Fundamentals of Nonparametric Bayesian Inference*, volume 44. Cambridge University Press, 2017.
- Subhashis Ghosal, Jayanta K Ghosh, and Aad W Van Der Vaart. Convergence rates of posterior distributions. *Annals of Statistics*, pages 500–531, 2000.
- Evarist Giné and Richard Nickl. *Mathematical Foundations of Infinite-Dimensional Statistical Models*. Cambridge University Press, 2021.
- Sander Greenland. An introduction to instrumental variables for epidemiologists. *International Journal of Epidemiology*, 29(4):722–729, 2000.
- Jason Hartford, Greg Lewis, Kevin Leyton-Brown, and Matt Taddy. Deep IV: A flexible approach for counterfactual prediction. In *International Conference on Machine Learning*, pages 1414–1423, 2017.
- Bobby He, Balaji Lakshminarayanan, and Yee Whye Teh. Bayesian deep ensembles via the neural tangent kernel. *arXiv preprint arXiv:2007.05864*, 2020.

- Joel L. Horowitz. Applied nonparametric instrumental variables estimation. *Econometrica*, 79(2):347–394, 2011.
- Joel L. Horowitz. Specification testing in nonparametric instrumental variable estimation. *Journal of Econometrics*, 167(2):383–396, 2012.
- Tommi Jaakkola, Marina Meila, and Tony Jebara. Maximum entropy discrimination. In *Proceedings of the 12th International Conference on Neural Information Processing Systems*, pages 470–476, 1999.
- Arthur Jacot, Franck Gabriel, and Clement Hongler. Neural tangent kernel: Convergence and generalization in neural networks. In *Advances in Neural Information Processing Systems*, 2018.
- Motonobu Kanagawa, Philipp Hennig, Dino Sejdinovic, and Bharath K Sriperumbudur. Gaussian processes and kernel methods: A review on connections and equivalences. *arXiv preprint arXiv:1807.02582*, 2018.
- Kengo Kato. Quasi-Bayesian analysis of nonparametric instrumental variables models. *The Annals of Statistics*, 41(5):2359–2390, 2013.
- Jae-Young Kim. Limited information likelihood and Bayesian analysis. *Journal of Econometrics*, page 19, 2002.
- Frank Kleibergen and Herman K Van Dijk. Bayesian simultaneous equations analysis using reduced rank structures. *Econometric Theory*, pages 701–743, 1998.
- Frank Kleibergen and Eric Zivot. Bayesian and classical approaches to instrumental variable regression. *Journal of Econometrics*, 114(1):29–72, 2003.
- B. T. Knapik, A. W. van der Vaart, and J. H. van Zanten. Bayesian inverse problems with Gaussian priors. *The Annals of Statistics*, 39(5):2626–2657, 2011.
- Bartek Knapik and Jean-Bernard Salomond. A general approach to posterior contraction in nonparametric inverse problems. *Bernoulli*, 24(3), 2018.
- Jaehoon Lee, Lechao Xiao, Samuel Schoenholz, Yasaman Bahri, Roman Novak, Jascha Sohl-Dickstein, and Jeffrey Pennington. Wide neural networks of any depth evolve as linear models under gradient descent. In *Advances in Neural Information Processing Systems*, volume 32, 2019.
- Greg Lewis and Vasilis Syrgkanis. Adversarial generalized method of moments. *arXiv preprint arXiv:1803.07164*, 2018.
- Luofeng Liao, You-Lin Chen, Zhuoran Yang, Bo Dai, Zhaoran Wang, and Mladen Kolar. Provably efficient neural estimation of structural equation model: An adversarial approach. *arXiv preprint arXiv:2007.01290*, 2020.
- Yuan Liao and Wenxin Jiang. Posterior consistency of nonparametric conditional moment restricted models. *The Annals of Statistics*, 39(6):3003–3031, 2011.

- Hedibert F Lopes and Nicholas G Polson. Bayesian instrumental variables: priors and likelihoods. *Econometric Reviews*, 33(1-4):100–121, 2014.
- Afsaneh Mastouri, Yuchen Zhu, Limor Gultchin, Anna Korba, Ricardo Silva, Matt J Kusner, Arthur Gretton, and Krikamol Muandet. Proximal causal learning with kernels: Two-stage estimation and moment restriction. *arXiv preprint arXiv:2105.04544*, 2021.
- Wang Miao, Zhi Geng, and Eric J Tchetgen Tchetgen. Identifying causal effects with proxy variables of an unmeasured confounder. *Biometrika*, 105(4):987–993, 2018.
- Marcelo Moreira, Jack R Porter, and Gustavo A Suarez. Bootstrap and higher-order expansion validity when instruments may be weak, 2004.
- Krikamol Muandet, Arash Mehrjou, Si Kai Lee, and Anant Raj. Dual instrumental variable regression. *arXiv preprint arXiv:1910.12358*, 2020.
- Radford M Neal. *Bayesian Learning for Neural Networks*, volume 118. Springer Science & Business Media, 2012.
- Whitney K Newey and James L Powell. Instrumental variable estimation of nonparametric models. *Econometrica*, 71(5):1565–1578, 2003.
- Ian Osband, John Aslanides, and Albin Cassirer. Randomized prior functions for deep reinforcement learning. In *Proceedings of the 32nd International Conference on Neural Information Processing Systems*, pages 8626–8638, 2018.
- Tim Pearce, Felix Leibfried, and Alexandra Brintrup. Uncertainty in neural networks: Approximately Bayesian ensembling. In *Proceedings of the 23rd International Conference on Artificial Intelligence and Statistics*, volume 108, pages 234–244, 2020.
- Ali Rahimi, Benjamin Recht, et al. Random features for large-scale kernel machines. In *Advances in Neural Information Processing Systems*. Citeseer, 2007.
- Judith Rousseau and Botond Szabo. Asymptotic behaviour of the empirical Bayes posteriors associated to maximum marginal likelihood estimator. *The Annals of Statistics*, 45(2), 2017.
- Alessandro Rudi, Raffaello Camoriano, and Lorenzo Rosasco. Less is more: Nyström computational regularization. *arXiv preprint arXiv:1507.04717*, 2016.
- Rahul Singh, Maneesh Sahani, and Arthur Gretton. Kernel Instrumental variable regression. *arXiv preprint arXiv:1906.00232*, 2019.
- Niranjan Srinivas, Andreas Krause, Sham M. Kakade, and Matthias Seeger. Gaussian process optimization in the bandit setting: No regret and experimental design. *IEEE Transactions on Information Theory*, 58(5):3250–3265, 2012.
- Bharath K Sriperumbudur, Kenji Fukumizu, and Gert RG Lanckriet. Universality, characteristic kernels and RKHS embedding of measures. *Journal of Machine Learning Research*, 12(7), 2011.

- Ingo Steinwart. Convergence types and rates in generic Karhunen-Loève expansions with applications to sample path properties. *Potential Analysis*, 51(3):361–395, 2019.
- Ingo Steinwart and Andreas Christmann. *Support Vector Machines*. Springer Science & Business Media, 2008.
- Ingo Steinwart and Clint Scovel. Mercer’s theorem on general domains: On the interaction between measures, kernels, and RKHSs. *Constructive Approximation*, 35(3):363–417, 2012.
- Ingo Steinwart, Don R Hush, Clint Scovel, et al. Optimal rates for regularized least squares regression. In *COLT*, pages 79–93, 2009.
- James H Stock, Jonathan H Wright, and Motohiro Yogo. A survey of weak instruments and weak identification in generalized method of moments. *Journal of Business & Economic Statistics*, 20(4):518–529, 2002.
- Robert S Strichartz. Analysis of the Laplacian on the complete Riemannian manifold. *Journal of Functional Analysis*, 52(1):48–79, 1983.
- Andrew M Stuart. Inverse problems: a Bayesian perspective. *Acta Numerica*, 19:451–559, 2010.
- Botond Szabó, A. W. van der Vaart, and J. H. van Zanten. Frequentist coverage of adaptive nonparametric Bayesian credible sets. *The Annals of Statistics*, 43(4):1391–1428, 2015.
- Hans Triebel. *Theory of Function Spaces*. Springer Basel, Basel, 1983. ISBN 978-3-0346-0415-4 978-3-0346-0416-1.
- A. W. van der Vaart and J. H. van Zanten. Rates of contraction of posterior distributions based on Gaussian process priors. *The Annals of Statistics*, 36(3), 2008a.
- A. W. van der Vaart and J. H. van Zanten. Reproducing kernel Hilbert spaces of Gaussian priors. *arXiv preprint arXiv:0805.3252*, pages 200–222, 2008b.
- A. W. van der Vaart and J. H. van Zanten. Information rates of nonparametric Gaussian process regression. *Journal of Machine Learning Research*, 12:2095–2119, 2011.
- Martin J Wainwright. *High-Dimensional Statistics: A Non-Asymptotic Viewpoint*, volume 48. Cambridge University Press, 2019.
- Ziyu Wang, Yuhao Zhou, Tongzheng Ren, and Jun Zhu. Scalable quasi-bayesian inference for instrumental variable regression. In *Advances in Neural Information Processing Systems*, 2021.
- Manuel Wiesenfarth, Carlos Matías Hisgen, Thomas Kneib, and Carmen Cadarso-Suarez. Bayesian nonparametric instrumental variables regression based on penalized splines and dirichlet process mixtures. *Journal of Business & Economic Statistics*, 32(3):468–482, 2014.

- Liyuan Xu, Yutian Chen, Siddarth Srinivasan, Nando de Freitas, Arnaud Doucet, and Arthur Gretton. Learning deep features in instrumental variable regression. *arXiv preprint arXiv:2010.07154*, 2020.
- Yun Yang, Anirban Bhattacharya, and Debdeep Pati. Frequentist coverage and sup-norm convergence rate in Gaussian process regression. *arXiv preprint arXiv:1708.04753*, 2017.
- Arnold Zellner. Bayesian method of moments (BMOM) analysis of mean and regression models. *arXiv preprint arXiv:bayes-an/9511001*, 1995.
- Rui Zhang, Masaaki Imaizumi, Bernhard Schölkopf, and Krikamol Muandet. Maximum moment restriction for instrumental variable regression. *arXiv preprint arXiv:2010.07684*, 2020.
- Tong Zhang. From ϵ -entropy to KL-entropy: Analysis of minimum information complexity density estimation. *The Annals of Statistics*, 34(5):2180–2210, 2006.
- Jun Zhu and Eric P Xing. Maximum entropy discrimination Markov networks. *Journal of Machine Learning Research*, 10(11), 2009.